CATALYSIS BY SURFACES

- 7.1 Introduction
 - 7.1.1 Brief History of Surface Catalysis
- 7.2 Catalytic Action
 - 7.2.1 Kinetic Expressions
 - 7.2.2 Selective Catalysis
 - 7.2.3 Tabulated Kinetic Parameters for Catalytic Reactions
- 7.3 Catalyst Preparation, Deactivation, and Regeneration
 - 7.3.1 Catalyst Preparation
 - 7.3.2 Catalyst Deactivation
 - 7.3.3 Catalyst Regeneration
- 7.4 Metal Catalysis
 - 7.4.1 Trends Across the Periodic Table
 - 7.4.2 Some Frequently Used Concepts of Metal Catalysis
- 7.5 Catalysis by Ions at Surfaces. Acid-Base Catalysis
 - 7.5.1 Acid Catalysis in Solutions
 - 7.5.2 Solid Acids
 - 7.5.3 Carbenium Ion Reactions
- 7.6 Most Frequently Used Catalyst Materials
- 7.7 Surface-Science Approach to Catalytic Chemistry
 - 7.7.1 Techniques to Characterize and Study the Reactivity of Small-Area Catalyst Surfaces
 - 7.7.1.1 High-Pressure Reactors
 - 7.7.1.2 Comparison of the Reactivities of Small- and Large-Surface-Area Catalysts
- 7.8 Case Histories of Surface Catalysis
 - 7.8.1 Ammonia Synthesis
 - 7.8.1.1 Thermodynamics and Kinetics
 - 7.8.1.1.1 Kinetics
 - 7.8.1.2 Catalyst Preparation
 - 7.8.1.3 Activity for Ammonia Synthesis Using Transition Metals Across the Periodic Table
 - 7.8.1.4 Surface Science of Ammonia Synthesis
 - 7.8.1.4.1 Structure Sensitivity of Ammonia Synthesis
 - 7.8.1.4.2 Kinetics of Dissociative Nitrogen Adsorption
 - 7.8.1.4.3 Effects of Aluminum Oxide in Restructuring Iron Single-Crystal Surfaces for Ammonia Synthesis
 - 7.8.1.4.4 Characterization of the Restructured Surfaces
 - 7.8.1.4.5 Effect of Potassium on the Dissociative Chemisorption of Nitrogen on Iron Single-Crystal Surfaces in UHV

- 7.8.1.4.6 Temperature-Programmed Desorption Studies of Ammonia from Iron Surfaces in the Presence of Potassium
- 7.8.1.4.7 Effects of Potassium on Ammonia Synthesis Kinetics
- 7.8.1.4.8 Effects of Potassium on the Adsorption of Ammonia on Iron Under Ammonia Synthesis Conditions
- 7.8.1.5 Mechanism and Kinetics of Ammonia Synthesis
- 7.8.2 Hydrogenation of Carbon Monoxide
 - 7.8.2.1 Thermodynamics
 - 7.8.2.2 Catalyst Preparation
 - 7.8.2.3 Methanation. Kinetics, Surface Science, Mechanisms
 - 7.8.2.4 Promotion of the Rates of C—O Bond Hydrogenation by the Oxide-Metal Interface
 - 7.8.2.5 Methanol Production. Kinetics, Surface Science, and Mechanisms
 - 7.8.2.6 Production of Higher-Molecular-Weight Hydrocarbons. Kinetics, Surface Science, and Mechanisms
 - 7.8.2.7 Formation of Oxygenated Hydrocarbons from CO and H₂ and Organic Molecules
- 7.8.3 Hydrocarbon Conversion on Platinum
 - 7.8.3.1 Introduction
 - 7.8.3.2 Structure Sensitivity of Hydrocarbon Conversion Reactions on Platinum Surfaces
 - 7.8.3.3 Carbonaceous Overlayers
 - 7.8.3.4 Catalysis on Top of a Strongly Adsorbed Overlayer
 - 7.8.3.5 Structure Modifiers
 - 7.8.3.5.1 Site Blocking by Sulfur
 - 7.8.3.5.2 Ensemble Effect in Alloy Catalysis and the Creation of New Sites by Alloys
 - 7.8.3.6 The Building of Improved Platinum and Other Metal Catalysts
- 7.9 Summary and Concepts
- 7.10 Problems

References

7.1 INTRODUCTION

In a surface catalytic process, the reaction occurs repeatedly by a sequence of elementary steps that includes adsorption, surface diffusion, the chemical rearrangements (bond breaking, bond forming, molecular rearrangement) of the adsorbed reaction intermediates and the desorption of the products.

Catalytic reactions play all important roles in our life. Most biological reactions that build the human body, as well as the reactions that control the functioning of the brain and other vital organs, are catalytic. Photosynthesis and the majority of chemical processes that are utilized in chemical technology are also catalytic reactions. These range from oil refining and the production of chemicals by hydrogenation, dehydrogenation, partial oxidation, and organic molecular rearrangements (isomerization, cyclization), to ammonia synthesis and fermentation. The chemical bonds that form during these processes that can turn over repeatedly are very differ-

ent from those that form during stoichiometric reactions that characterize the formation of the chemisorption bond.

7.1.1 Brief History of Surface Catalysis

In 1814 Kirchhoff reported that acids aid the hydrolysis of starch to glucose. The oxidation of hydrogen by air over platinum was observed by H. Davy (1817) and E. Davy (1820) as well as by Döbereiner (1823), who constructed a "tinderbox" to produce flame when a small dose of hydrogen generated by the reaction of zinc and hydrochloric acid reacts with air in the presence of platinum. His device sold handily in the early part of the 19th century when matches were not yet available. Platinum was also found to aid the oxidation of CO and ethanol (Döbereiner).

Faraday was the first to carry out experiments to explore why platinum facilitates the oxidation reactions of different molecules. He found that ethylene adsorption deactivates the platinum surface temporarily while the adsorption of sulfur deactivates platinum permanently. He measured the rate of hydrogen oxidation, suggested a mechanism, and observed its deactivation and regeneration. Thus, Faraday was the first scientist who studied catalytic reactions. In 1836 Berzelius [1, 2] defined the phenomenon and called it *catalysis* and suggested the existence of a "catalytic force" associated with the action of catalysts.

Catalyst-based technologies were introduced in the second half of the 19th century. The Deacon process $(2HCl + \frac{1}{2}O_2 + \stackrel{CuCl_2}{\longrightarrow} H_2O + Cl_2)$ was discovered in 1860, and the oxidation of SO_2 to SO_3 by platinum was discovered by Messel in 1875. Mond introduced the nickel-catalyzed reaction of methane with steam $(CH_4 + H_2O \stackrel{N_1}{\longrightarrow} CO + 3H_2)$. In the early 20th century, Ostwald developed the process of ammonia oxidation $(2NH_3 + \frac{5}{2}O_2 \stackrel{Pt}{\longrightarrow} 2NO + 3H_2O)$ to form nitric oxide, the precursor to nitric acid manufacture (1902); and in 1902, Sebatier developed a process for the hydrogenation of ethylene $(C_2H_4 + H_2 \stackrel{N_1}{\longrightarrow} C_2H_6)$. In 1905, Ipatieff used the catalytic action of clays to carry out different organic reactions: dehydrogenation, isomerization, hydrogenation, and polymerization.

Better understanding of thermodynamics established the limits of reaction rates in catalyzed reactions. A catalyst can bring a reaction closer to equilibrium but cannot produce molecules in excess of equilibrium concentrations. The ammonia synthesis from N₂ and H₂ became the reaction to provide the testing ground for both catalysis science and technology. The quality of the catalyst could be tested based on how closely chemical equilibrium could be attained. High-pressure reactors were designed to shift the chemical equilibrium during catalyzed ammonia production.

Catalyzed reactions of carbon monoxide and hydrogen were utilized to produce methanol (CO + 2H₂ CH₃OH) in 1923 and higher-molecular-weight liquid hydrocarbons by 1930. The production of motor fuels became one of the chief aims of catalysis during the 1930–1950 period. The cracking of long-chain hydrocarbons to produce lower-molecular-weight products was achieved over oxide catalysts composed mostly of alumina and silica. Acid-catalyzed alkylation reactions provided high-octane fuel and important organic molecules.

In the meantime, catalysis science was developed (1915–1940) through the efforts of Langmuir (sticking probability, adsorption isotherm, dissociative adsorption, role of monolayers). Emmett (surface area measurements, kinetics of ammonia synthe-

sis), Taylor (active sites, activated adsorption), Bonhoeffer, Rideal, Roberts, Polanyi, Farkas (kinetics and molecular mechanisms of ethylene hydrogenation, *orthopara* hydrogen conversion, isotope exchange, intermediate compound theories), and many others.

The discovery of abundant and inexpensive oil in Arabia in the early 1950s focused the development of catalytic processes to convert petroleum crude to fuels and chemicals. Oil and oil-derived intermediates (ethylene, propylene) became the dominant feedstocks.

Platinum (metal)- and acid (oxide)-catalyzed processes were developed to convert petroleum to high-octane fuels. Hydrodesulfurization catalysis removed sulfur from the crude to prevent catalyst deactivation. The discovery of microporous crystalline alumina silicates (zeolites) provided more selective and active catalysts for many reactions, including cracking, hydrocracking, alkylation, isomerization, and oligomerization. Catalysts that polymerize ethylene, propylene, and other molecules were discovered. A new generation of bimetallic catalysts that were dispersed on high-surface-area (100–400 m²/g) oxides was synthesized.

The energy crisis in the early 1970s renewed interest in chemicals and fuels, producing technologies using feedstocks other than crude oil. Intensive research was carried out utilizing coal, shale, and natural gas to develop new technologies and to improve on the activity and selectivity of older catalyst-based processes. Increasing concern about environmental quality led to the development of the catalytic converter for automobiles and to other, nitrogen-oxide-reducing catalysts.

Modern surface science developed during the same period and has been applied intensively to explore the working of catalysts on the molecular level, to characterize the active surface, and to aid the development of new catalysts for new chemical reactions. Indeed, surface science provided the means to explore the molecular structure and mechanisms of elementary reaction steps and to provide for rational design for modification of catalyst activity and selectivity. This was carried out usually by altering the structure of the surface and by using coadsorbed additives as bonding modifiers for reaction intermediates on the surface.

In this chapter we describe the important macroscopic and molecular concepts of surface catalysis that emerged from studies of recent decades. Then we shall review what is known about a few important catalytic reactions that provide case histories of the state of modern surface science of catalysis and of catalytic science.

7.2 CATALYTIC ACTION

One of the major functions of a catalyst is to aid in rapidly achieving chemical equilibrium for certain chemical reactions.

Two of the simpler, although important, reactions that demonstrate this type of catalytic action are the formation of water from oxygen and hydrogen (${}_{2}^{1}O_{2} + H_{2} \rightarrow H_{2}O$) and the formation of ammonia from hydrogen and nitrogen ($3H_{2} + N_{2} \rightarrow 2NH_{3}$). Water has a standard free energy of formation $\Delta G_{298}^{0} = -58$ kcal/mole (232 kJ/mole). Yet O_{2} and H_{2} gas mixtures may be stored indefinitely in a glass bulb without showing signs of any chemical reaction. Just by dropping a high-surface-area platinum gauze into the mixture, the reaction occurs instantaneously and explosively—as demonstrated to the delight of freshman chemistry students in the

introductory chemistry courses. The reason for this striking effect can be explained as follows. H₂ and O₂ have large activation energies for several of the elementary steps for the reaction in the gas phase. First, one of the diatomic molecules must be dissociated. Dissociation energies are very large compared with thermal energies, RT (103 kcal/mole (412 kJ/mole) for H₂ and 117 kcal/mole (468 kJ/mole) for oxygen [3]). The subsequent atom-molecule reactions (H + O_2 or H_2 + O) still require an activation energy of about 10 kcal/mole (40 kJ/mole) [4]. Thus the gasphase reaction is very improbable under any circumstances. In the presence of a properly structured platinum surface, however, both molecules dissociate to atoms with zero activation energies (2Pt + $H_2 \rightarrow 2Pt-H$, or 2Pt + $O_2 \rightarrow 2Pt-O$) [5, 6], as shown by low-pressure surface studies. In addition, the atom-atom or atommolecule reactions that subsequently take place on the surface have very low or no activation energies in contrast to that in the gas phase [5]. Thus the surface catalytic action involves its ability to atomize the large-binding-energy diatomic molecules by forming chemisorbed atomic intermediates and to lower the activation energy for the reaction on the surface that follows.

Similarly, the synthesis of ammonia from dinitrogen and hydrogen ($N_2 + 3H_2 \rightarrow 2NH_3$) required the "activation" of the N-N bond to dissociate the molecule. The nitrogen atoms that form then must react with hydrogen atoms or molecules to produce NH₃. The very large dissociation energy of N_2 ($\Delta E = 280$ kcal/mole or 1120 kJ/mole) makes it virtually impossible for this reaction to occur in the gas phase. On an iron surface, however, N_2 dissociates on a properly structured surface [the (111) crystal face, for example] with a small activation energy (3 kcal or 12 kJ/mole). This is the key initiation step for the catalytic reaction. Iron also readily atomizes the hydrogen molecules. The chemisorbed nitrogen atoms then react with hydrogen atoms on the surface to produce NH, NH₂, and finally NH₃ molecules that desorb into the gas phase.

7.2.1 Kinetic Expressions

Catalysis is a kinetic phenomenon; we would like to carry out the same reaction with an optimum rate over and over again using the same catalyst surface. Therefore, in the sequence of elementary reactions leading to the formation of the product molecule, the rate of each step must be of steady state. Let us define the catalytic reaction turnover frequency, \mathcal{J} , as the number of product molecules formed per second. Its inverse, 1/3, yields the turnover time, the time necessary to form a product molecule. By dividing the turnover frequency by the catalyst surface area, α , we obtain the specific turnover rate, \Re (molecules/cm²/sec) = \Im/\Re (\Re often called the turnover frequency also, in the literature). This type of analysis assumes that every surface site is active. Although the number of catalytically active sites could be much smaller (usually uncertain) than the total number of available surface sites, the specific rate defined this way gives a conservative lower limit of the catalytic turnover rate. If we multiply \Re by the total reaction time, δt , we obtain the turnover number, the number of product molecules formed per surface site. A turnover number of one corresponds to a stoichiometric reaction. Because of the experimental uncertainties, the turnover number must be on the order of 10² or larger for the reaction to qualify as catalytic.

While the turnover number provides a figure of merit for the activity of the cat-

alyst sites, the reaction probability RP reveals the overall efficiency of the catalytic process under the reaction conditions. The reaction probability is defined as

$$RP = \frac{\text{rate of formation of product molecules}}{\text{rate of incidence of reactant molecules}}$$
(7.1)

RP can be readily obtained by dividing \Re by the rate of molecular incidence F which is obtained from the kinetic theory expression $F = P/(2\pi MRT)^{1/2}$.

The specific catalytic reaction rate \Re can often be expressed as the product of the rate constant k and a reactant pressure (or concentration)-dependent term

$$\Re = k \times f(P_i) \tag{7.2}$$

where P_i is the partial pressure of the reactants. The rate constant for the overall catalytic reaction may contain the rate constants of many of the elementary reaction steps that precede the rate-determining step. Because the slowest rate-reaction step may change as the reaction conditions vary (temperature, pressure, relative surface concentrations of reactants, catalyst structure), k may also change to reflect the changing reaction mechanism. Nevertheless, k can be defined using the Arrhenius expression

$$k = A \exp\left(-\frac{\Delta E^*}{RT}\right) \tag{7.3}$$

where A is the temperature-independent preexponential factor and ΔE^* is the apparent activation energy measured under the catalytic reaction conditions.

Ranges of turnover rates for hydrocarbon reactions are shown in Figure 7.1. Turnover rates between 10^{-4} and 100 are used in the various technologies, and thus the temperature employed is adjusted to obtain the desired rates. The more complex isomerization, cyclization, dehydrocyclization, and hydrogenolysis reactions have activation energies ΔE^* in the range of 35-45 kcal/mole (140-180 kJ/mole); and thus according to the Arrhenius expression for the rate constant k, k = A exp $(-\Delta E^*/RT)$, high temperatures are required to carry them out at the desired rates. Hydrogenation reactions have activation energies of 6-12 kcal/mole (24-28 kJ/mole) and therefore may be performed at high rates at 300 K or below. Thus, there are at least two classes of reactions distinguishable by their very different activation energies that may be carried out at high and at low temperature, respectively, under very different experimental conditions.

The rates of surface catalyzed reactions are usually measured by monitoring the concentrations of reactants and products as a function of time under steady-state conditions. Such studies tell us relatively little about the elementary surface reaction steps. Dynamic methods that alter the flow of reactants or introduce pulses of isotopically labeled reacting species have been useful to distinguish between reacting intermediates and adsorbed spectator species on surfaces. These investigations are carried out by following changes of the concentrations of adsorbates beginning when changes in flow rate commence, as a function of time, and by monitoring the time-dependent changes in the concentrations of isotopically labeled product molecules.

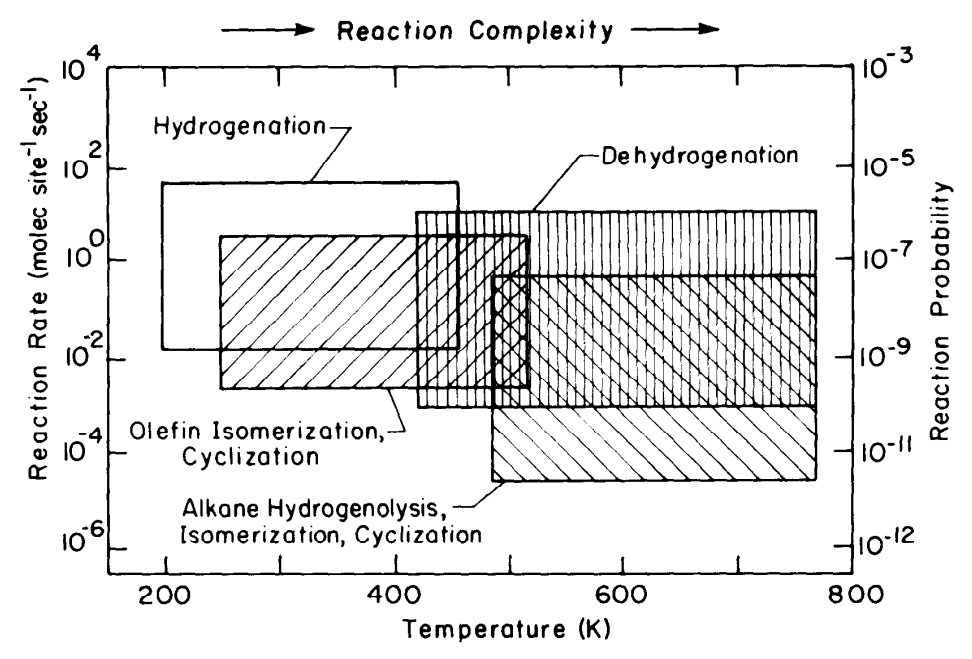


Figure 7.1. Block diagram of hydrocarbon conversion over platinum catalysts showing the approximate range of reaction rates and temperature ranges that are most commonly studied.

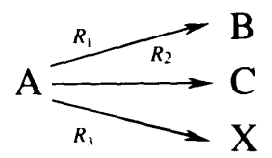
7.2.2 Selective Catalysis

A good catalyst is also selective and permits the formation of only one type of product when reactions may occur along several reaction paths. CO and H₂ react to produce methane (CH₄) exclusively when nickel is used as a catalyst, whereas only methanol (CH₃OH) is formed when the catalyst is copper and zinc oxide. The reaction of *n*-hexane in the presence of excess hydrogen can produce benzene, cyclic molecules, branched isomers, or shorter-chain species as shown in Figure 7.2. A selective catalyst will produce only one of these products.

In more general terms, catalyzed reactions involve either (a) successive kinetic steps leading to the final product or (b) alternative, simultaneous reaction paths yielding two or more products. The former reaction scheme may be represented by

$$A \xrightarrow{R_1} B \xrightarrow{R_2} C \tag{7.4}$$

and a good example is the stepwise dehydrogenation of cyclohexane to cyclohexene and then to benzene. When two or more parallel reaction paths are operative as is the case during n-hexane conversion, the reaction scheme is



We define the fractional catalytic selectivity, S_i , as the fraction of reacting mol-

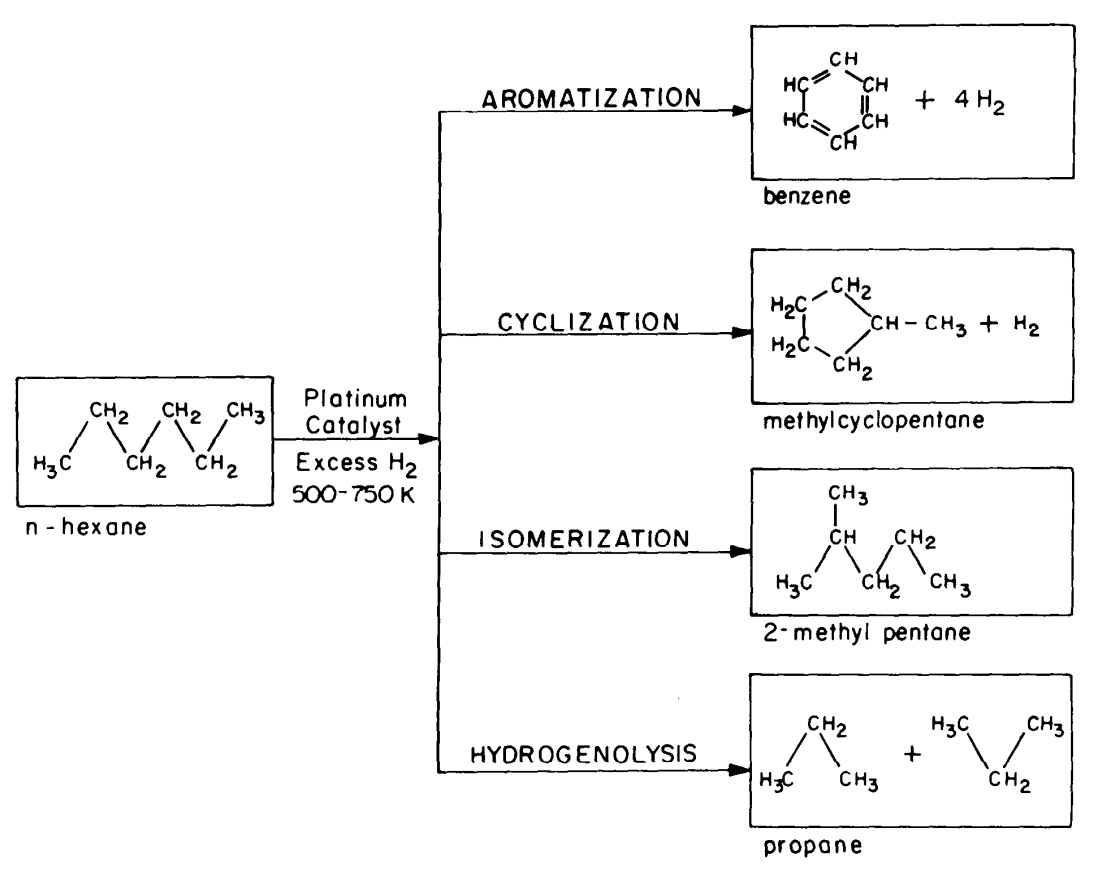


Figure 7.2. Various organic molecules that can all be produced by the catalyzed reactions of *n*-hexane [188].

ecules which are converted along a specified pathway

$$S_j = \frac{R_j}{\sum_{i=1}^n R_i} \tag{7.5}$$

An additional possibility is provided by competitive parallel reactions

$$A \xrightarrow{R_1} B \qquad (7.6)$$

$$X \longrightarrow Y \qquad (7.7)$$

$$X \longrightarrow Y \tag{7.7}$$

Here the ratio of rates, R_1/R_2 , defines the kinetic selectivity. The activity (rate) and the selectivity are the key parameters of any catalytic reaction.

7.2.3 Tabulated Kinetic Parameters for Catalytic Reactions

A great deal of kinetic information has been obtained for different types of catalyzed hydrocarbon reactions carried out over metal catalyst surfaces. These reactions include dehydrogenation, hydrogenation, hydrogenolysis and cracking, ring opening, dehydrocyclization, and isomerization. The kinetic parameters for these reactions are listed in Tables 7.1 to 7.41. In these tables the catalyst systems that were used are listed together with the temperature range of the investigation. Because these reactions are always carried out in the presence of hydrogen, both the hydrocarbon and hydrogen concentrations (in molecules/cm³) are tabulated in a logarithmic form. These exponents are also displayed whenever they were determined. From these data the changes of the reaction rates with reactant concentrations can be determined. The rate of reaction at a given temperature, in the range used in the experimental study, is also calculated and listed, together with the apparent activation energy for the reaction, ΔE^* , and the logarithm of the preexponential factor, $\ln A$. From the rate and reactant concentrations a reaction probability (RP) can be calculated. This is also displayed in Tables 7.1 to 7.41 for the various catalytic reactions, as $-\ln$ RP. Fractional selectivities, S, are also supplied when reported. These are defined as the ratio of the rate of the specific reaction to the total reaction rate.

There is a great deal of scatter in the kinetic parameters obtained for a given reaction on different catalyst systems. This is expected, since the structure and bonding characteristics of the different metal catalysts vary widely. Nevertheless, several conclusions may be reached from the inspection of the data. The reaction probabilities are very low under the conditions where these reactions were carried out. They range from 10^{-8} to 10^{-5} for hydrogenation to 10^{-12} to 10^{-8} for most of the other reactions. The apparent activation energies are the lowest for hydrogenation and cyclopropane ring opening, 9-15 kcal/mole (36-60 kJ/mole). For dehydrogenation of cyclohexane and for the hydrogenolysis of C_4 to C_6 alkanes, ΔE^* is in the range 16-25 kcal/mole (64-100 kJ/mole). For most of the other reactions, which include (a) hydrogenolysis (the most frequently studied reaction) of ethane, propane, and other alkanes, (b) cracking of olefins and benzene, (c) dehydrogenation of alkanes, and (d) isomerization of C_5 to C_6 hydrocarbons, the apparent activation energies are in the range 25-50 kcal/mole (100-200 kJ/mole).

The kinetic information displayed in Tables 7.1 to 7.41 can be useful in establishing the optimum reaction conditions and catalyst systems. It is hoped that reliable kinetic parameters will become available for many other important catalyzed hydrocarbon reactions in the near future.

7.3 CATALYST PREPARATION, DEACTIVATION, AND REGENERATION

7.3.1 Catalyst Preparation

The higher the active surface area of the catalyst, the greater the number of product molecules produced per unit time. Therefore, much of the art and science of catalyst preparation deals with high-surface-area materials. Usually materials with 100- to $400\text{-m}^2/g$ surface area are prepared from alumina, silica, or carbon; and more recently other oxides (Mg, Zr, Ti, V oxides), phosphates, sulfides, or carbonates have been used. These are prepared in such a way that they are often crystalline with well-defined microstructures and behave as active components of the catalyst system in spite of their accepted name "supports." Transition-metal ions or atoms are then deposited in the micropores, which are then heated and reduced to produce small metal particles $10\text{--}10^2$ Å in size with virtually all the atoms located on the surface

(unity dispersion). The surface structure of the metal particles can often be controlled by the method of preparation. Usually more than one metal component is used, with bimetallic systems being the most popular in recent years. Frequently another oxide (e.g., TiO₂) is dispersed on the high-surface-area oxide (alumina) to impart unique catalytic properties as well. Additives [7] that are usually electron donors (alkali metals) or electron acceptors (halogens) are adsorbed on the metal or on the oxide to act as bonding modifiers for the coadsorbed reactants (see Chapter 4). This complex and intricately fabricated catalyst system is used for hundreds or thousands of hours and often millions of turnovers to produce the desired molecules at high rates and selectivity before their deactivation.

7.3.2 Catalyst Deactivation

Catalysts live long and active lives, but they do not last forever. The type of supported metal catalysts that are used in petroleum refining produces in the range of 200-800 barrels of products per pound of catalyst (1 barrel = 42 gallons). Once the catalyst is deactivated, it is either regenerated or replaced. There can be many reasons for the deactivation. At the operating temperatures some of the reactant hydrocarbons may completely decompose and deposit a thick layer of inactive carbon on the catalyst surface (coke). For many catalysts the deactivation is slow enough that they are used in steady-state operation. The liquid or gaseous reactants are passed through the catalyst with a well-defined "space velocity" that is normally measured as the weight hourly space velocity (WHSV)—that is, the pound of liquids or gas passed over the unit weight of catalyst per hour. For other active catalysts, deactivation is so rapid that they are used in a cyclic fashion; the reactors "swing" between running the catalytic reactions and regenerating. Thus understanding the causes of deactivation and developing new catalysts that are more resistant to "poisoning" are constant concerns of the catalytic chemist.

Many of the catalyst poisons act by blocking active surface sites. In addition, poisons may change the atomic surface structure in a way that reduces the catalytic activity. Sulfur, for example, is known to change the surface structure of nickel [8]. By forming chemical bonds of different strengths on the different crystal planes, it provides a thermodynamic driving force for the restructuring of the metal particles. Sometimes the rate of deactivation of metal catalysts by small concentrations of sulfur can indeed be dramatic. The automobile catalytic converter necessitated the removal of tetraethyl-lead from gasoline, one of the best antiknocking agents, because it readily poisoned the Pt-Pd catalyst by depositing lead sulfate on the noblemetal surfaces. One of the major causes of deactivation in crude oil cracking catalysts is the deposition on the catalyst surface of metallic impurities that are present as compounds in the reactant mixture. Vanadium- and titanium-containing organometallic compounds decompose and not only deactivate the catalyst surface but often plug the pores of the high-surface-area supports, thereby impeding the reactant-catalyst contact during petroleum refining.

A freshly prepared catalyst may not exhibit optimum catalytic activity upon its first introduction into the reactant stream. There may be efficient but undesirable side reactions that need to be eliminated. For this purpose a small amount of "poison" is often added to the reaction mixture or introduced in the form of pretreatment. Thus deactivating impurities may also be used, in small quantities, to improve the selectivity of the working catalyst.

7.3.3 Catalyst Regeneration

The regeneration treatment of the catalyst depends on the causes of deactivation. Most frequently, carbon deposition is the primary source of deactivation during hydrocarbon conversion reactions. In this circumstance, heating the spent catalyst in air or in oxygen burns off the carbon. The heat generated in this exothermic combustion reaction can be used beneficially in the overall catalytic process. Sintering of catalyst particles due to exposure to high temperatures for extended periods leads to loss of surface area. Oxygen can often oxidize the metal component of the catalyst to alter the shape and size of the metal particles. Metal oxides have lower surface energy than metals, and therefore oxidation could lead to better "wetting" of the high-surface-area oxide support. Subsequent reduction of the metal oxides in hydrogen may lead to redispersion of the metal constituent as small particles with increased total surface area. Additives such as chlorine that may form volatile metal halides can also help the redispersion of some of the catalyst components.

At high enough temperatures the micropores of the high-surface-area catalyst may collapse by sintering or melting. It is therefore essential that the materials chemistry be understood and that compounds with the proper surface and bulk thermodynamic properties be chosen to maintain their thermal stability under diverse (oxidizing or reducing) reaction conditions.

The removal of impurities that deposit from the reactant mixture poses particular challenge. Sulfur, arsenic, phosphorous, and vanadium are often deposited during oil refining. The reader is referred to publications that deal with these special problems of catalyst deactivation and regeneration (e.g., see references [9, 10]).

7.4 METAL CATALYSIS

Transition metals and their compounds, oxides, sulfides, and carbides are uniquely active as catalysts, and they are used in most surface catalytic processes. The effective-medium theory of the surface chemical bond (Chapter 6) emphasizes the dominant contribution of d-electrons to bonding of atoms and molecules at surfaces. Other theories [11] also point out that d-electron metals in which the d-bond is mixed with the s and p electronic states provide a large concentration of low-energy electronic states and electron vacancy states. This is ideal for catalysis because of the multiplicity of degenerate electronic states that can readily donate or accept electrons to and from adsorbed species. Those surface sites where the degenerate electronic states have the highest concentrations are most active in breaking and forming chemical bonds. These electronic states have high charge fluctuation probability (configurational and spin fluctuations) especially when the density of electron vacancy or hole states is high.

7.4.1 Trends Across the Periodic Table

One prediction of these theoretical models is that the heat of chemisorption of atoms should increase from right to left in the periodic table. This trend is well-documented in Chapter 6, and there is good agreement between experiments and theory. Thus, one of the important functions of transition metals in catalytic reactions is to atomize

diatomic molecules and then to supply the atoms to other reactants and reaction intermediates. H₂, O₂, N₂, and CO are the diatomic molecules of importance, in order of increasing bond energy. The strength of bonding of hydrogen, carbon, nitrogen, and oxygen atoms on transition-metal surfaces provides the thermodynamic driving force for the atomization and for the release of atoms for reactions with other molecules. If the surface bonds are too strong, the reaction intermediates block the adsorption of new reactant molecules because of their long surface residence times and the reaction stops. For too weak adsorbate-surface bonds, the necessary bondscission processes may be absent. Hence the catalytic reaction will not occur. A good catalyst is thought to be able to form chemical bonds of intermediate strength. These bonds should be strong enough to induce bond dissociation in the reactant molecules. However, the bond should not be too strong, thereby ensuring only short residence times for the surface intermediates and rapid desorption of the product molecules so that the reaction can proceed with a large turnover number.

These considerations are strikingly demonstrated by the volcano-shaped pattern of variation of catalytic activity as shown schematically in Figure 7.3. While the heat of adsorption is steadily decreasing from left to right, the catalytic reaction rates peak at the group VIII metals in the periodic table. Figure 7.3 shows the pattern of variation of catalytic reaction rates across the series of transition metals Re, Os, Ir, Pt, and Au for the hydrogenolysis of the C-C bond in ethane, the C-N bond in methylamine, and the C-Cl bond in methyl chloride.

The influence of the electronic structure of surface atoms show up not only in producing the volcano-shaped trends of transition metal catalytic activity across the periodic table, but also in producing the structure sensitivity of certain catalytic reactions on a given transition metal. A catalytic reaction is defined as *structure-sensitive* if the rate changes markedly as the particle size of the catalyst is changed. Reaction studies on single crystals revealed the importance of steps of atomic height and of kinks in the steps in increasing reaction rates for H_2/D_2 exchange, for dehydrogenation and hydrogenolysis. Theoretical studies indicate large changes in the local density of electronic states at the surface defect sites that correlate with changes in catalytic activity.

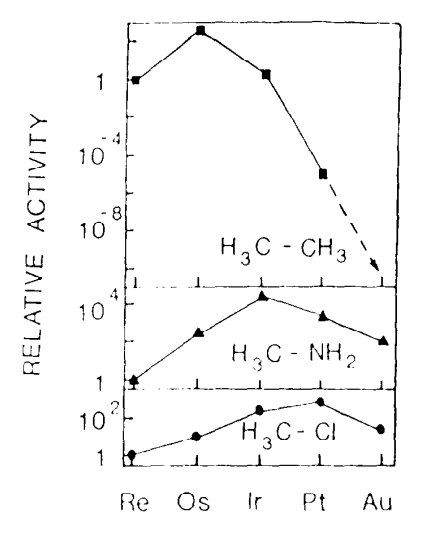


Figure 7.3. Catalytic activities of transition metals across the periodic table [188] for the hydrogenolysis of the C-C bond in ethane, the C-N bond in methylamine, and the C-Cl bond in methyl chloride.

7.4.2 Some Frequently Used Concepts of Metal Catalysis

During the operation of complex catalyst systems, several macroscopic experimental parameters have been uncovered that provide useful practical information about the nature of the catalyst or the catalyzed surface reaction. A catalytic reaction is defined to be *structure-sensitive* if the rate changes markedly as the particle size of the catalyst changes [12]. Conversely, the reaction is *structure-insensitive* on a given catalyst if its rate is not influenced appreciably by changing the dispersion of the particles under the usual experimental conditions. In Table 7.42 we list several reactions that belong to these two classes. Clearly, variations of particle size give rise to changes of atomic surface structure. The relative concentrations of atoms in steps, kinks, and terraces are altered. Nevertheless, no quantitative correlation has been made to date between variations of macroscopic particle size and the atomic surface structure.

During the development of mechanistic interpretations of catalytic reactions using the macroscopic rate equations that were determined by experiments, two types of reaction models found general acceptance. In one of them the rate-determining surface reaction step involves interaction between two atoms or molecules, both in the adsorbed state. This reaction model is called the *Langmuir-Hinshelwood* mechanism [13, 14]. In the other the rate-determining reaction step involves a chemical reaction between a molecule from the gas phase and one in the adsorbed state. This is called the *Rideal-Eley* mechanism [15]. Most reactions have rate equations that fit the first of these two mechanisms. Recently, the oxidation of CO has been identified by molecular-scale studies as obeying the Langmuir-Hinshelwood reaction mechanism [16]. However, correlation of these reaction mechanisms (suggested by inspection of the macroscopic rate equations) with molecular-level studies of the elementary surface reactions remains one of the future challenges of catalysis.

During studies of a given catalyzed reaction over catalysts that were prepared in different ways, an interesting phenomenon was found, called the *compensation effect* [17]. Using the Arrhenius expression for the rate constant, both the preexponential factor and the activation energy for the reaction were found to have varied greatly from catalyst to catalyst. However, they varied in such a way as to compensate each other, so that the rate constant (or the reaction rate under the same conditions of pressure and temperature) remained almost constant. For example, for the methanation reaction (that is, the hydrogenation of CO), the following empirical relationship was found to hold between A and ΔE^* :

$$\ln A = \alpha + \frac{\Delta E^*}{R\Theta} \tag{7.8}$$

where α is a constant and Θ is called the *isokinetic temperature*, at which the rates on all the catalysts are equal. For the methanation reaction [18], $\alpha \approx 0$ and $\Theta = 436$ K. Thus $\ln A_{\text{CH}_4} \approx 1.1 \Delta E^*$ kcal/mole. Figure 7.4 shows the compensation effect for the methanation reaction for eight different metal catalysts. The $\ln A_{\text{CH}_4}$ versus ΔE^* plots yield a straight-line relationship. Figure 7.5 shows the compensation effect for the hydrogenolysis reactions whose rates are displayed in Figure 7.3.

The compensation effect has been rationalized in a variety of ways. It is thought

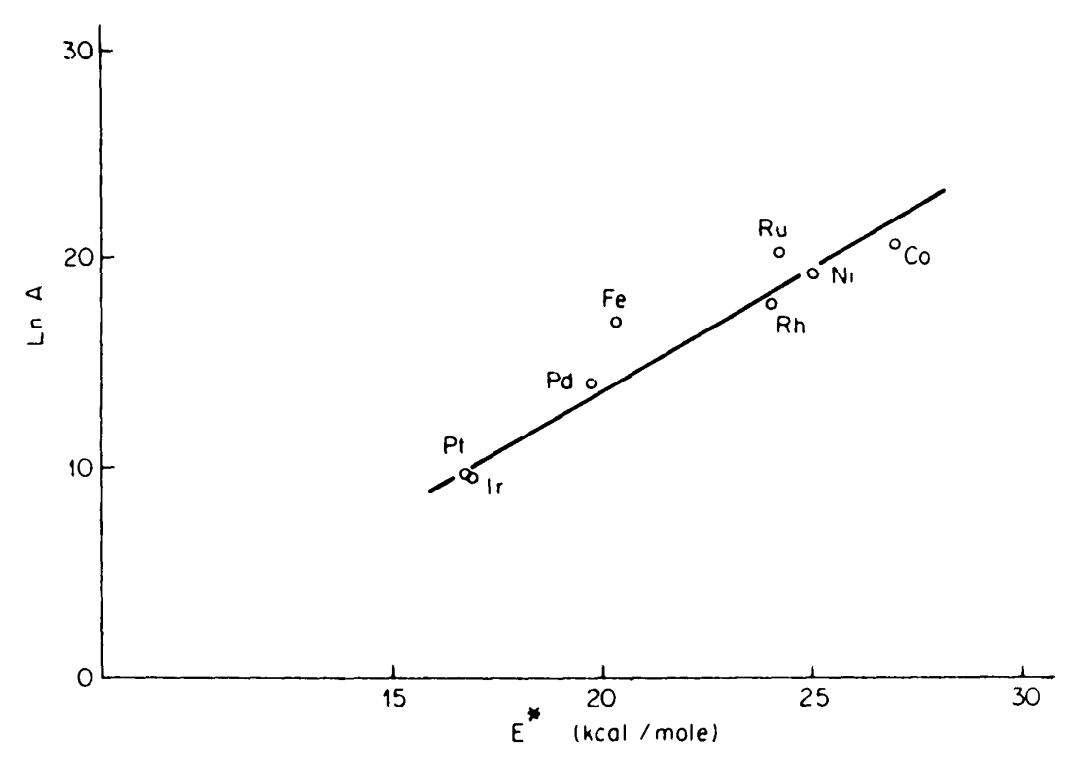


Figure 7.4. Compensation effect for the methanation reaction. The logarithm of the preexpontial factor is plotted againt the apparent activation energy, ΔE^* , for this reaction over several transition-metal catalysts [18].

that one catalyst may have a large concentration of active sites where the reaction requires a high activation energy, while the other catalyst, which is prepared differently, has a small concentration of active sites that have low activation energies for the same surface reaction. An atomic-level explanation of the compensation effect remains the task of scientists in the future.

During most reactions, the surface of the active metal catalyst is covered with a strongly chemisorbed overlayer that remained tenaciously bound to the surface for 10^2-10^6 turnovers. During hydrocarbon reactions, this is a carbonaceous overlayer with a composition of about $(H/C) \approx 1$, during ammonia syntheses it is chemisorbed nitrogen, and during hydrodesulfurization it is a mixture of sulfur and carbon. It is believed that this overlayer may play a role in restructuring the surface to create new active sites and in altering the bonding of reactants, intermediates, and prod-

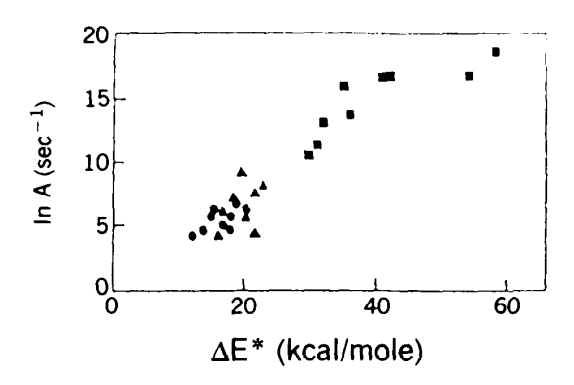


Figure 7.5. Compensation effect for the hydrogenolysis reaction. The logarithm of the preexponential factor is plotted against the apparent activation energy, ΔE^* , for this reaction over several transition-metal catalysts. The squares, triangles, and circles represent values for ethane, methylamine, and methyl chloride hydrogenolysis, respectively [188].

ucts. However, more experimental evidence is needed before the precise role of these strongly held surface deposits can be identified.

Structure modifiers and bonding modifiers are often introduced as important additives when formulating the complex catalyst systems. Structural promoters can change the surface structure that is often the key to catalyst selectivity. Aluminum oxide facilitates the restructuring of iron in the presence of nitrogen to produce surfaces that are most active during ammonia synthesis. Alloy components may not participate in the reaction chemistry but modify structure and site distribution on the catalyst surface. Site blocking could improve selectivity as has been proven for many working catalyst systems. Sulfur and silicon or other strongly adsorbed atoms that seek out certain active sites can block undesirable side reactions.

Bonding modifiers are employed to weaken or strengthen the chemisorption bonds of reactants and products. Strong electron donors (such as potassium) or electron acceptors (such as chlorine) that are coadsorbed on the catalyst surface are often used for this purpose. Alloying may create new active sites (mixed metal sites) that can greatly modify activity and selectivity. New catalytically active sites can also be created at the interface between the metal and the high-surface-area oxide support. In this circumstance the catalyst exhibits the so-called strong metal-support interaction (SMSI). Titanium oxide frequently shows this effect when used as a support for catalysis by transition metals. Often the sites created at the oxide-metal interface are much more active than the sites on the transition metal.

7.5 CATALYSIS BY IONS AT SURFACES. ACID-BASE CATALYSIS

Most surface reactions and the formation of surface intermediates involve charge transfer—either an electron transfer or a proton transfer. These processes are often viewed as modified acid-base reactions. It is common to refer to an oxide catalyst as acidic or basic according to its ability to donate or accept electrons or protons [19].

The electron transfer capability of a catalyst is expressed according to the Lewis definition. A surface site capable of receiving a pair of electrons from the adsorbate is a Lewis acid. A site having a free pair of electrons that can be transferred to the adsorbate is a Lewis base. The acidity of metal ions of equal radius increases with the increasing charge of the metal ions: $Na^+ < Ca^{2+} < Y^{3+} < Th^{4+}$. The strength of the Lewis acidity is measured by determining the binding energies of the charge-transfer complexes that form by this type of electron-transfer process.

The proton-transfer capability of a catalyst is expressed according to the Brønsted definition. A surface site capable of losing a proton to the adsorbate is a Brønsted acid. A site that can accept a proton from the adsorbed species is a Brønsted base. The Brønsted acidity of the catalyst is usually determined by ion exchange from solution (surface proton is substituted by alkali ions Li⁺, Na⁺, etc.) or by the adsorption of weak acids or bases, such as phenol and pyridine, or the surface. In this way the proton-transfer ability of the surface can be titrated. The Brønsted acidity for oxides has also been related to the metal—oxygen bond energies. In general, the acidity increases with an increase of charge on the metal ion. In the series of oxides Na₂O, CaO, MgO, Ag₂O, BeO, Al₂O₃, CdO, ZnO, SnO, H₂O, B₂O₃, FeO, SiO₂,

Ca₂O₃, Fe₂O₃, P₄O₆, SnO₂, GeO₂, TiO₂, SO₂, N₂O₅, and Cl₂O₇, those that are to the left of water are bases, and those to the right are acids [19].

7.5.1 Acid Catalysis in Solutions

In aqueous solutions of acids the hydronium ion H_3O^+ has been identified as a proton donor. Undissociated acids in high concentrations of acid solutions, HF for example, can also act as proton donors. The stronger the acid, the more active the catalyst. This acid strength is related to the dissociation constant of the acid, K_{HA} :

$$K_{\rm HA} = \frac{a_{\rm H} + a_{\rm A}}{a_{\rm HA}} \tag{7.9}$$

where $a_{\rm H^+}$, and $a_{\rm A^-}$, and $a_{\rm HA}$ are the activities of the ionic and undissociated species, respectively. The rate of acid-catalyzed reactions can be represented by the Brønsted relation

$$\ln k = \alpha \ln K_{\rm HA} + {\rm const.} \tag{7.10}$$

where k is the second-order rate constant for the reaction and α is a constant with a value between 0 and 1. The Brønsted relation is one of the so-called free energy relations encountered in physical organic chemistry that relate the kinetic parameters of a reaction (the rate constant, for example) to an equilibrium constant.

In concentrated strong acid solutions there can be many different proton donors. A useful function, the Hammett acidity function measures the tendency of the solution to donate a proton to a neutral base, B (e.g., a neutral organic molecule). The protonation of the base can be expressed as

$$H^+ + B \leftrightharpoons BH^+ \tag{7.11}$$

The dissociation equilibrium constant of BH⁺ can be written as

$$K_a = \frac{a_{\rm H} + a_{\rm B}}{a_{\rm RH} +} = \frac{a_{\rm H} + \gamma_{\rm B}}{\gamma_{\rm RH} +} \cdot \frac{C_{\rm B}}{C_{\rm RH} +}$$
 (7.12)

where γ_B , γ_{BH^+} , and C_B , C_{BH^+} are the activity coefficients and the concentrations of the neutral and the protonated base, respectively. C_B/C_{BH^+} can be measured experimentally. The negative logarithm of K_a defines the Hammett acidity function H_0 as

$$-\log K_a = pK_a = H_0 + \log \frac{C_{\rm BH}^+}{C_{\rm B}}$$
 (7.13)

The H_0 values for aqueous solutions for several strong acids are given in Figure 7.6. There are acids with values of the Hammett acidity function of -20 or less; these are called *superacids* because the H_0 value for pure H_2SO_4 is only -12. These

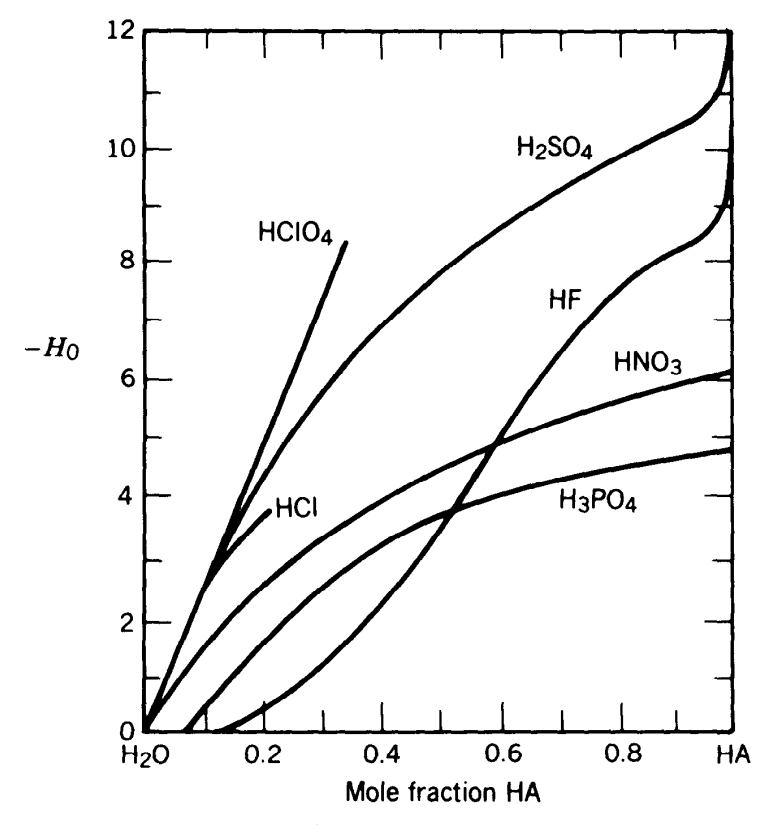


Figure 7.6. The Hammett acidity function, H_0 , for several acids as a function of their mole fraction in aqueous solution [189].

extremely strong acids can be formed from the combination of Lewis and Brønsted acids. These include:

Brønsted Acid	Lewis Acid
HF	BF_3
HF	SbF ₅
FSO ₃ H	SbF ₅

The great proton donor strength of superacids is due to the stabilization of the protonated forms of the Brønsted acid in an ion pair; $H_2F^+SbF_6^-$ for example.

7.5.2 Solid Acids

There are solid acids with Hammett acidity functions that are greater than sulfuric acid and similar to that of the superacids. Many of these are alumina silicates (commonly called zeolites), which are among the most common minerals in nature. The acid strength of these materials often depends on the Si/Al ratio. The aluminum ion, having one less valence electron than the silicon ion, has high electron affinity, thereby stabilizing a proton (Brønsted acid) near the AlO₄ tetrahedra by weakening the O-H bond in the hydrogen-form zeolite:

When this material is heated to high temperatures, water is driven off and coordinately unsaturated Al³⁺ ions are formed; these are strong electron-acceptor Lewis acid sites.

Very high internal surface area zeolites $(10^2 \text{m}^2/\text{g})$ can be synthesized with controlled pore sizes of 8-20 Å and controlled acidity [(Si/Al) ratio]. These find applications in the cracking and isomerization of hydrocarbons that occur in a shape-selective manner as a result of the uniform pore structure and are the largest-volume catalysts utilized in petroleum refining at present [20]. They are also the first of the "high-technology" catalysts where the chemical activity is tailored by atomic-scale study and control of the internal surface structure and composition.

7.5.3 Carbenium Ion Reactions

Hydrocarbons may be viewed as weak bases that can be protonated by strong acids to form carbenium ions. For an olefin this reaction may be written as

$$R-CH=CH-R' + H^+ = R-CH_2-CH-R'$$
 (7.14)

Tertiary carbenium ions are more stable than secondary ions, which are more stable than primary ions:

$$R_3C - \overset{+}{C} - CR'_3 > R_3C - \overset{+}{C}H - CR'_2 > R_3C - CH_2 - \overset{+}{C}H_2$$
 (7.15)

Isomerization, carbon-carbon bond scission (cracking), and carbon-carbon bond formation (alkylation) are among the most important hydrocarbon conversion reactions catalyzed by acids. Zeolites are often used to carry out these reactions during the refining of petroleum. Some of the zeolites are particularly active to convert olefins and cycloparaffins to paraffins and aromatics to produce jet fuel and gasoline.

7.6 MOST FREQUENTLY USED CATALYST MATERIALS

It may be instructive to review how widely catalysts are applied in the various technologies and to identify some of the most frequently used materials. There are three major areas of catalyst application at present [21]: automotive [22, 23], fossil-fuel refining, and production of chemicals. Table 7.43 lists the chemical processes that are the largest users of heterogeneous catalysts and the catalyst systems that are employed most frequently at present.

The automotive industry uses mostly noble metals (platinum, rhodium, and palladium) for catalytic control of car emissions: unburned hydrocarbons, CO, and NO. These highly dispersed metals are supported on oxide surfaces, and the catalyst system is specially prepared to be active at the high space velocities of the exhaust gases and over a wide temperature range. In petroleum refining, zeolites are most widely used for cracking of hydrocarbon in the presence of hydrogen. The important hydrodesulfurization process uses mostly sulfides of molybdenum and cobalt on an alumina support. The "reforming" reactions to produce cyclic and aromatic molecules and isomers from alkanes to improve the octane number are carried out mostly over platinum or platinum-containing bimetallic catalysts, such as Pt-Re and Pt-Sn. Sulfuric and hydrofluoric acids are the catalysts for alkylation. In the chemical technologies, steam reforming of natural gas (mostly methane) to produce hydrogen and CO is an important large-volume catalytic process. The purified natural gas is reacted with steam to form CO and H₂, mostly over supported nickel catalyst. The water-gas shift reaction (CO + $H_2O \rightarrow CO_2 + H_2$) is then employed to produce more hydrogen. The most frequently used catalyst for this purpose is iron-based. Methanol is produced from CO and H_2 , and ammonia is produced from H_2 and N_2 . Copper oxide and zinc oxide are also used for the shift reaction, as well as for the production of methanol from CO and H₂. Nickel is the catalyst for methanation from CO and H₂, and iron is the major catalyst for the ammonia synthesis.

Catalytic hydrogenation processes primarily use nickel and palladium as catalysts. Hydrogenation of nitrile groups to amines and various edible and inedible oils for the preparation of margarine, salad oils, and stearine are some of the major applications. Selective hydrogenation of olefins is also an important catalytic process. Among the larger-volume oxidation reactions, the oxidation of ammonia to nitric oxide to produce nitric acid uses noble metals: Pt, Pt-Rh, and Pt-Pd-Rh. The oxidation of SO₂ to SO₃ to produce sulfuric acid uses mostly vanadium oxide as catalyst. Ammoxidation, which makes acrylonitrile from propylene, oxygen and ammonia uses bismuth and molybdenum oxides as catalysts. Oxychlorination to make vinyl chloride from acetylene and HCl uses copper chloride as a catalyst. Polymerization reactions of ethylene and propylene are catalyzed by titanium trichloride, aluminum alkyls, chrome oxide on silica, and peresters. While these are the catalysts that are used in the largest quantity, many other highly selective catalysts serve as the basis of entire chemical technologies. In fact, the value of a very selective catalyst that aids a complex chemical transformation and the production of precious lifesaving pharmaceuticals is without compare.

Most of the catalysts employed in the chemical technologies are heterogeneous. The chemical reaction takes place on surfaces, and the reactants are introduced as gases or liquids. Homogeneous catalysts, which are frequently metalloorganic molecules or clusters of molecules, also find wide and important applications in the chemical technologies [24]. Some of the important homogeneously catalyzed processes are listed in Table 7.44. Carbonylation, which involves the addition of CO and H_2 to a C_n olefin to produce a C_{n+1} acid, aldehyde, or alcohol, uses rhodium and cobalt complexes. Cobalt, copper, and palladium ions are used for the oxidation of ethylene to acetaldehyde and to acetic acid. Cobalt(II) acetate is used mostly for alkane oxidation to acids, especially butane. The air oxidation of cyclohexane to cyclohexanone and cyclohexanol is also carried out mostly with cobalt salts. Further oxidation to adipic acid uses copper(II) and vanadium(V) salts as catalysts. The

hydrocyanation of butadiene to adiponitrile uses zero-valent nickel complexes. Polymerization technologies also frequently use homogeneous catalysts. The manufacture of polyethylene terephthalate uses antimony salts, and the copolymerization of ethylene and propylene to produce rubber uses alkylvanadium compounds.

7.7 SURFACE-SCIENCE APPROACH TO CATALYTIC CHEMISTRY

The purpose of surface-science studies of heterogeneous catalyst systems is to understand how they work on the atomic scale. One aims to identify the active sites where bond breaking and rearrangement take place and to detect surface intermediates that form. Studies are conducted to determine how the atomic surface structure and surface composition determine activity and selectivity. Once such an atomic-scale understanding is obtained, more active and selective catalysts can be designed, or one might find substitutes for precious-metal catalysts that are not readily available. Working catalyst systems have complicated structures, however, that do not lend themselves easily to atomic-scale investigations. The large-surface-area internal pore structure of the support hides the metal particles and makes it difficult to study their structure, oxidation state, and composition, which determine both activity and selectivity. Characterization of these complex but practical catalyst systems are the aims of many laboratories.

There is a different approach to the study of catalyst systems, which I would like to call the model system or synthetic approach [25]. It is similar to the technique used by synthetic organic chemists to prepare complex organic molecules by linking the smaller segments one by one until the final product is obtained. The catalyst particle is viewed as composed of single-crystal surfaces, as shown in Figure 7.7. Each surface has different reactivity, and the product distribution reflects the chemistry of the different surface sites. One may start with the simplest single-crystal surface [e.g., the (111) crystal face of platinum] and examine its reactivity. It is expected that much of the chemistry of the dispersed catalyst system would be absent on such a homogeneous crystal surface. Then high-Miller-index crystal faces are prepared to expose surface irregularities, steps, and kinks of known structure and concentration, and their catalytic behavior is tested and compared with the activity of the dispersed supported catalyst under identical experimental conditions. If there are still differences, the surface composition is changed systematically or other variables are introduced until the chemistries of the model system and the working catalyst become identical. This approach is described by the following sequence:

Studies of the structure of crystal surfaces when clean and in the presence of chemisorbed reactants and products. Chemisorption, structure, and bonding studies of reactants and products at low pressures ($\leq 10^{-4}$ torr)

Û

Surface reactions on external surfaces (small area $(\approx 1 \text{ cm}^2)$ crystals, foils, thin films, deposited particles) at high pressures $(10^3 \text{ to } 10^5 \text{ torr})$

Û

Reactions on dispersed (high surface area) catalysts at high pressures (10³ to 10⁵ torr)

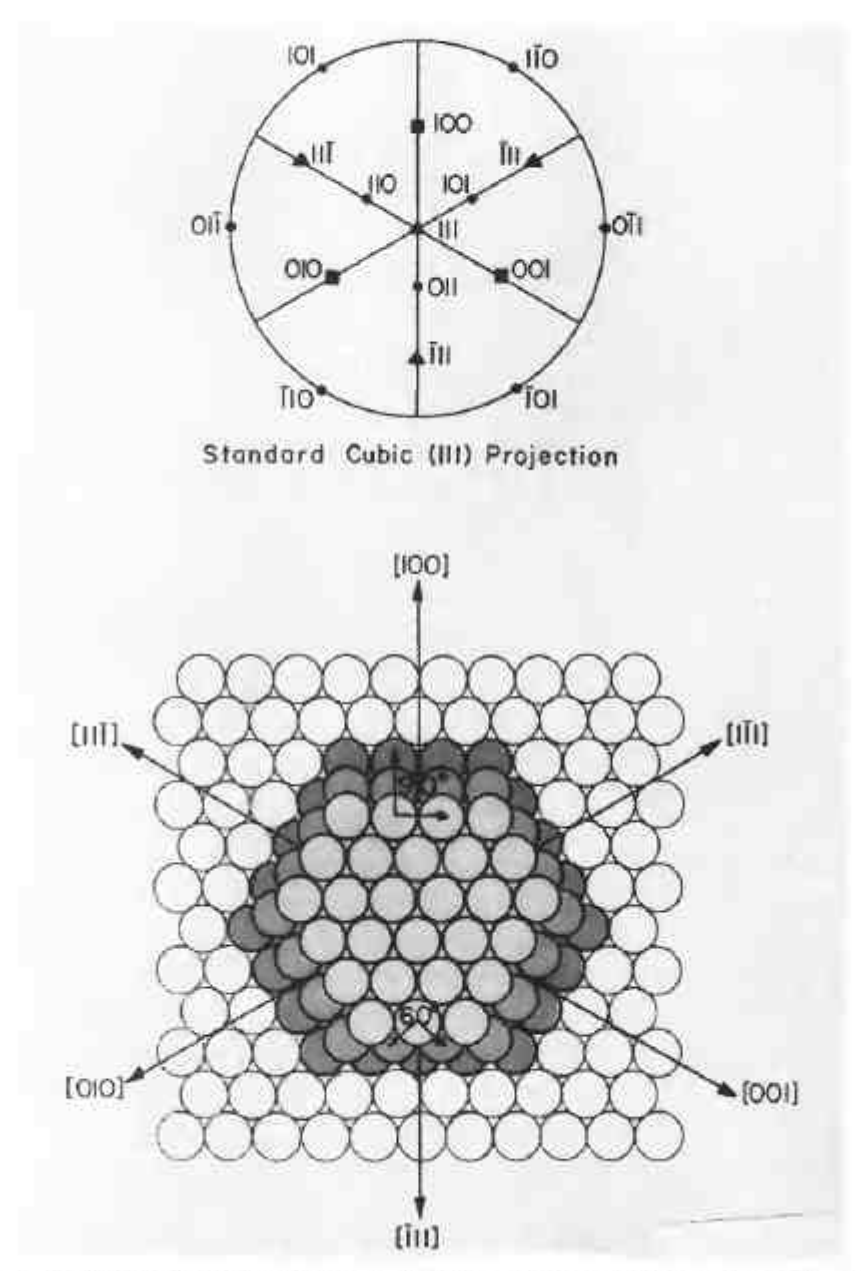


Figure 7.7. Catalyst particle viewed as a crystallite, composed of well-defined atomic planes, steps, and kink sites.

Investigations in the first step define the surface structure and composition on the atomic scale and the chemical bonding of adsorbates. Studies in the second phase reveal many of the elementary surface reaction steps and the dynamics of surface reactions. Combined studies in the second and third steps establish the similarities and differences between the model systems and the dispersed catalysts under practical reaction conditions.

The advantage of using small-area (1 cm²) catalyst samples is that their surface structure and composition can be prepared with uniformity and can be characterized by the many available surface diagnostic techniques. However, the small catalyst area that must be used in studies of this type necessitated the development of new instrumentation, which will be described next.

7.7.1 Techniques to Characterize and Study the Reactivity of Small-Area Catalyst Surfaces

7.7.1.1 High-Pressure Reactors In our synthetic approach to catalytic reaction studies, it is imperative that we determine the surface composition and surface structure in the same chamber where the reactions are carried out, without exposing the crystal surface to the ambient atmosphere. This necessitates the combined use of an ultrahigh-vacuum enclosure, where the surface characterization is to be carried out, and a high-pressure isolation cell, where the catalytic studies are performed. Such an apparatus is shown in Figure 7.8. The small-surface-area (approximately 1 cm²) catalyst is placed in the middle of the chamber, which can be evacuated to 10⁻⁹ torr. The surface is characterized by LEED and AES and by other desired surface diagnostic techniques. Then the lower part of the high-pressure isolation cell is lifted to enclose the sample in a 0.5-liter volume that is sealed by a copper gasket (approximately 2000 psi pressure is needed to provide a leak-free seal). The isolation chamber can be pressurized to 100 atm if desired and is connected to a gas chro-

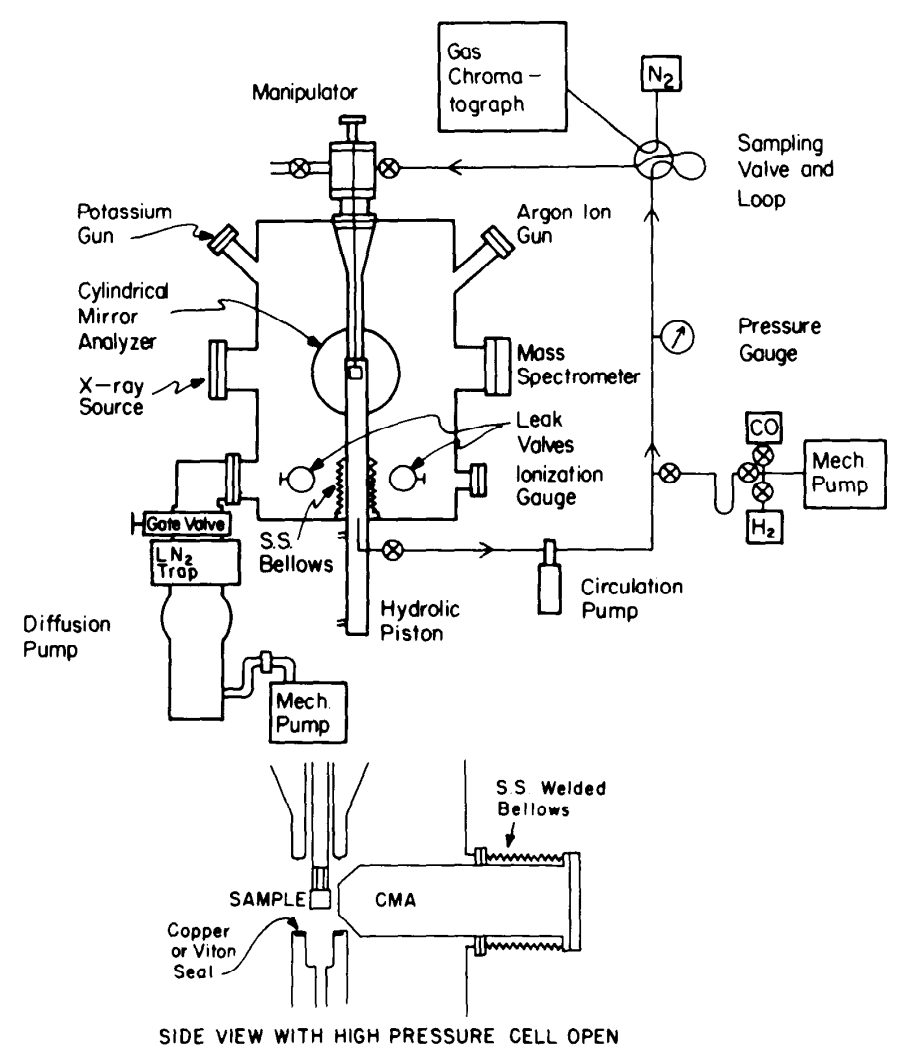


Figure 7.8. Schematic representation of one type of apparatus capable of carrying out catalytic-reaction-rate studies on single-crystal surfaces of low surface area at high pressures (atmospheres) and also to perform surface characterization in ultrahigh vacuum.

matograph that detects the product distribution as a function of time and surface temperature. The sample may be heated resistively, both at high pressure or in ultrahigh vacuum. After the reaction study, the isolation chamber is evacuated and opened, and the catalytic surface is again analyzed by the various surface-diagnostic techniques. Ion-bombardment cleaning of the surface or means to introduce controlled amounts of surface additives by vaporization are also available. The reaction at high pressures may be studied in the batch or the flow mode.

There are many different designs available for combined high-pressure reaction studies and ultrahigh-vacuum surface science investigations. Transfer rods that move the sample from the environmental cells to the UHV chamber and reaction cells that permit liquid-phase or gas-phase reaction studies have been described in the literature.

7.7.1.2 Comparison of the Reactivities of Small- and Large-Surface-Area Catalysts It is essential to test the high-pressure chamber to make sure that the measured reaction rates using the small-surface-area sample can be readily compared to reaction rates obtained on large-surface-area catalysts. This comparison has been made using the ring opening of cyclopropane [26] and the hydrogenation of carbon monoxide [27] as test reactions. Table 7.45 shows the turnover numbers and the activation energies obtained for the ring opening of cyclopropane to form propane on small-area single-crystal platinum and on dispersed platinum catalysts under identical experimental conditions. The agreement is indeed excellent. This is a structure-insensitive reaction at high pressures that lends itself well to such correlative studies. For structure-sensitive reactions, marked differences are found, with the single-crystal catalyst being much more active in general. Similarly, excellent agreements among rates, activation energies, and the product distribution were obtained for the hydrogenation of carbon monoxide over polycrystalline rhodium foils and dispersed, silica-supported rhodium catalyst particles. This is shown in Table 7.46. Figures 7.9 and 7.10 show the agreement reached between studies of the same re-

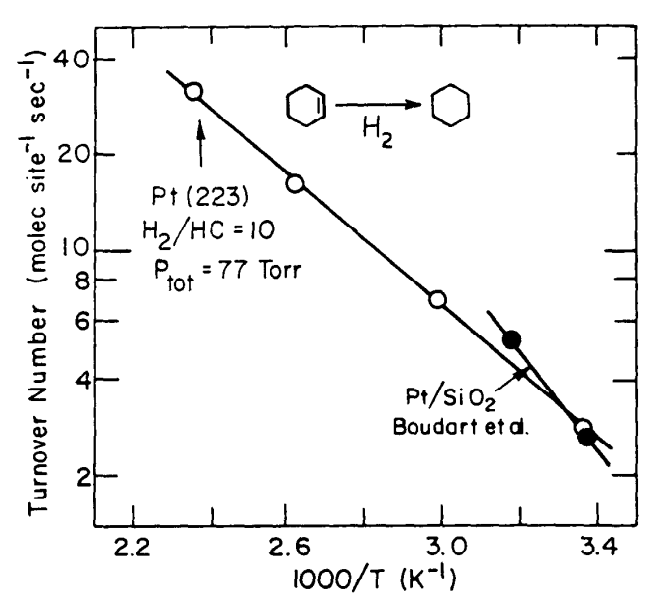


Figure 7.9. Arrhenius plot of the rate of cyclohexene hydrogenation to cyclohexane on Pt(111) crystal surfaces and on platinum particles dispersed on silica. Both the rates and activation energies are similar [190].

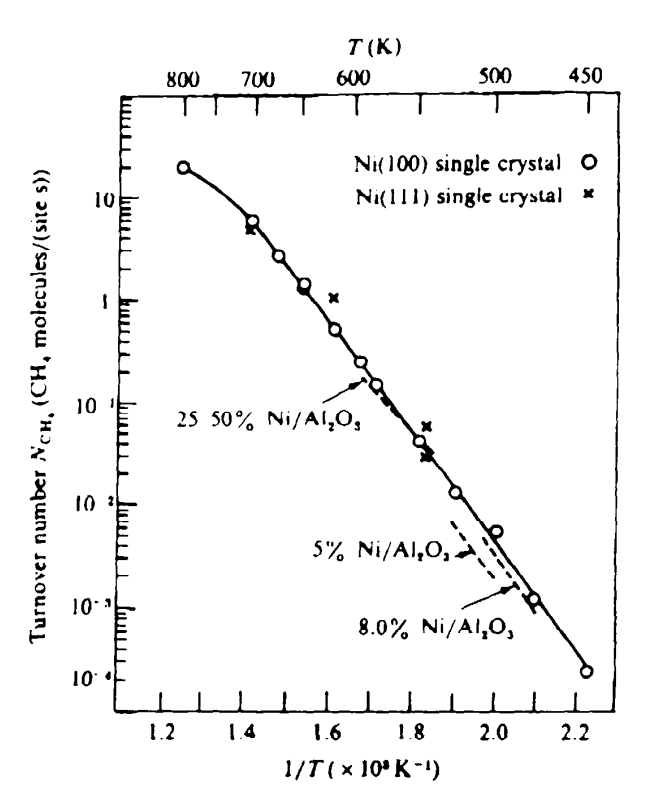


Figure 7.10. Arrhenius plot of the rate of methane production from hydrogen and carbon monoxide over Ni(111) and (100) compared to the production over supported Ni/Al₂O₃ dispersed catalyst. Both the rates and the activation energies are the same [191].

actions (benzene hydrogenation over Pt and CO hydrogenation over Ni) over low-surface-area model single crystal and high-surface-area dispersed catalysts.

7.8 CASE HISTORIES OF SURFACE CATALYSIS

Surface-science studies succeeded to identify many of the molecular ingredients of surface catalyzed reactions. Each catalyst system that is responsible for carrying out important chemical reactions with high turnover rate (activity) and selectivity has unique structural features and composition. In order to demonstrate how these systems operate, we shall review what is known about (a) ammonia synthesis catalyzed by iron, (b) the selective hydrogenation of carbon monoxide to various hydrocarbons, and (c) platinum-catalyzed conversion of hydrocarbons to various selected products.

7.8.1 Ammonia Syntheses

7.8.1.1 Thermodynamics and Kinetics The reaction of nitrogen and hydrogen to produce ammonia, $N_2 + 3H_2 \rightarrow 2NH_3$, is somewhat exothermic. The free energy of ammonia formation as a function of temperature is shown in Figure 7.11. The reaction is carried out over iron catalyst that is "promoted" by adding alumina and potassium most frequently. The reaction temperature is around 400°C, and total pressures utilized are in the range of 150-300 atm.

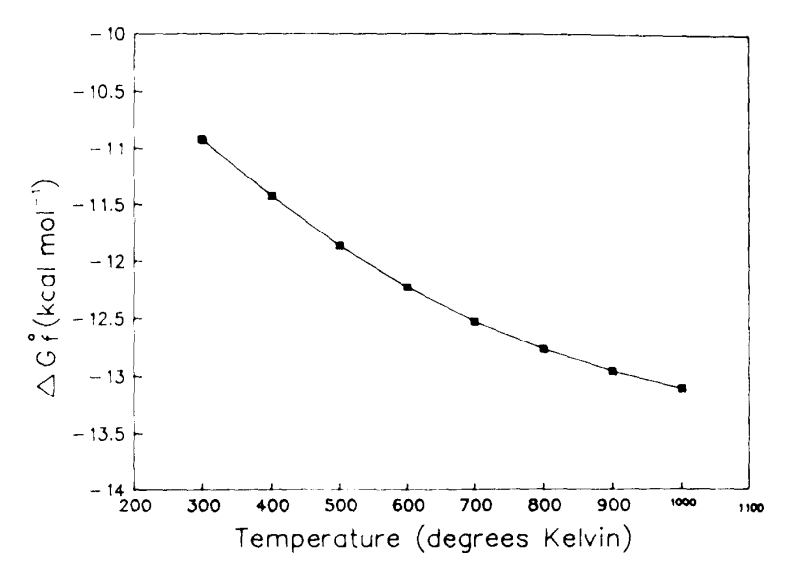


Figure 7.11. The free energy of ammonia formation as a function of temperature [33].

7.8.1.1.1 Kinetics From the experimental data, the observed dependencies of the rate on N_2 and H_2 pressures several rate laws have been proposed; the best known is perhaps the one by Temkin [28, 29]. An extension of this rate law by Nielsen [30, 31] yields

$$\frac{dP_{\text{NH}_3}}{dt} = \frac{k(P_{\text{N}_2}K_a - P_{\text{NH}_3}^2/P_{\text{H}_2}^3)}{(1 + K_3P_{\text{NH}_3}/P_{\text{H}_2}^w)^{2\alpha}}$$
(7.16)

where w = 1.5 and $\alpha = 0.75$. k, K_a , and K_3 are constants. The rate of ammonia formation depends in a rather complex manner on the partial pressures of N_2 , H_2 , and NH_3 mostly because of the possibility of a back-reaction. Far from equilibrium this may be neglected, and in this circumstance the rate depends only on the nitrogen pressure. This conclusion indicates that the rate-limiting step is the dissociative adsorption of nitrogen on the catalyst surface—a conclusion that is shared by most of the practitioners.

Other important rate equations that are applicable in a variety of experimental conditions have been proposed by Ozaki, Taylor, and Boudart [32].

The net activation energy for the reaction is 76 kJ/mole (e.g., see references [33-36]), which is in excellent agreement with the 81-kJ/mole value determined using single-crystal iron surfaces [37].

7.8.1.2 Catalyst Preparation The industrial catalyst is prepared by the reduction of iron oxide, Fe₃O₄ (94 wt%). It is in the shape of small porous particles with a surface area in the range of $10-15 \text{ m}^2/\text{g}$. Additives that improve its performance include Al₂O₃ (2.3 wt%), K₂O (0.8 wt%), and often CaO (1.7 wt%), MgO (0.5 wt%), and SiO₂ (0.4 wt%). Al, Mg, Ca, and Si oxides stabilize the pore structure and the surface structure of the iron catalyst K₂O, although decreases the iron surface area somewhat still greatly increases the ammonia yield at 613 K from 0.2 mol% to 0.34 mol%.

7.8.1.3 Activity for Ammonia Synthesis Using Transition Metals Across the Periodic Table There are two factors that are all important in determining the ammonia synthesis rate. One is the N_2 dissociative sticking probability. N_2 dissociation turns out to be rate-limiting, and at low conversions the total rate of the reaction equals the dissociation rate of N_2 . The other factor is the nitrogen atom chemisorption energy. Chemisorbed atomic nitrogen is by far the most stable reaction intermediate. Therefore, the surface is mainly covered by nitrogen atoms up to 90% of a monolayer; and the number of free sites on the surface where the nitrogen can adsorb is proportional to $(1 - \theta_N)$, where θ_N is the nitrogen coverage.

Using a kinetic model that was reported by A. Nielsen [30], the ammonia formation rate can be calculated as a function of the number of d-electrons in the transition metals. The results are shown in Figure 7.12. It produces a volcano curve similar to that observed experimentally by Ozaki and Aika, who have plotted the variation of the activity of various transition metals for the ammonia synthesis reaction as a function of the degree of filling of the d-band (Figure 7.13). The calculated results, and those found by experiments, overlap very well indeed. On the right side of the maximum in the volcano curve, the ammonia production decreases because the rate of N_2 dissociation drops as a consequence of the increase in the activation energy for dissociation. To the left of the tip of the volcano, the dissociation rate increases; but since the nitrogen chemisorption bond also increases in strength, the number of surface sites where the nitrogen molecule can dissociate decreases so fast that the overall rate decreases.

7.8.1.4 Surface Science of Ammonia Synthesis

7.8.1.4.1 Structure Sensitivity of Ammonia Synthesis An ultrahigh vacuum chamber equipped with a high-pressure cell was developed to study the ammonia synthe-

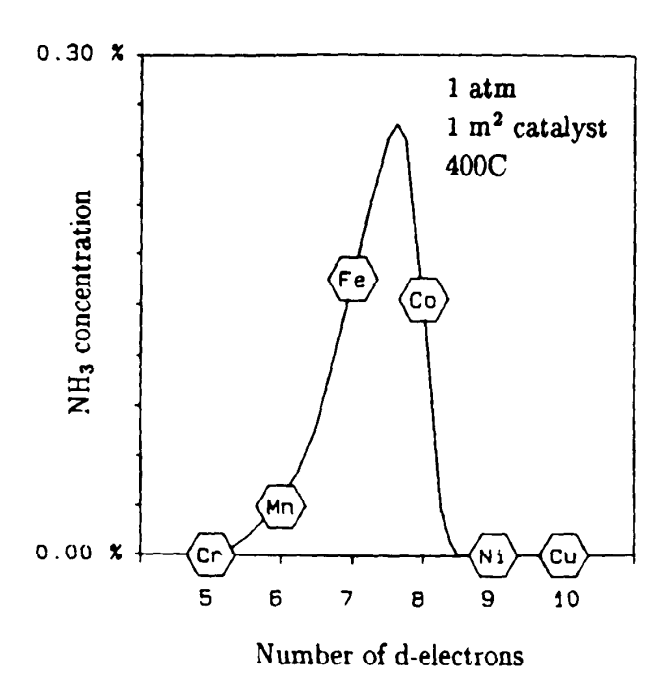


Figure 7.12. The calculated ammonia concentration for a fixed set of reaction conditions as a function of the number of d-electrons [71].

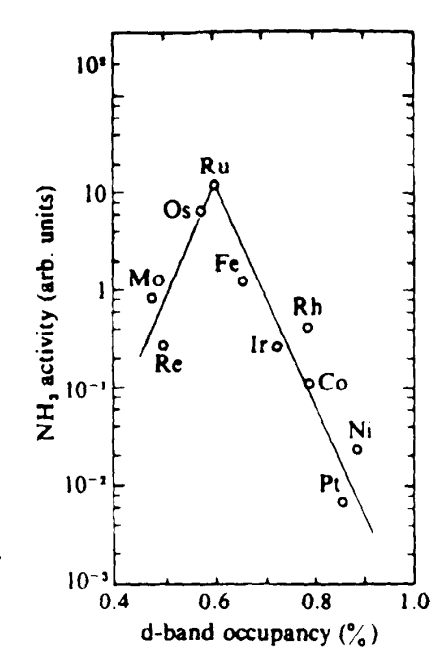


Figure 7.13. The activity of various transition metals for ammonia synthesis as a function of the degree of filling of the d-band [66].

sis reaction on iron single-crystal surfaces. A single crystal is enclosed in a high-pressure cell which constitutes part of a microbatch reactor. High pressures of gases—15 atm of hydrogen and 5 atm of nitrogen, for example—are introduced and the sample is heated to reaction temperatures, 600–700 K. The ammonia production is monitored using a selective photoionization detector with such photon energy that it ionizes ammonia and not nitrogen or hydrogen. After the reaction is completed, the reaction loop is evacuated and the cell opened, returning the sample to the ultrahigh vacuum environment where surface characterization is performed by Auger electron spectroscopy, low-energy electron diffraction, and temperature-programmed desorption.

In Figure 7.14 the rates of ammonia synthesis are shown over five iron crystal orientations. The Fe(111) and Fe(211) surfaces are by far the most active in ammonia synthesis and they are followed in reactivity by Fe(100), Fe(210), and Fe(110) [38]. Schematic representations of the idealized unit cells for these surfaces are shown in Figure 7.15. There are two possible reasons for the high activity of the (111) and (211) faces compared to the other (210), (100), and (110) orientations: their exceptionally high surface roughness or the presence of unique active sites the other crystal faces may not possess.

The (111) surface can be considered a rough surface, since it exposes secondand third-layer atoms to reactant gases in contrast to the (110) surface which only exposes first-layer atoms. Work functions are related to the roughness of a surface [39], and it is useful to quantify the corrugation of a plane in this way. Open faces, such as the (111) surface, have lower work functions than do close-packed faces, such as the (110) surface. The work functions of all the iron faces are not currently available but they are for tungsten [40], another body-centered cubic (bcc) metal which also shows structure sensitivity for ammonia decomposition [41]. The order of decreasing work function (ϕ) is as follows: $\phi_{110} > \phi_{211} > \phi_{100} > \phi_{111} > \phi_{210}$. However, the order of decreasing work function from crystal face to crystal face does not correlate with variations of catalytic activity.

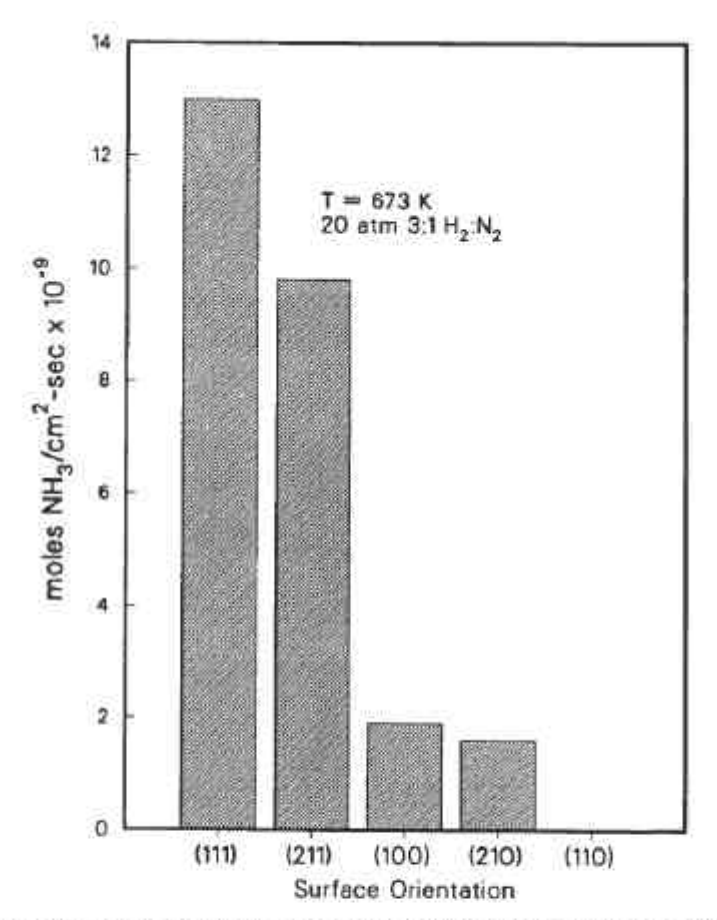


Figure 7.14. Rates of ammonia synthesis over five iron single-crystal surfaces with different orientations: (111), (211), (100), (210), and (110) [38].

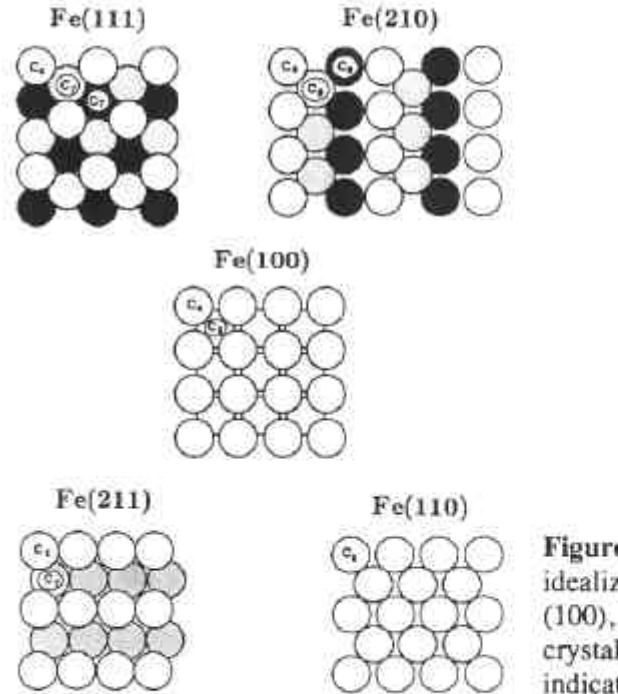


Figure 7.15. Schematic representations of the idealized surface structures of the (111), (211), (100), (210), and (110) orientation of iron single crystals. The coordination of each surface atom is indicated [38].

The second possible explanation for the structure sensitivity of ammonia synthesis rate of iron involves the nature of the active sites. The (111) and (211) faces of iron are the only surfaces which expose C_7 sites (iron atoms with seven nearest neighbors) to the reactant gases. Theoretical work by Falicov and Somorjai [11] has suggested that highly coordinated surface atoms would show increased catalytic activity due to low-energy charge fluctuations in the d-bands of highly coordinated surface atoms. Examination of the results suggests that the latter argument of active sites is the key to the structure sensitivity of ammonia synthesis over iron.

The reaction rates, in Figure 7.14, show that the (211) face is almost as active as the (111) plane of iron, while Fe(210) is less active than Fe(100). The Fe(210) and Fe(111) faces are open faces which expose second- and third-layer atoms. The Fe(211) face is more close-packed, but it exposes C_7 sites. If either surface roughness or a low work function were the important consideration for an active ammonia synthesis catalyst, then the Fe(210) would be expected to be the most active face. However, in marked contrast, Fe(111) and Fe(211) faces are much more active, indicating that the presence of C_7 sites is more important than surface roughness in an ammonia synthesis catalyst.

The idea of C_7 sites being the most active site in ammonia synthesis on iron has been suggested in the past. Dumesic et al. [42] found that the turnover number for ammonia synthesis was lower on small iron particles than on larger ones. Pretreatment of an Fe/MgO catalyst with ammonia enhanced the turnover number over small iron particles, but did not affect the larger particles. This result was explained by noting that the concentration of C_7 sites would be expected to be higher on the smaller iron particles and that restructuring induced by ammonia enhanced the number of these sites on the catalyst.

7.8.1.4.2 Kinetics of Dissociative Nitrogen Adsorption Because this step is ratedetermining for ammonia synthesis, considerable effort has been expended on its detailed investigation. It has turned out to be of great complexity so that, even now, complete understanding of the underlying microscopic dynamics is still lacking, although there exists general agreement about the experimental findings.

In Figure 7.16, the variation in the relative surface concentration of N_{ad} (as monitored by Auger electron spectroscopy) with N₂ exposure at elevated temperatures for the Fe(110), (100), and (111) surfaces [43, 44] is shown. The slopes of these curves yield the sticking coefficients for dissociative chemisorption which are obviously very small and depend markedly on the surface orientation. More specifically, the initial sticking coefficient (at 683 K) changes from 7×10^{-8} to 2×10^{-7} to 4×10^{-6} in the sequence Fe(110) < Fe(100) < Fe(111); that is, the (111) plane is about two orders of magnitude more active than the most densely packed (110) plane. This sequence of activity toward dissociative nitrogen adsorption at low pressures ($< 10^{-4}$ torr) is in agreement with that found for the rate of ammonia production at high pressure (20 atm) described in the previous section. Moreover, the sticking coefficients are approximately of the same orders of magnitude as the reaction probabilities derived from the high-pressure work. This remarkable result demonstrates that kinetic parameters derived from well-defined single-crystal surfaces are obviously transferable over the "pressure gap" and it confirms that the dissociative nitrogen adsorption is indeed the rate-limiting step, since the rate of NH₃ formation equals that of dissociative nitrogen adsorption.

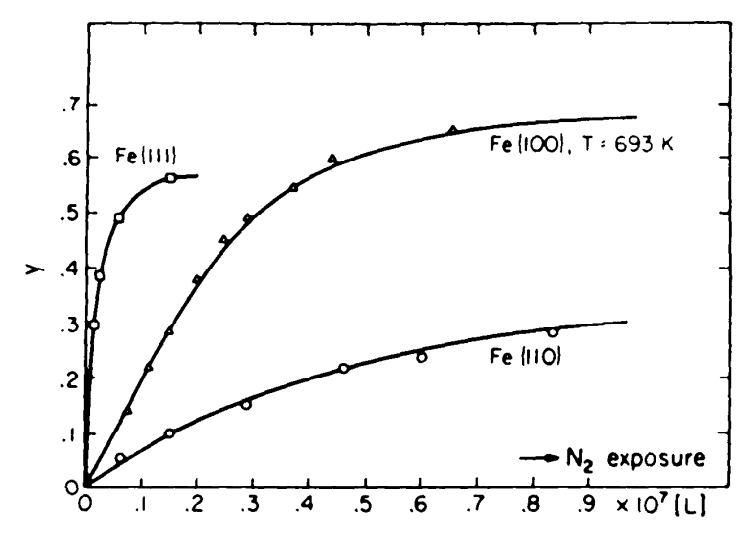


Figure 7.16. Variation of the relative surface concentration, y, of atomic nitrogen as a function of N_2 exposure [33]. 1 L (Langmuir) = 10^{-6} torr-sec.

Similar conclusions had already been reached many years ago by Emmett and Brunauer [45], who measured the uptake of nitrogen by commercial catalysts and concluded likewise that the sticking coefficient is only on the order of 10^{-6} .

The sticking coefficient can be formulated in terms of the usual Arrhenius equation for a rate constant, $s = A \exp(-\Delta E^*/RT)$, with the preexponential A and activation energy ΔE^* as parameters. Measurements at different temperatures revealed that the differences between the three crystal planes can essentially be traced back to differences in the net activation energy E^* for the overall process $N_2 \rightarrow 2N_{ad}$, which in the limit of zero coverage was found to be about 27 kJ/mole for Fe(110), about 21 kJ/mole for Fe(100), and about 0 kJ/mole for Fe(111). These activation energies increase continuously with increasing coverage, in qualitative agreement with previous measurements using supported Fe catalysts [46].

7.8.1.4.3 Effects of Aluminum Oxide in Restructuring Iron Single-Crystal Surfaces for Ammonia Synthesis The initial rate of ammonia synthesis has been determined over the clean Fe(111), Fe(100), and Fe(110) surfaces with and without aluminum oxide. The addition of aluminum oxide to the (110), (100), and (111) faces of iron decreases the rate of ammonia synthesis in direct proportion to the amount of surface covered [47]. This suggests that the promoter effect of aluminum oxide involves reaction with iron which cannot be achieved by simply depositing aluminum oxide on an iron catalyst.

Remembering that the industrial catalyst is prepared by fusion of 2-3% by weight of aluminum oxide and potassium with iron oxide (Fe₃O₄), experiments were performed in which Al_xO_y /Fe single-crystal surfaces were pretreated in an oxidizing environment prior to ammonia synthesis. These experiments were carried out by depositing about 2 ml of Al_xO_y on Fe(111), Fe(100), and Fe(110) surfaces and then treating them in varying amounts of water vapor at 723 K in order to oxidize the iron and to induce an interaction between iron oxide and aluminum oxide. After removal of the water vapor, high pressures of nitrogen and hydrogen were added to determine the rates of ammonia synthesis. The rate of ammonia synthesis over

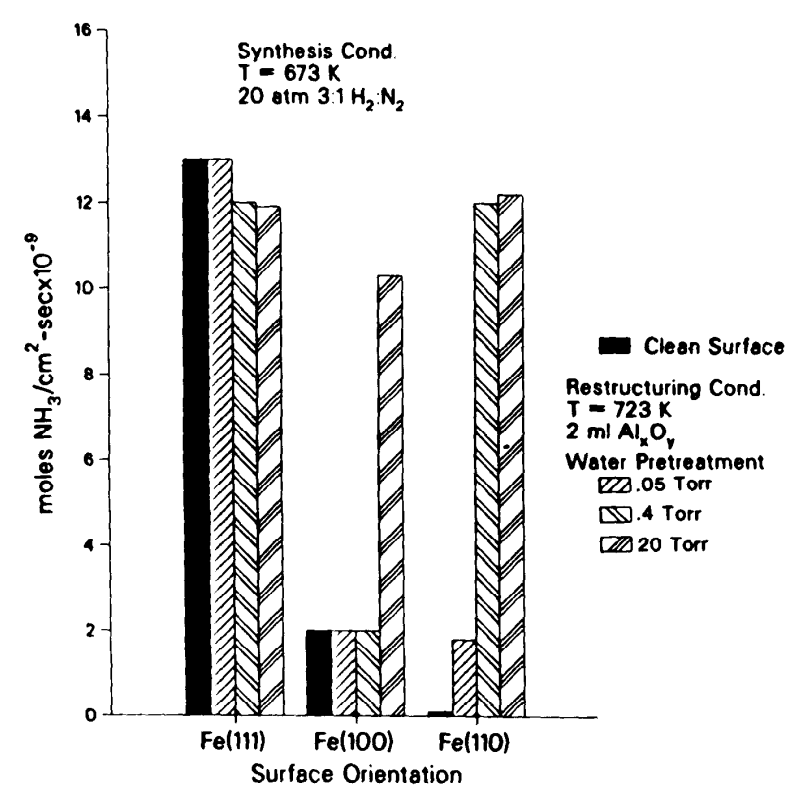


Figure 7.17. Rates of ammonia synthesis over clean iron single crystals and water-induced restructured Al_xO_y /Fe surfaces. Restructuring conditions are given in the figure [38].

 Al_xO_y/Fe surfaces pretreated with water vapor prior to ammonia synthesis is shown in Figure 7.17. The initially inactive $Al_xO_y/Fe(110)$ surface restructures and becomes as active as the Fe(100) surface after a 0.05-torr water vapor treatment and as active as the Fe(111) surface after a 20-torr water-vapor pretreatment. This is about a 400-fold increase in the rate of ammonia synthesis compared with clean Fe(110) [37]. The activity of the $Al_xO_y/Fe(100)$ surface can also be enhanced to that of the highly active Fe(111) surface by utilizing a 20-torr water-vapor pretreatment, and this high activity is maintained indefinitely as in the case for the restructured $Al_xO_y/Fe(110)$. Little change in the activity of the Fe(111) surface is seen experimentally when it is treated in water vapor in the presence of Al_xO_y .

The activity of the Fe(110) and Fe(100) surfaces for ammonia synthesis can also be enhanced to the level of Fe(111) by water-vapor pretreatments in the absence of aluminum oxide, but in this circumstance the enhancement in activity is only transient. Figure 7.18 shows the rate of ammonia synthesis as a function of reaction time for restructured Fe(110) and $Al_xO_y/Fe(110)$ surfaces. Both surfaces have an initial activity similar to that of the clean Fe(111) surface. The restructured $Al_xO_y/Fe(110)$ surface maintains this activity for over 4 hr while the restructured Fe(110) surface loses its activity for ammonia synthesis within 1 hr of reaction.

7.8.1.4.4 Characterization of the Restructured Surfaces The observation that the $Al_xO_y/Fe(110)$ and $Al_xO_y/Fe(100)$ become as active as the Fe(111) surface for ammonia synthesis suggests that new crystal orientations are being created upon restructuring the $Al_xO_y/Fe(110)$ and $Al_xO_y/Fe(100)$ surfaces in water vapor. A sug-

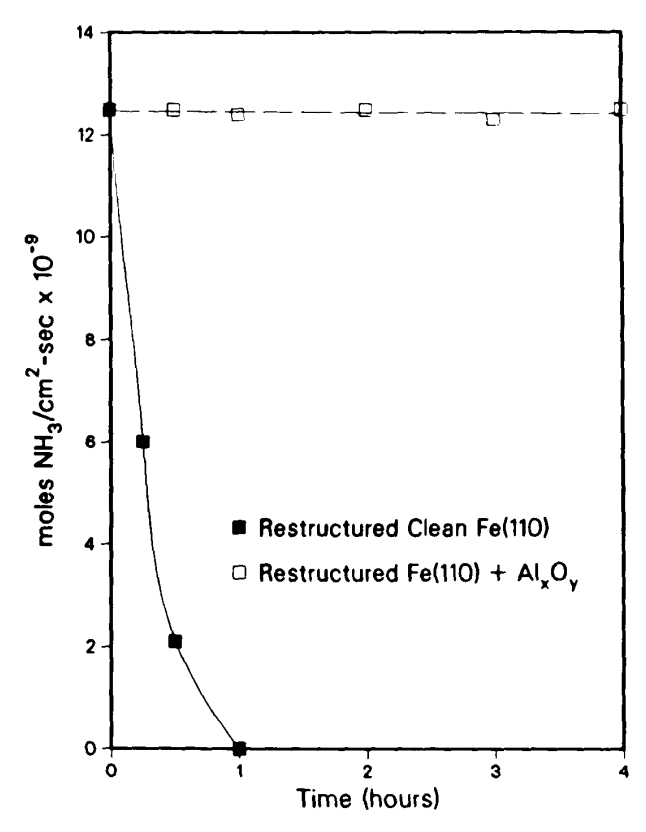


Figure 7.18. Deactivation of the restructured Fe(110) surface occurs within 1 hr while the restructured $Al_xO_y/Fe(110)$ surface maintains its activity under ammonia synthesis conditions [38].

gested increase in the surface area cannot account for the enhancement in rate, since it has been shown that about 40% less carbon monoxide adsorbs on restructured $Al_xO_y/Fe(110)$ and $Al_xO_y/Fe(100)$ relative to the clean respective surfaces [48] (i.e., the iron surface area actually decreases).

Electron spectroscopies, low-energy electron diffraction, temperature-programmed desorption (TPD), and scanning electron microscopy (SEM) have been used to characterize the restructured surfaces. SEM micrographs for restructured Fe(110) and $Al_xO_y/Fe(110)$ surfaces following a 20-torr water-vapor pretreatment show that the surfaces seem to be completely recrystallized. Auger electron spectroscopy finds that only about 5% of the iron surface is covered by aluminum oxide, and sputtering the surface with argon ions reveals aluminum oxide beneath the iron surface.

TPD of ammonia from iron single-crystal surfaces following high-pressure ammonia synthesis proves to be a sensitive probe of the new surface binding sites formed upon restructuring. Ammonia TPD spectra for the four clean surfaces are shown in Figure 7.19. Each surface shows distinct desorption sites. The Fe(110) surface displays one desorption peak (β_3) with a peak maximum at 658 K. Two desorption peaks are seen for the Fe(100) surface (β_2 and β_3) at 556 K and 661 K. The Fe(111) surface exhibits three desorption peaks (β_1 , β_2 , and β_3) with peak maxima at 495 K, 568 K, and 676 K, and the Fe(211) plane has two desorption peaks (β_2 and β_3) at 570 K and 676 K. PD spectra for the Al_xO_y/Fe(110), Al_xO_y/Fe(100), and Al_xO_y/Fe(111) surfaces restructured in 20 torr of water vapor are shown in

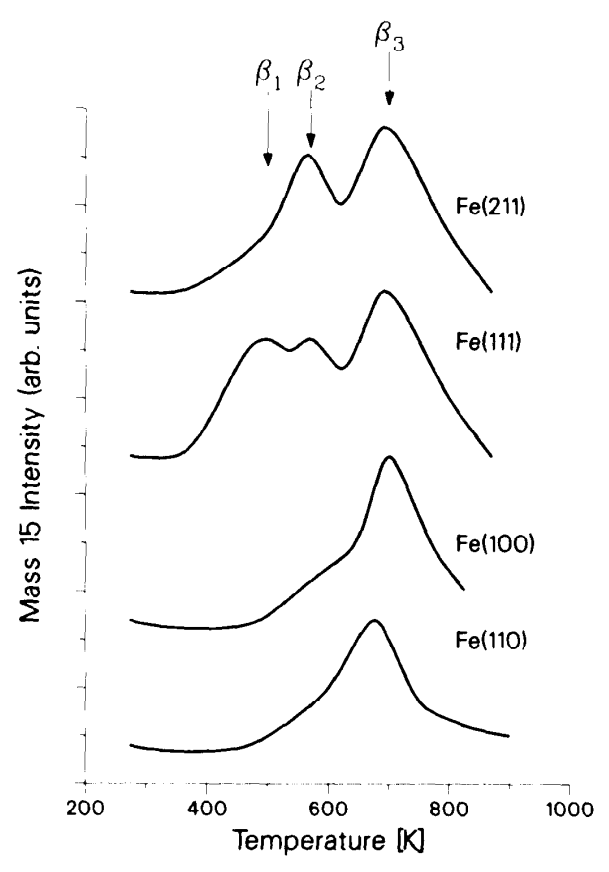


Figure 7.19. Ammonia TPD after high-pressure ammonia synthesis. The low-temperature peaks exhibited by Fe(111) and Fe(211) (β_1 and β_2) are attributed to the presence of C_7 sites [38].

Figure 7.20. A new desorption peak, β_2 , develops on the restructured $Al_xO_y/Fe(110)$ surface, and an increase in the β_2 peak occurs on the restructured $Al_xO_y/Fe(100)$ surface. The β_2 peaks from the restructured $Al_xO_y/Fe(110)$ and $Al_xO_y/Fe(100)$ surfaces grow in the same temperature range as the Fe(111) and Fe(211) β_2 peaks.

The ammonia TPD results point toward the formation of surface orientations which contain C_7 sites during water-vapor-induced restructuring. The growth of the β_2 peaks upon restructuring of the Fe(110) and Fe(100) surfaces suggests that the surfaces change orientation upon water-vapor treatment. The β_2 peaks also reside in the same temperature range as the Fe(111) β_2 peak. It seems likely that the TPD peaks in this temperature range act as a signature for the C_7 sites because the Fe(211) surface which contains C_7 sites is highly active in the ammonia synthesis reaction and also exhibits a β_2 peak after ammonia synthesis, with a peak maximum at 570 K. These results suggest that surface orientations which contain C_7 sites, such as the Fe(111) and Fe(211) planes, are formed during the reconstruction of clean and Al_xO_y -treated iron surfaces, but only in the presence of Al_xO_y does the active restructured surface remain stable under the ammonia synthesis conditions.

With the addition of Al_xO_y , the mobility of the iron is increased and restructuring can occur at lower pressure of water vapor. The SEM micrographs suggest that iron forms crystallites on top of the restructured $Al_xO_y/Fe(110)$ surface [as opposed to the uniform appearance of the restructured clean Fe(110) surface]. AES finds little

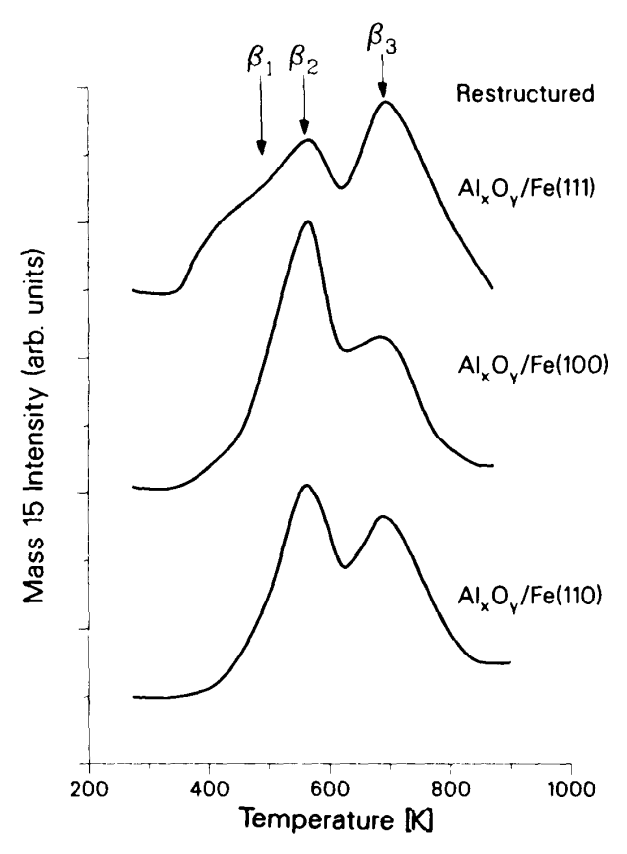


Figure 7.20. Ammonia TPD following ammonia synthesis from restructured $Al_xO_y/Fe(100)$ surfaces exhibit low-temperature peaks similar to those of Fe(111) and Fe(211). Thus, restructuring by water vapor creates active C_7 sites [38].

 Al_xO_y on the surface, suggesting that the iron has diffused through the Al_xO_y islands, covering them. These findings can be explained by considering wetting properties and the minimization of the free energy for the iron oxide-aluminum oxide system. The formation of iron aluminate (i.e., $FeAl_2O_4$) in the presence of an oxygen source was also postulated [49] on the basis of microelectron diffraction data.

The formation of an iron aluminate during reconstruction of the iron surface may be responsible for the stability of the restructured Al_xO_y /Fe surfaces. The presence of iron aluminate has been postulated from XPS studies on Fe-Al₂O₃ and Fe₃O₄-Al₂O₃ systems [50, 51] as well as in numerous studies on the industrial ammonia synthesis catalyst [52-54]. The low coverages of Al_xO_y on the restructured surfaces suggest that FeAl₂O₄ plays the role of support on which iron surfaces grow with (111) orientation that is most active in ammonia synthesis. This is supported by the fact that ion sputtering the restructured surfaces reveal subsurface Al_xO_y . This model of the role of alumina as a structure modifier of iron for ammonia synthesis is shown in Figure 7.21.

7.8.1.4.5 Effect of Potassium on the Dissociative Chemisorption of Nitrogen on Iron Single-Crystal Surfaces in UHV The rate-determining ammonia synthesis reaction is widely accepted to be the dissociation of nitrogen [32, 55-57]. Consequently the direct interaction between nitrogen and iron has been studied [43, 44] together with the addition of submonolayer amounts of potassium [56, 58]. All the

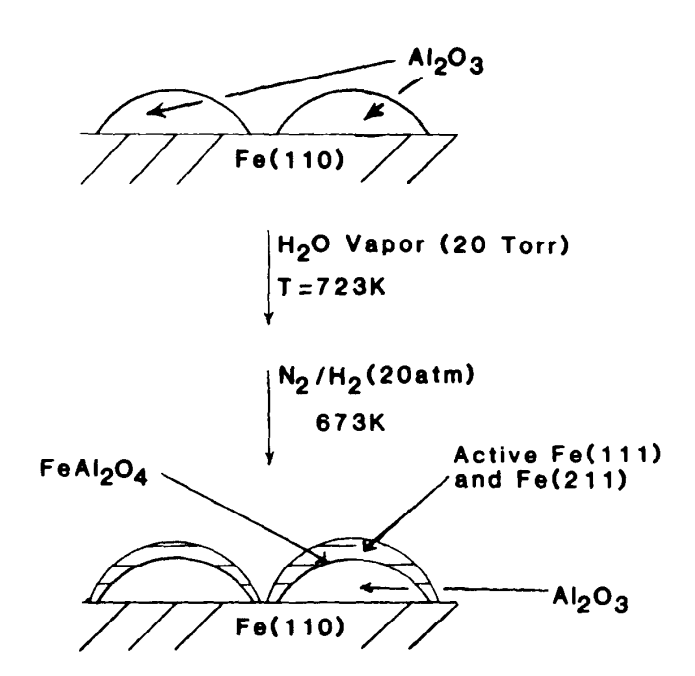


Figure 7.21. Scheme of the restructuring process of iron induced by water vapor and the presence of aluminum oxide. The oxidation of iron permits the migration of the metal on top of the aluminum oxide. The formation of $FeAl_2O_4$ may facilitate this process. Upon reduction in nitrogen and hydrogen, iron is left in active and stable (111) orientation for ammonia synthesis on top of $FeAl_2O_4$.

work that will be referred to in this section was carried out in a UHV chamber, which therefore limits the pressure range to lie between 10^{-4} torr and 10^{-10} torr.

Using both iron single crystals and polycrystalline foils, the sticking probability of molecular nitrogen on iron was found to be on the order of 10^{-7} . This result reveals why, in addition to thermodynamic considerations, ammonia synthesis from the elements is favored at high reactant gas pressures. Because the sticking probability of dissociating nitrogen is so low on iron, higher pressures of nitrogen enhance the kinetics of the rate-limiting step in ammonia synthesis. The structure sensitivity of the reaction is also revealed in the nitrogen chemisorption studies. It was found that the Fe(111) surface dissociatively chemisorbed nitrogen 20 times faster than the Fe(100) surface and 60 times faster than the Fe(110) surface. This agrees well with the structure sensitivity of ammonia synthesis and adds more credence to dissociative chemisorption being the rate-limiting step. The addition of submonolayer amounts of elemental potassium has dramatic effects on the nitrogen chemisorption properties of the (110), (100), and (111) faces of iron.

The effect of potassium on the initial sticking coefficient (S_0) of nitrogen on a Fe(100) surface is shown in Figure 7.22. For clean Fe(100), S_0 is 2×10^{-7} , but with the addition of potassium S_0 increases almost linearly, until at a potassium concentration of 1.5×10^{14} potassium atoms per cm², where S_0 maximizes at a value of 3.9×10^{-5} , a factor of $280 \times$ enhancement is seen. Higher coverages of potassium start to decrease S_0 , presumably due to the blocking of iron sites by potassium which would otherwise dissociatively chemisorb nitrogen. The maximum increase in S_0 , due to potassium adsorption, on Fe(111) is about a factor of 10 ($S_0 = 4 \times 10^{-5}$) at a potassium concentration of 2×10^{14} K atoms per cm². The potassium-induced enhancement of S_0 on the Fe(110) surface is greater than that

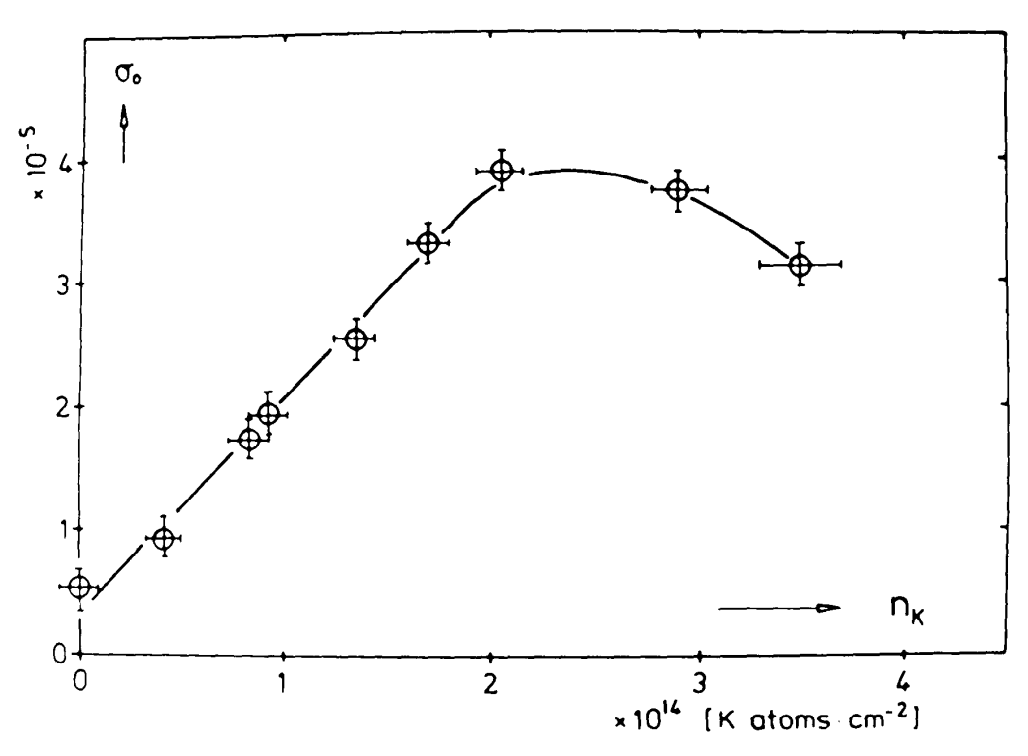


Figure 7.22. Variation of the initial sticking coefficient of N_2 , σ_0 , with the addition of potassium to Fe(100) at 430 K. The N_2 sticking coefficient can be enhanced by a factor of 280 relative to clean Fe(100) [56].

observed on either Fe(111) or Fe(100), so that the differences in activities for nitrogen dissociation seen on the clean surfaces is much smaller in the presence of potassium.

The mechanism by which potassium promotes nitrogen chemisorption is usually attributed to the lowering of the surface work function in the vicinity of a potassium ion. This effect is greatest at sufficiently low coverages (<0.15 ML) where the potassium-iron bond has strong ionic character, so that the local ionization potential of the surface iron atoms is greatest. This allows for more electron density to be transferred to the nitrogen $2\pi^*$ antibonding orbitals from the surface. This phenomenon increases the adsorption energy of molecular nitrogen and simultaneously lowers the activation energy for dissociation. For example, on the Fe(100) surface the addition of 1.5×10^{14} K atoms per cm² decreases the work function by about 1.8 eV and increases the rate of nitrogen dissociation by more than a factor of 200. This enhancement in rate is accompanied by an increase in the adsorption energy of nitrogen on Fe(100) by 11.5 kcal/mole, which decreases the activation barrier for dissociation, in the presence of potassium, from 2.5 kcal/mole to about 0 kcal/mole.

7.8.1.4.6 Temperature-Programmed Desorption Studies of Ammonia from Iron Surfaces in the Presence of Potassium The TPD of ammonia from clean Fe(111) and K/Fe(111) is shown in Figure 7.23 [59]. Ammonia desorbs through a wide temperature range, resulting in a broad peak with a maximum rate of desorption occurring at around 300 K. With the addition of 0.1 ML of potassium, the temperature of the peak maximum is reduced by about 40 K. Assuming first-order desorption for ammonia, the 40-K decrease corresponds to a 2.4-kcal/mole drop in the

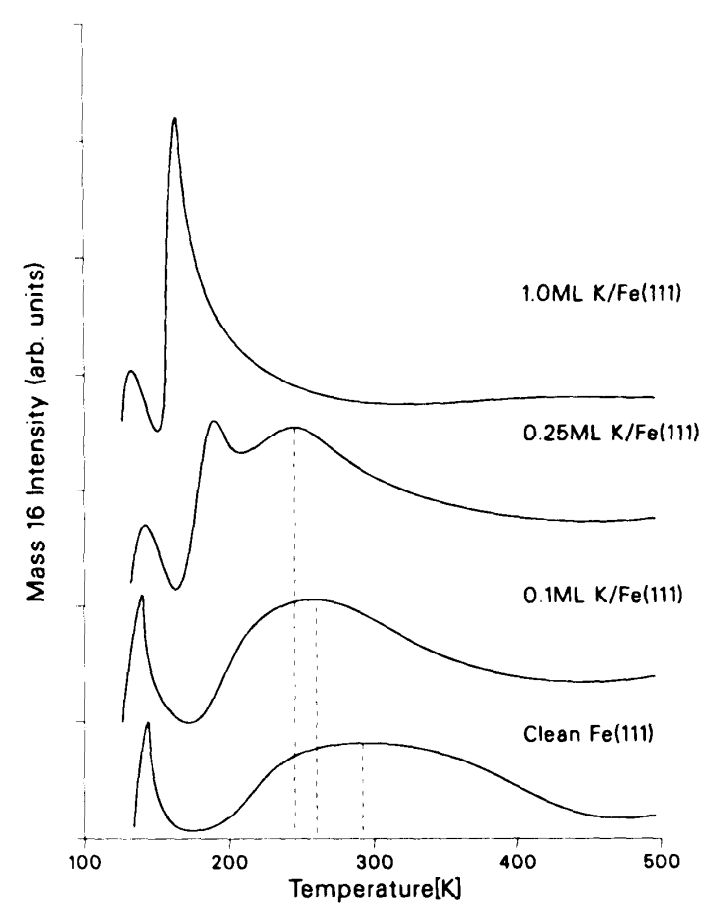


Figure 7.23. Ammonia TPD from clean Fe(111) and K/Fe(111) surfaces. The desorption temperature of ammonia from Fe(111) is lowered in the presence of potassium. Thus potassium lowers the adsorption energy of ammonia on the iron surface [59].

adsorption energy of ammonia on iron in the presence of 0.1 ML potassium. The peak maximum continuously shifts to lower temperature with increasing amounts of coadsorbed potassium. At a coverage of 0.25 ML a new desorption peak appears at about 189 K. Increasing coverages of potassium now increase the intensity of the new peak (it also shifts to lower temperatures) and decreases the intensity of the original ammonia desorption peak. At a potassium coverage of about 1.0 ML, only a weakly bound ammonia species is present, with a maximum rate of desorption occurring at 164 K. This observation of decreasing adsorption energy for ammonia with the coadsorption of potassium on iron is similar to what is found for ammonia desorption from nickel and ruthenium with adsorbed sodium [60, 61].

7.8.1.4.7 Effects of Potassium on Ammonia Synthesis Kinetics Extensive research has been completed in which the effects of potassium on ammonia synthesis over iron single-crystal surfaces of (111), (100), and (110) orientations [59] have been determined. The apparent order of ammonia and hydrogen for ammonia synthesis over iron and K/Fe surfaces has been determined in addition to the effect of potassium on the apparent activation energy (E_a) for the reaction. In all the experiments, potassium was coadsorbed with oxygen because only about 0.15 ML of potassium coadsorbed with oxygen is stable under ammonia synthesis conditions (20)

atm total pressure: 3 to 1 H_2 to N_2 : T = 673 K) [47, 59, 62]. It has been shown that the addition of 0.15 ML of potassium to Fe(111) and Fe(100) increases the ammonia partial pressure dependence from -0.60 for the clean iron surfaces to -0.35 for the 0.15 ML K/Fe(111) and 0.15 ML K/Fe(100) surfaces under high-pressure ammonia synthesis conditions (Figure 7.24). The apparent order in hydrogen partial pressure has been found to decrease from 0.76 for clean Fe(111) to 0.44 for the 0.15 ML K/Fe(111) surface (Figure 7.25). The Fe(110) is inactive for ammonia synthesis under these conditions with or without potassium. These changes in both the apparent order of hydrogen and ammonia pressure dependence occurring with no change in the activation energy suggests that potassium does not change the elementary steps of ammonia synthesis (Figure 7.26). The data show that the promotional effect of potassium is enhanced as the reaction conversion increases (i.e., increasing ammonia partial pressure.

These results are consistent with earlier literature [63, 64] in which the effects of potassium on doubly promoted (aluminum oxide and potassium) catalysts were studied. It was shown that the turnover number for ammonia synthesis is roughly the same over singly (aluminum oxide) and double promoted iron when 1 atm reactant

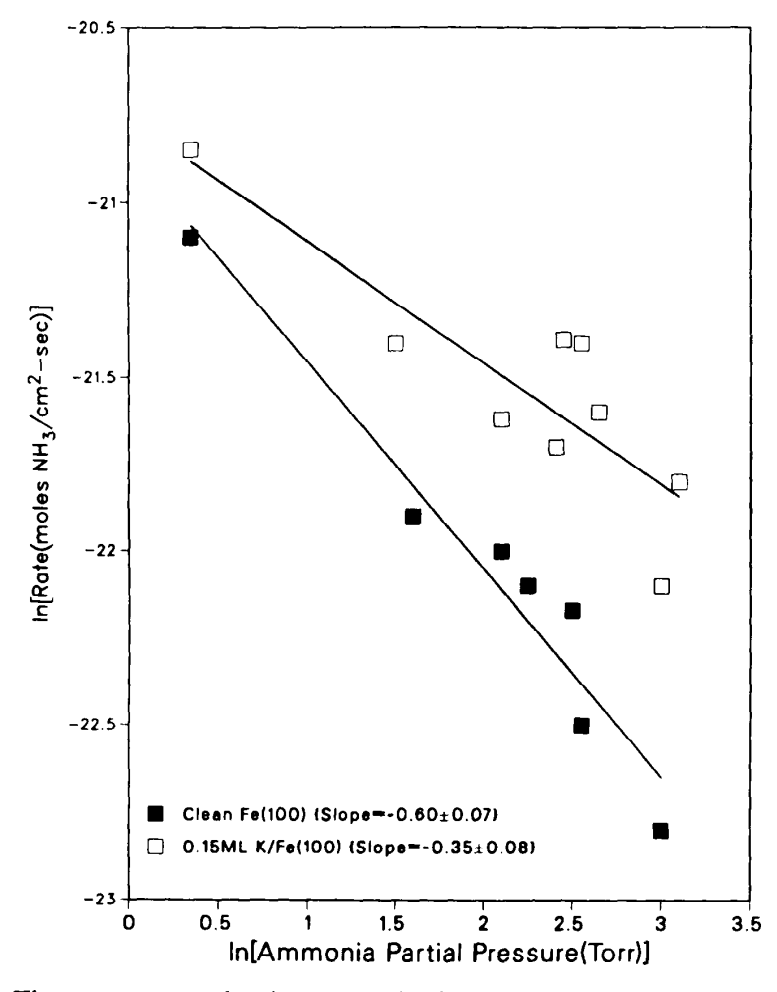


Figure 7.24. The apparent order in ammonia for ammonia synthesis over Fe(100) and K/Fe(100) surfaces. The order in ammonia becomes less negative when potassium is present. The same values were found for Fe(111) and K/Fe(111) surfaces [59].

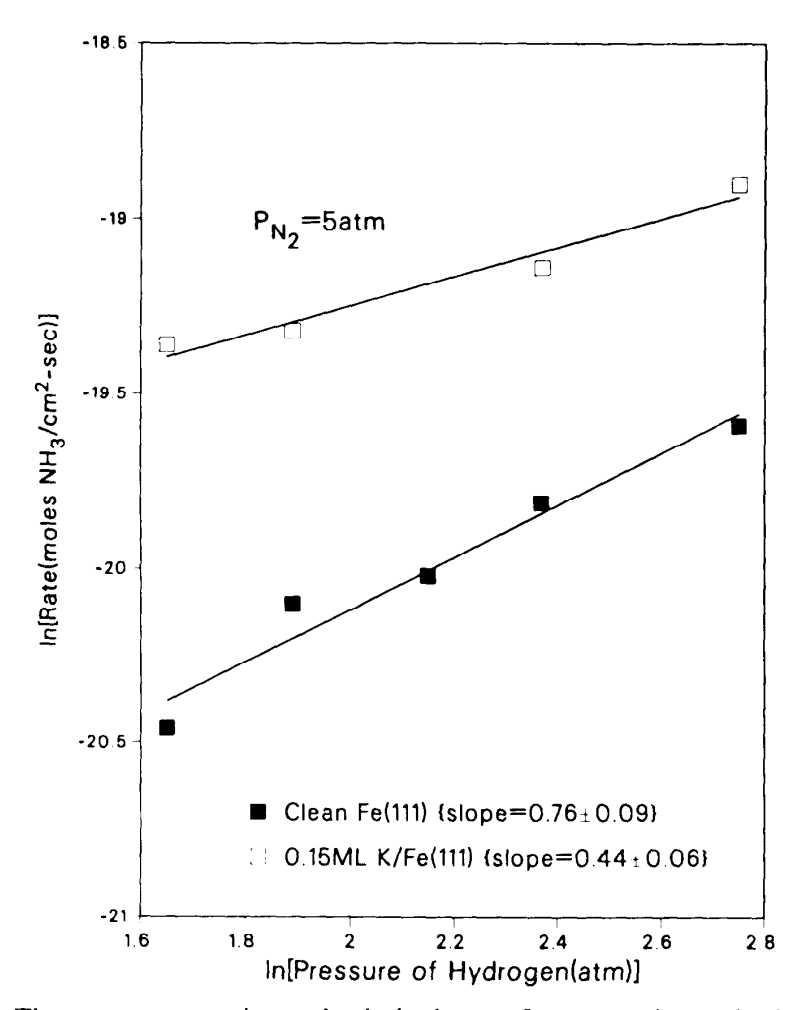


Figure 7.25. The apparent reaction order in hydrogen for ammonia synthesis over Fe(111) and K/Fe(111) surfaces. The order in hydrogen decreases in the presence of potassium [59].

pressure of nitrogen and hydrogen is used [64]. This implies that at low-pressure conditions, the gas-phase ammonia concentration is not high enough for potassium to exert a promoter effect. As higher reactant pressures are achieved (95–200 atm), the promoter effect of potassium becomes significant. It was found that doubly promoted catalysts became increasingly more active than catalysts without potassium when the concentration of ammonia in the gas phase increased [63]. This implies that potassium makes the apparent reaction order dependence in ammonia partial pressure less negative over commercial catalysts, in agreement with the single-crystal work.

7.8.1.4.8 Effects of Potassium on the Adsorption of Ammonia on Iron Under Ammonia Synthesis Conditions The changes in the apparent reaction order dependence in ammonia partial pressure suggest that to elucidate the effects of potassium on both iron single crystals and the industrial catalyst, it is necessary to understand the readsorption of gas-phase ammonia on the catalyst surface during ammonia synthesis; The fact that the rate of ammonia synthesis is negative order in ammonia synthesis. Once adsorbed, the ammonia has a certain residence time (τ) on the catalyst which is determined by its adsorption energy (ΔH_{ads}) on iron $[\tau \propto \tau_0]$ exp $(\Delta H_{ads}/RT)$

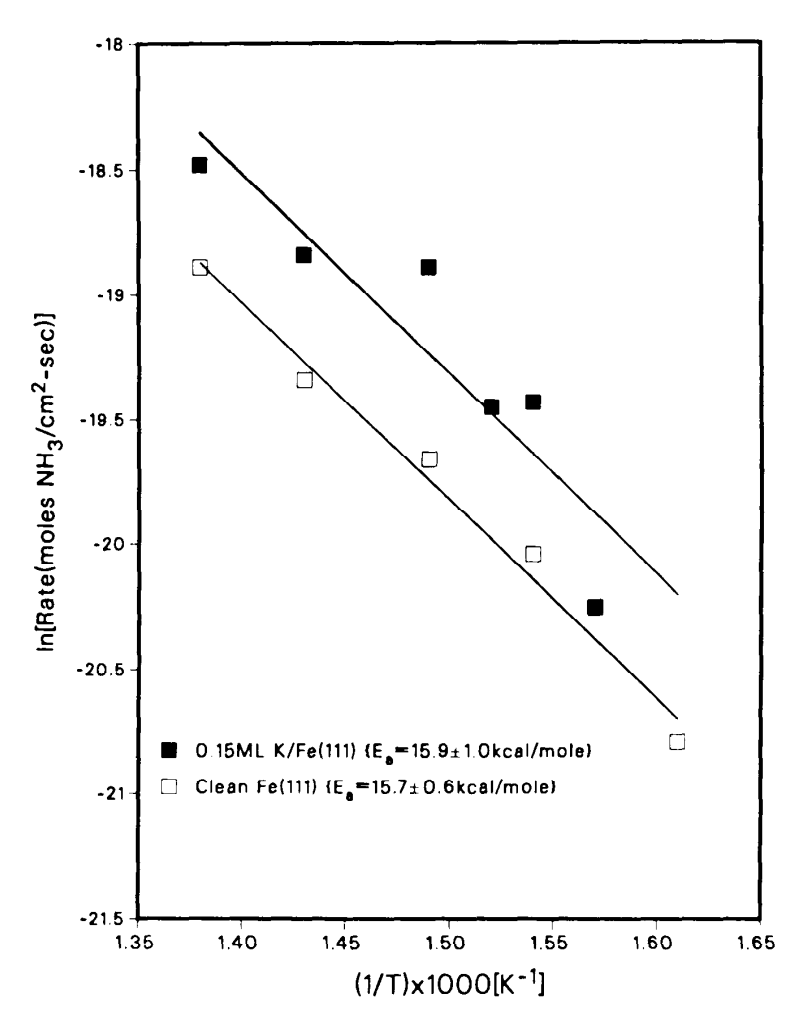


Figure 7.26. The activation energy for ammonia synthesis on Fe(111) and K/Fe(111). Within experimental error there is no change, suggesting that potassium does not change the reaction mechanism of ammonia synthesis [59].

[65]. During this residence on the catalyst, ammonia can either diffuse on the surface or decompose to atomic nitrogen and hydrogen [28, 29, 32]. In both cases the species produced by ammonia might reside on surface sites that would otherwise dissociatively chemisorb gas-phase nitrogen and thereby decrease the rate of ammonia synthesis [28, 29, 32, 66]. The promoter effect of potassium then involves lowering the adsorption energy of the adsorbed ammonia so that the concentration of adsorbed ammonia is decreased. This is supported by the TPD results, which show that ammonia desorption from Fe(111) shifts to lower temperatures when potassium is adsorbed on the surfaces. Even at a 0.1-ML coverage of potassium (coverage roughly equivalent to that stable under ammonia synthesis conditions), the adsorption energy of ammonia is decreased by 2.4 kcal/mole. Thus, the residence time for the adsorbed ammonia is reduced and more of the active sites are available for the dissociation of nitrogen. At higher coverages of potassium, the adsorption energy of ammonia decreases to an even greater extent, but these coverages could not be maintained under ammonia synthesis conditions. There also seems to be an additional adsorption site for ammonia when adsorbed on iron at high coverages of potassium as indicated by the TPD results. The development of a new desorption peak

with coverages of potassium greater than 0.25 ML might result from ammonia molecules interacting directly with potassium atoms, with the negative end of the ammonia dipole interacting with the potassium ion on the iron surface [60]. This interaction appears to be weak, since at a potassium coverage of 1 ML, ammonia desorbs from the surface at 164 K.

Additional experimental evidence supporting the notion that ammonia blocks active sites comes from the post-reaction Auger data. Within experimental error, there is no change in the intensity of the nitrogen Auger peak between a Fe surface and a K/Fe surface after a high-pressure ammonia synthesis reaction. This suggests that potassium does not change the coverage of atomic nitrogen, but instead the presence of potassium helps to inhibit the readsorption or promote the desorption of molecular ammonia on the catalyst. High-pressure reaction conditions are probably needed to stabilize this ammonia product on the iron surface at 673 K, so it will not be present in the ultrahigh vacuum environment. Thus, only the more strongly bound atomic nitrogen will be detected by AES in UHV.

7.8.1.5 Mechanism and Kinetics of Ammonia Synthesis If all the experimental evidence presented in the preceding sections is put together, the reaction scheme for the catalytic synthesis of ammonia on iron-based catalysts can unequivocally be formulated in terms of the following steps:

$$H_2 + * \rightleftharpoons 2H_{ad}$$
 $N_2 + * \rightleftharpoons N_{2,ad}$
 $N_{2,ad} + * \rightleftharpoons 2N_{ad}$
 $N_{ad} + H_{ad} \rightleftharpoons NH_{ad}$
 $NH_{ad} + H_{ad} \rightleftharpoons NH_{2,ad}$
 $NH_{2,ad} + H_{ad} \rightleftharpoons NH_{3,ad}$
 $NH_{3,ad} \rightleftharpoons NH_3 \uparrow$

where * denotes schematically an ensemble of atoms forming an adsorption site.

The progress of the reaction may be rationalized in terms of its energy profile as reproduced in Figure 7.27.

Attempts at theoretical modeling of the kinetics along these lines were recently performed independently by two groups: Bowker et al. [67, 68] and Stolze and Nørskov [69–74]. The latter group starts with the experimentally well-established fact that dissociation of adsorbed nitrogen is rate-limiting. The overall rate can then be calculated from the rate of this step and the equilibrium constants of all the other steps. This reduces the number of input parameters significantly. The adsorption-desorption equilibria are treated with the approximation of competitive Langmuir-type adsorption and by evaluation of the partition functions for the gaseous and adsorbed species. The data for the potassium-promoted Fe(111) surface were used for the rate of dissociative nitrogen adsorption and are also representative of the other crystal planes of the promoted catalyst, as outlined above. The active area of the commercial catalyst was assumed to equal that derived from selective carbon monoxide chemisorption as a well-established standard procedure. A particular

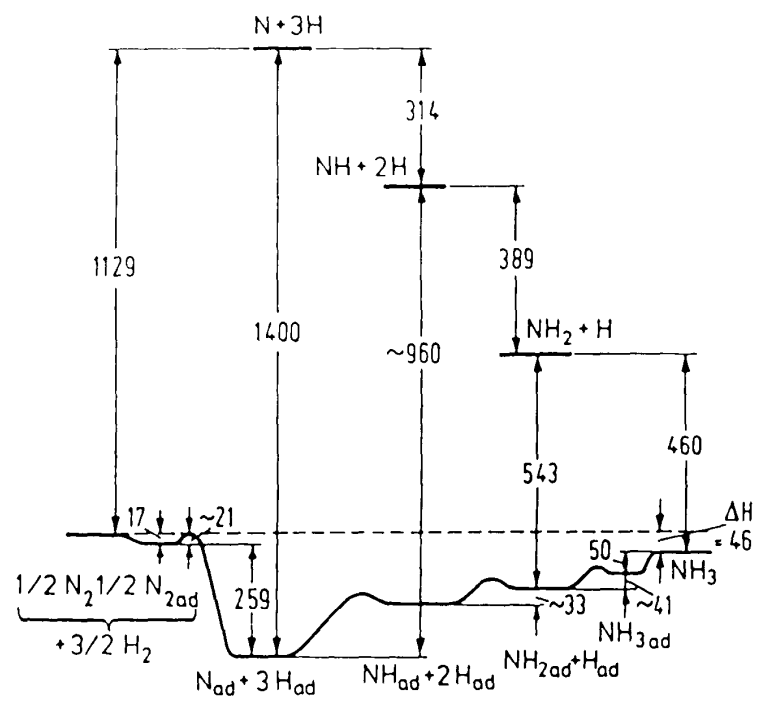


Figure 7.27. Schematic energy profile of the progress of ammonia synthesis on iron (in kJ/mole) [33].

strength of this model is the fact that experimental data from single-crystal studies (such as TPD traces) are reproduced well with the same set of parameters and the same model as used for the determination of the rate under "real" conditions. Comparison of the resulting yields against those determined experimentally with a commercial catalyst yielded general agreement to within a factor better than 2. In Figure 7.28, a compilation of data over a wide range of conditions is presented that demonstrate this almost-too-perfect agreement.

A general conclusion from these models based on single-crystal data is that the most abundant surface species under practical synthesis conditions will be adsorbed atomic nitrogen (>90%), despite the fact that its formation is the rate-limiting step of the overall reaction.

7.8.2 Hydrogenation of Carbon Monoxide

7.8.2.1 Thermodynamics Using relatively easily available small molecules (e.g., CO, H_2 , CO_2 , and H_2O), all of the smaller or larger hydrocarbon molecules could be synthesized by reactions that are thermodynamically feasible. For example, the standard free energies of three of the four reactions that produce methane from these molecules are negative:

CO +
$$3H_2 \rightleftharpoons CH_4 + H_2O$$
 $\Delta G_{298}^0 = -33.4 \text{ kcal/mole}$
 $4CO + 2H_2O \rightleftharpoons CH_4 + 3CO_2$ $\Delta G_{298}^0 = -54.1 \text{ kcal/mole}$
 $CO_2 + H_2 \rightleftharpoons CH_4 + 2H_2O$ $\Delta G_{298}^0 = -26.2 \text{ kcal/mole}$
 $CO_2 + 2H_2O \rightleftharpoons CH_4 + 2O_2$ $\Delta G_{298}^0 = +19.1 \text{ kcal/mole}$

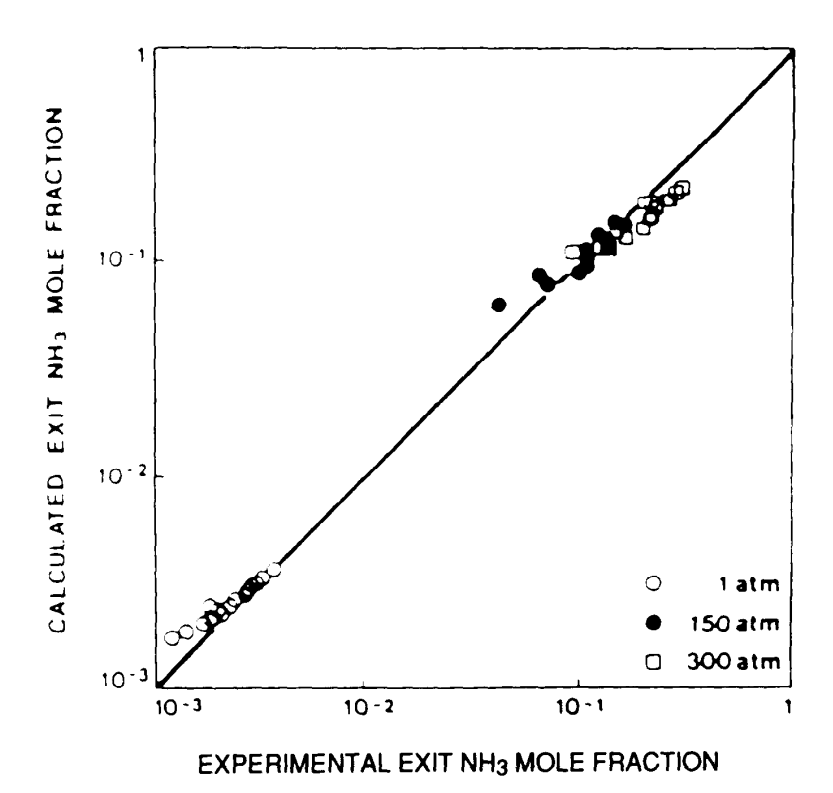


Figure 7.28. Comparison of calculated and measured ammonia production over commercial iron-based catalysts for a broad range of temperatures, pressures, N/H ratios, and gas flows [192].

The only reaction that is thermodynamically uphill is the one between CO₂ and H₂O, which produces oxygen as well. This type of reaction is the basis of photosynthesis, which requires external energy and has played an important role in the evolution of this planet. The other three reactions can be readily carried out using transition metals and their compounds as catalysts.

The usual sources of CO, CO₂, and H₂ are coal or natural gas, which is mostly methane (≈ 72 mole %). The gasification of coal using steam at high temperatures produces predominantly carbon monoxide and hydrogen, a gas mixture that is appropriately called "water gas" or "synthesis gas" ("syn gas"):

Coal +
$$H_2O \rightleftharpoons CO + H_2$$
 $G_{298}^0 = +88 \text{ kJ/mole}$ (7.17)

At lower gasification temperatures ($\approx 900 \text{ K}$) in the presence of appropriate catalysts (CaO and K₂O, for example) the gasification produces almost exclusively CO₂ and H₂:

Coal +
$$2H_2O \stackrel{CaO, K_2O}{\Longrightarrow} CO_2 + 2H_2 \qquad \Delta G_{298}^0 = +60 \text{ kJ/mole}$$
 (7.18)

Both of these reactions are endothermic, and the heat needed to carry them out is often obtained by combustion of some of the coal.

The reaction of steam with methane is another method of obtaining syn gas:

$$CH_4 + H_2O \rightleftharpoons CO + 3H_2 \qquad \Delta G_{298}^0 = +136 \text{ kJ/mole}$$
 (7.19)

This reaction [75] is often called "steam reforming." Once CO, CO₂, and H₂ are obtained, their molar ratio can be adjusted to the desired value using the water-gas shift reaction

$$CO + H_2O \rightleftharpoons CO_2 + H_2 \qquad \Delta G_{298}^0 = -28 \text{ kJ/mole}$$
 (7.20)

This is a virtually thermoneutral reaction that can readily be catalyzed by copper oxide at low temperatures ($\approx 600 \text{ K}$) and by potassium promoted iron oxide at elevated temperatures ($\approx 1000 \text{ K}$).

In recent years the reaction of CH₄ with CO₂ instead of steam was also used to produce syn gas. This is also an endothermic reaction, but in some circumstances there are advantages in using carbon dioxide as an oxidizing agent.

One of the most promising new methods of producing syn gas from methane is by partial oxidation with oxygen directly (e.g., see reference [76]):

CH₄ +
$$\frac{1}{2}$$
O₂ \rightleftharpoons CO + H₂
 $\Delta G_{298}^0 = -20.7 \text{ kcal/mole}, \quad \Delta H_{298}^0 = -8.5 \text{ kcal/mole}$ (7.21)

This is an exothermic reaction that produces H_2 and CO in the 2:1 ratio, which is desirable for the synthesis of many hydrocarbons. By the use of appropriate catalysts, this reaction may be carried out at much lower temperatures than the reactions 7.17 and 7.19.

Using various ratios of carbon monoxide and hydrogen, the production of hydrocarbons of different types is thermodynamically feasible.

Let us consider the formation of alkanes according to the reaction

$$(n + 1)H_2 + 2nCO = C_nH_{2n+2} + nCO_2$$
 (7.22)

$$(2n + 1)H_2 + nCO = C_nH_{2n+2} + nH_2O$$
 (7.23)

Both reactions are thermodynamically feasible, although reaction 7.22 has a somewhat lower negative free energy of formation. Thus the by-product of alkane formation is either CO₂ or H₂O. These reactions are not independent but are related through the water–gas shift reaction. Catalysts that carry out the water–gas shift readily (iron, for example) may produce alkanes and both CO₂ and H₂O, depending on the reaction conditions. Other catalysts that are poor for catalyzing the water–gas shift may produce alkanes and mostly water or mostly CO₂. Catalysts that produce alkanes and CO₂ are often more desirable, because less hydrogen is used up in this circumstance. Hydrogen is generally the costlier of the two reactants. Let us write only one of these reactions for the formation of alkanes, alkenes, and alcohols, which are also produced from CO and H₂, and compare their free energies for formation:

$$(2n + 1)H_2 + nCO \rightleftharpoons C_nH_{2n+2} + nH_2O$$
 (7.24)

$$2nH_2 + nCO \rightleftharpoons C_nH_{2n} + nH_2O \tag{7.25}$$

$$2nH_2 + nCO \rightleftharpoons C_nH_{2n+1}OH + (n-1)H_2O$$
 (7.26)

The reactions that produce higher-molecular-weight hydrocarbon from CO and H₂ are often called Fischer-Tropsch reaction processes, named after their discoverers. The standard free energies of formation of the various products, as a function of temperature, are shown in Figures 7.29, 7.30, and 7.31. Because these are all exothermic reactions, low temperatures favor the formation of the products. At present, however, none of the known catalysts for the hydrogenation of CO can produce hydrocarbons at high enough rates to approach the concentrations that are predicted from thermodynamic equilibrium consideration. In fact, the reaction rates are orders of magnitude lower than the maximum rates calculable at equilibrium. Thus these thermodynamic calculations provide only guidance and boundary conditions of the product distribution that may be produced under various experimental conditions. Because a slow surface reaction step (or perhaps several steps that have large activation energies) controls the rate of the reaction as well as the product distribution (they have low turnover frequencies, 10^{-6} to 10 molecules/surface-atom/sec), higher temperatures (in the range 500-700 K) are usually employed to optimize the rates of formation of the products.

Another reaction that appears to play an important role in the synthesis of hydrocarbons from CO and H_2 is the disproportionation of carbon monoxide:

$$2CO \rightleftharpoons C + CO_2 \qquad \Delta G_{298}^0 = -116 \text{ kJ/mole}$$
 (7.27)

There is a great deal of experimental evidence, which is presented later in the section on methanation, that the hydrogenation of the active form of carbon that

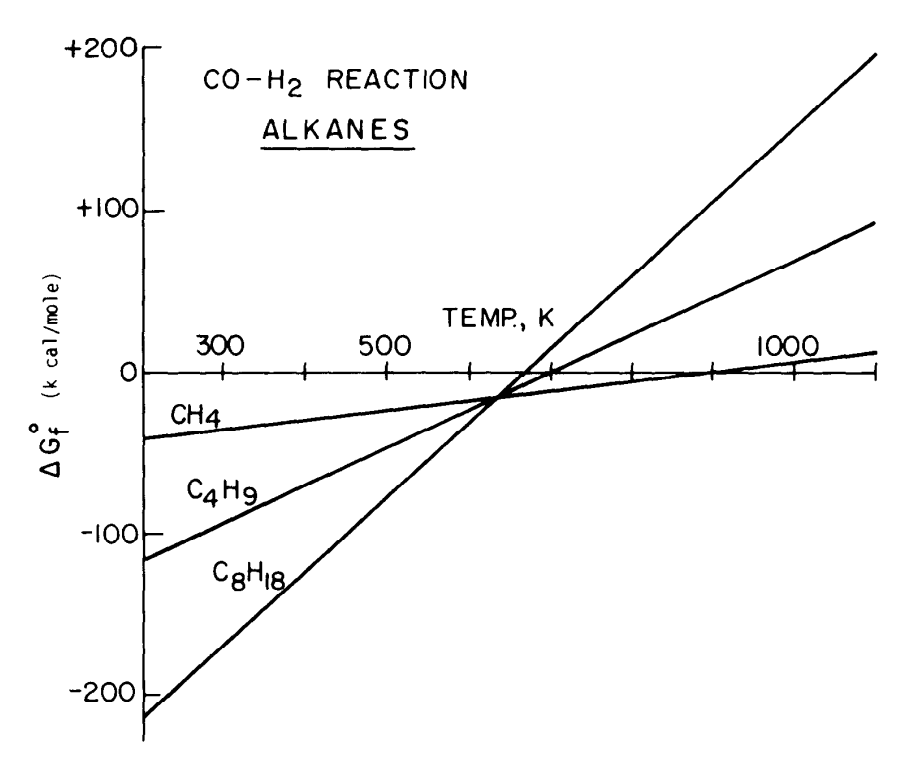


Figure 7.29. Free energies of formation of alkanes from CO and H₂ as a function of temperature.

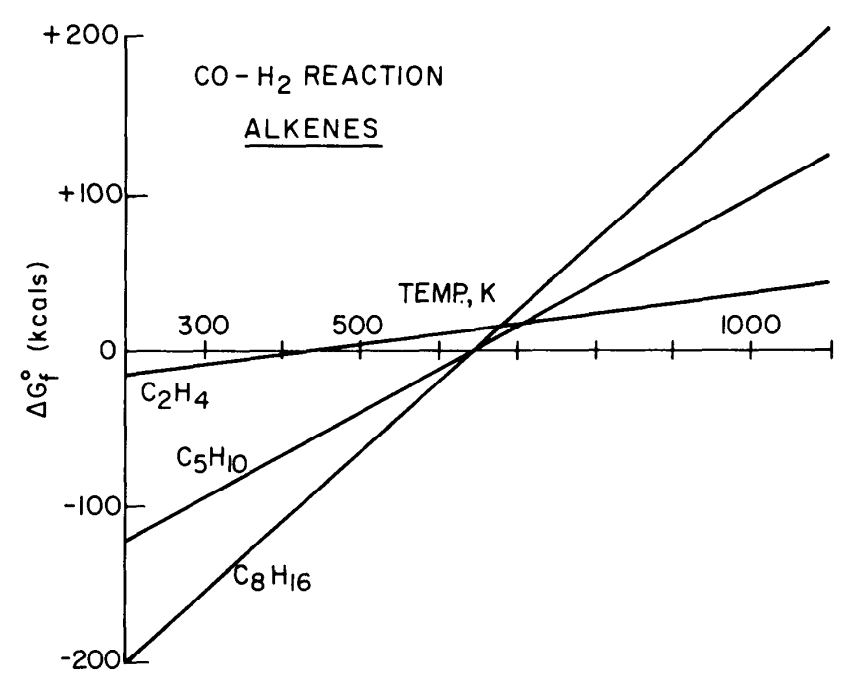


Figure 7.30. Free energies of formation of alkenes from CO and H_2 as a function of temperature.

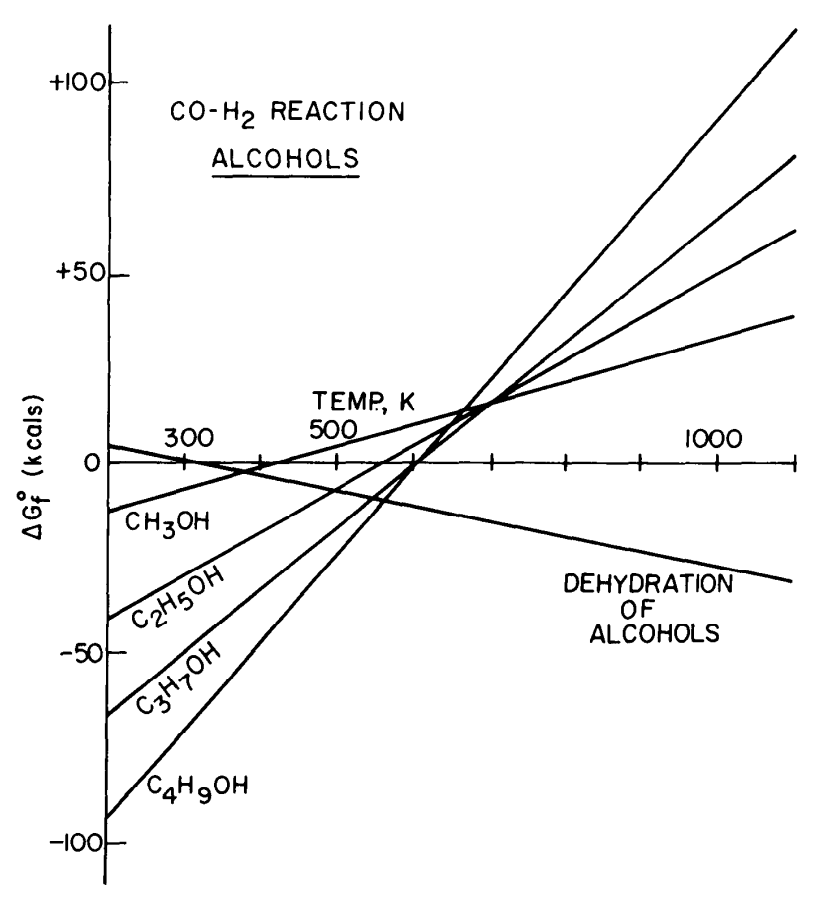


Figure 7.31. Free energies of formation of alcohols from CO and H_2 as a function of temperature.

deposits as a result of the reaction in Eq. 7.27—frequently called the *Boudouard* reaction—leads to the formation of hydrocarbons.

According to the Le Chatelier principle, high pressures favor the association reactions, which are accompanied by a decrease in the number of moles in the reaction mixture as the product molecules are formed. Thus the formation of higher-molecular-weight products is more favorable at high pressures. To demonstrate this [27], let us consider the reaction $aA + bB \rightleftharpoons cC + dD$. The equilibrium constant in terms of partial fugacities is

$$K_f = \frac{(f_{\rm C})^c (f_{\rm D})^d}{(f_{\rm A})^a (f_{\rm B})^b}$$
(7.28)

In terms of partial pressures, this becomes

$$K_P = \frac{(Px_{\rm C})^c (Px_{\rm D})^d}{(Px_{\rm A})^a (Px_{\rm B})^b}$$
 (7.29)

where P is the total pressure and x_A , x_B , and so on, are the mole fractions. It follows that $K_f = K_p K_\gamma$, where $\gamma = f/p$ and

$$K_{\gamma} = \frac{(\gamma x_{\rm C})^{c} (\gamma x_{\rm D})^{d}}{(\gamma x_{\rm A})^{a} (\gamma x_{\rm B})^{b}}$$
(7.30)

The approximation $K_{\gamma} \approx 1$ for Fischer-Tropsch reaction conditions (less than 100 atm) yields

$$\frac{(x_{\rm C})^c (x_{\rm D})^d}{(x_{\rm A})^a (x_{\rm B})^b} = K_f P^{-\Delta n}$$
 (7.31)

where $-\Delta n = a + b - c - d$. Thus, associative reactions, where (a + b) is larger than (c + d), are favored by a pressure increase. For all of the Fischer-Tropsch reactions, (a + b) is larger than (c + d), as a general rule. As an example, for the reaction $3H_2 + CO = CH_4 + H_2O \Delta G_f$ at 730 K and 1 atm equals -11.42 kcal/mole and K equals 3.68×10^3 . At 10^{-4} torr total pressure, $K_f P^2 = 3.68 \times 10^3 \times 1.78 \times 10^{-14} = 6.4 \times 10^{-11}$.

7.8.2.2 Catalyst Preparation Nickel is used most frequently as a catalyst to produce methane. It is usually deposited on high-surface-area oxides such as γ -Al₂O₃ and TiO₂. Potassium is used frequently as a promoter in the catalyst formulation. Copper, copper oxide, and zinc oxide together are used to produce methanol selectively. Small particles of the mixed oxides are used usually without support.

Iron and its compounds (carbide, nitride), as well as ruthenium, cobalt, rhodium, and molybdenum compounds (sulfide, carbide), are used most frequently to produce high-molecular-weight hydrocarbons. Iron can be prepared as a high-surface-area catalyst ($\approx 300~\text{m}^2/\text{g}$) even without using a microporous oxide support. γ -Al₂O₃, TiO₂, and silica are frequently used as supports of the dispersed transition-metal particles. Recently zeolites, as well as thorium oxide and lanthanum oxide, have

been employed with success as catalyst supports and as active catalyst components that alter the product distribution.

Potassium is used most frequently as a promoter to increase the molecular weight of the organic products and reduce the hydrogenation rate during the reactions that leads to the formation of unsaturated hydrocarbon. Bimetallic systems are utilized frequently to change the product distribution during CO hydrogenation. Copper and manganese, rhodium, platinum, palladium with iron, and two catalytically active transition metals with various combinations (Fe-Co, Fe-Ru) are used to alter product selectivity.

7.8.2.3 Methanation. Kinetics, Surface Science, Mechanisms One of the main products of the hydrogenation of CO is methane. It is produced almost exclusively over nickel, while it forms together with higher-molecular-weight hydrocarbons over many other transition-metal surfaces. Vannice [77] has determined the relative activity of various transition metals for methanation at 1 atm total pressure under conditions in which most other hydrocarbon molecules are not likely to form because of thermodynamic limitation. The order of decreasing activity is Ru > Fe > Ni > Co > Rh > Pd > Pt > Ir. The activation energy for methanation from CO and H₂ is in the range 23-25 kcal/mole for ruthenium, iron, nickel, cobalt, and rhodium metals, for which this has been determined. The nearly identical activation energies indicate that the mechanism of methanation is likely to be similar. Recent studies in several laboratories clearly show that the dominant mechanism involves the dissociation of CO followed by the hydrogenation of the surface carbon atoms to methane. The adsorbed oxygen is removed from the surface as CO₂ by reaction with another CO molecule. The net process by which the active surface carbon that is to be hydrogenated forms is often described as the disproportionation of CO:

$$2CO \rightleftharpoons C + CO_2 \tag{7.32}$$

This is called the *Boudouard reaction*. This mechanism has been confirmed in several ways. The formation of a carbonaceous overlayer has been detected on polycrystalline rhodium [27] and on iron and nickel surfaces [78, 79] in CO- H_2 mixtures in the temperature range 500-700 K. After pumping out the reaction mixture and introducing hydrogen, methane is produced at the same rate as in the presence of water gas. Ventrcek et al. [80] and Rabo et al. [81] have been able to titrate the amount of surface carbon by quantitative measurement of the amount of CO_2 evolved $(2CO \rightleftharpoons C + CO_2)$ over nickel, ruthenium, and cobalt catalyst surfaces, respectively. Rabo et al. [81] have introduced pulses of H_2 after forming the surface carbon to produce predominantly methane. Biloen et al. [82] have deposited the active surface carbon on nickel, cobalt, and ruthenium by dissociating labeled ^{13}CO . The isotopically labeled carbon layer is readily hydrogenated subsequently in the presence of a $CO-H_2$ mixture to yield labeled $^{13}CH_4$.

The active surface carbon that forms from the dissociation of CO maintains its activity to produce methane only in a rather narrow temperature range. Above 700 K the carbon layer becomes graphitized and loses its reactivity with hydrogen. At temperatures below 450 K, the dissociation rate of CO to produce the active carbon is too slow to produce the active surface carbon in high enough concentrations. The temperature dependence of the nature of the CO and carbon chemical bonds intro-

duces a narrow range of conditions for the production of methane. The fact that the dissociation of molecules on surfaces is an activated process is well established by many studies of the formation of surface chemical bonds.

However, changes in the chemical activity of the surface carbon that forms are less well established. The unique hydrogenation activity of the carbon that forms upon the dissociation of carbon monoxide on transition-metal surfaces in the range 450-700 K indicates the formation of active carbon-metal bonds that deserve further experimental scrutiny. The formation of reactive carbene or carbyne species is not unlikely, because these active metal-carbon bonds can yield the hydrogenation activity that was detected. Araki and Ponec [79] have compared the catalytic activity of nickel and nickel-copper alloys for methanation. Upon the addition of less than 10 atom % of copper, the activity drastically decreased. Their results indicate that more than one nickel atom is involved in forming the strong and active metal-carbon bond that yields methane by direct hydrogenation. Because ethylidyne molecules were detected on the Pt(111) crystal face upon adsorption of C_2H_4 and C_2H_2 , where the strongly bound carbon is in a threefold site [83], a similar location for the carbon or CH fragments on nickel surfaces [84], which would bind them to three or four nickel atoms, seems likely. The active carbon is metastable with respect to the formation of graphite, however. Heating to above 700 K produces a stable graphite surface layer that is unreactive with hydrogen. Once the graphitic carbon is formed, the catalyst loses its activity for the formation of hydrocarbons of any type. The rate of methane formation is usually positive order (often first order) in hydrogen pressure and negative order in CO pressure.

While the hydrogenation of the active surface carbon that forms from CO dissociation appears to be the predominant mechanism of CH₄ formation, it is not the only mechanism that produces methane. Poutsma et al. [85] have detected the formation of CH₄ over palladium surfaces that do not readily dissociate carbon monoxide. They also observed methane formation over nickel surfaces at 300 K under conditions in which only molecular carbon monoxide appears to be present on the catalyst surfaces [81]. Vannice [86] also reported the formation of methane over platinum, palladium, and iridium surfaces, and independent experiments indicate the absence of carbon monoxide dissociation over these transition-metal catalysts in most cases. It appears that the direct hydrogenation of molecular carbon monoxide can also occur but that this reaction has a much lower rate than methane formation via the hydrogenation of the active carbon that is produced from the dissociation of carbon monoxide in the appropriate temperature range.

Another mechanism, proposed by Pichler [87] and Emmettt [88, 89], involves the direct hydrogenation of molecular carbon monoxide to an enol species, followed by dehydration and further hydrogenation to produce methane. It is likely that this mechanism provides an additional reaction channel that may compete over certain transition-metal catalysts with CH₄ formation via the dissociation of carbon monoxide. Recent studies of methane formation over molybdenum indicate positive CO and H₂ pressure dependencies of the reaction rate

$$R_{\rm CH_4} \propto (P_{\rm H_2})^{1.0} (P_{\rm CO})^{0.5}$$
 (7.33)

This could be an indication of the formation of an enol intermediate.

The chemistry of C_{Ni} formed from CO disproportionation and from other carbon

sources has been further investigated by Rabo et al. [90]. It was found that the $C_{\rm Ni}$ reacts readily with water. Upon injecting a pulse of steam at 600 K over freshly prepared $C_{\rm Ni}$, this species rapidly reacted with water to form equimolar CO_2 and CH_4 according to the equation

$$2C_{N_1} + 2H_2O \stackrel{600K}{\rightleftharpoons} CO_2 + CH_4$$
 (7.34)

These experimental results are consistent with the thermodynamics of the reaction between carbon and water. At low temperatures they favor the formation of methane, in contrast to the same reaction occurring at high temperatures where the product is $CO + H_2$. The fresh C_{N_i} species reacts readily with both H_2 and H_2O , whereas this species aged at higher temperatures is rendered substantially inert to both. The reaction of C_{N_i} with H_2O , similar to the reaction of C_{N_i} with H_2 , is rapid at about 600 K, reaching 90% conversion of the C_{N_i} layer in a few minutes.

The formation of C_{Ni} from CO, according to the Boudouard reaction, is exothermic. The reaction of C_{Ni}^{CO} with H_2O is also exothermic. This latter observation is in contrast to the reaction of graphite and water, which is calculated to be endothermic at about 600 K by about 3 kcal/mole. The exothermic nature of the reaction between C_{Ni} and H_2O indicates a higher-energy state for C_{Ni} relative to graphite.

An interesting change in the kinetics of methanation was observed by Castner et al. [91] when the reaction rates were monitored over clean rhodium and oxidized rhodium surfaces in CO-H₂ and CO₂-H₂ gas mixtures. The rates obtained at 600 K, the activation energies, and the preexponential factors for methanation are listed in Table 7.47. The turnover frequencies are much greater and the activation energies are much lower over the preoxidized metal surface. It appears that the oxidized metal surface is not only a better catalyst, but the mechanism of methanation is very different, as indicated by the large change in the kinetic parameters. The activation energy for methane formation is in the 12- to 15-kcal range over the oxidized surface and also when CO₂-H₂ gas mixtures are used for the reaction instead of CO and H₂, in contrast with the 24-kcal activation energy for this reaction on clean metal surfaces. High-resolution electron spectroscopy studies revealed that CO₂ dissociates on the clean rhodium surface to CO and O, and thus the molecule may act as an oxidizing agent on the clean metal surface. It is then likely that the CO₂-H₂ reaction occurs on a partially oxidized rhodium surface, and for this reason it exhibits similar kinetics to the CO-H₂ reaction on the oxidized metal surface.

Surface-science studies using nickel single-crystal surfaces revealed that the methanation reaction is surface-structure-insensitive. Both the (111) and (100) crystal faces yield the same reaction rates over a wide temperature range. These specific rates are also the same as those found for alumina-supported nickel, further proving the structure insensitivity of the process. This is also the case for the reaction over ruthenium, rhodium, molybdenum, and iron.

7.8.2.4 Promotion of the Rates of C—O Bond Hydrogenation by the Oxide-Metal Interface CO hydrogenation catalysis has benefited greatly from the rediscovery of the unique catalytic behavior of oxide-metal interfaces first observed by Schwab [92]. The effect is commonly referred to as strong metal-support interaction, or SMSI (see also reference [93]). Tauster et al. [94, 95] reported large enhancement

in the CO hydrogenation rates for transition-metal catalysts when supported on highsurface-area titanium oxide. This effect is clearly shown in Figure 7.32, where the rate of methane formation from CO and H₂ is compared for different nickel catalysts. These include unsupported nickel and nickel deposited on silica, alumina, and titanium oxide. As can be seen, the nickel deposited on titanium oxide is orders of magnitude more active for CO hydrogenation than the pure, unsupported nickel catalyst. Subsequent studies of catalyst activation involving reduction and reoxidation using H₂ and O₂, respectively, indicated that the catalyst is activated by optimizing the oxide-metal interface area. Because the same catalytic behavior can be obtained by depositing the metal on the oxide support or by deposition of oxide islands on the transition metal, the oxide-metal periphery area is implicated as the active site responsible for the increased reaction rates. A typical reaction rate behavior exhibits a maximum with increasing oxide coverage over a transition-metal catalyst as shown in Figure 7.33 for CO₂ hydrogenation over TiO₂ on Rh. The oxide alone is inactive while the metal is active for methane formation. At about 50% of a monolayer of oxide coverage, which corresponds to the optimum oxide-metal interface area, the reaction rate exhibits a maximum.

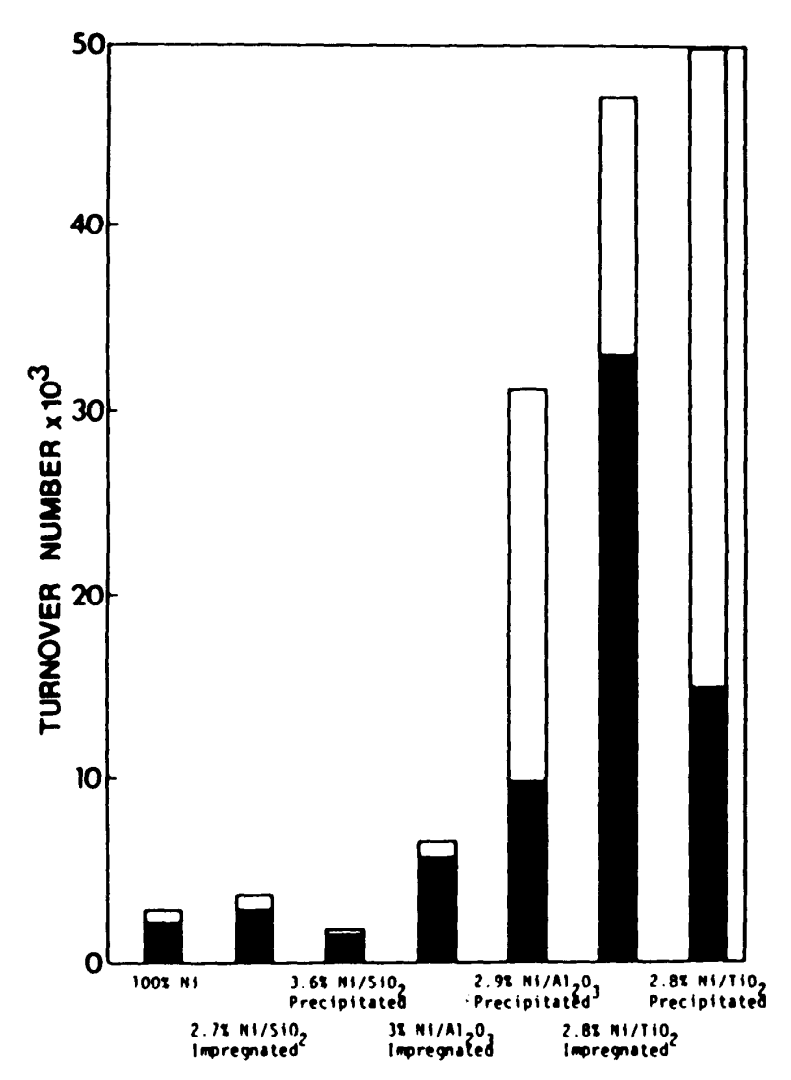


Figure 7.32. Effect of support on CO hydrogenation over Ni catalysts [193].

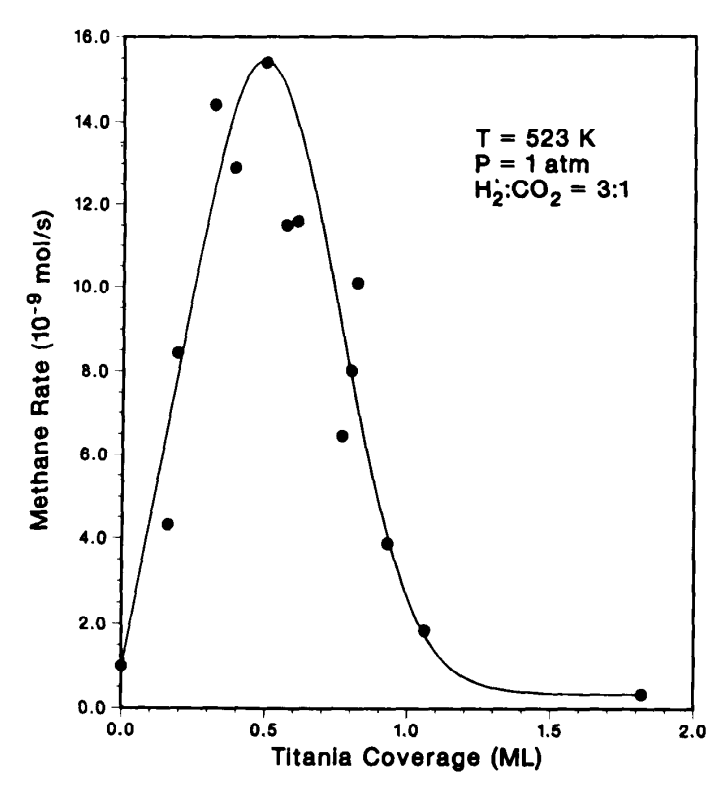


Figure 7.33. CO₂ hydrogenation rate over the rhodium-titanium oxide catalyst as a function of oxide coverage of the metal [194].

This large oxide-metal interface catalysis effect is observed for several transition metals (including Ni, Rh, Co, and Fe) and for several oxides (including TiO_2 , La_2O_3 , Nb_2O_5 , and Ta_2O_5). In addition to CO activation, other molecules that have CO bonds (CO_2 , acetone, alcohols) are also activated for hydrogenation.

This oxide-metal interface activation phenomenon is under intense investigation in many laboratories because several new catalyst systems have been reported based on SMSI [96-126]. Recent studies indicate a correlation between the Lewis acidity of high oxidation state transition metal oxides (utilized as supports) and the enhancement of the reaction rates: The stronger the Lewis acidity of the oxide, the greater the activity of the oxide-metal interface catalyst. The scanning tunneling microscope (STM) has been able to image the oxide-metal interface on the atomic scale. It is suggested that the periodic restructuring of metal atoms that drives the catalytic reaction can occur at faster rates at the oxide-metal interface, leading to enhanced catalytic activity. It is hoped that STM experiments that are performed while the reaction is occurring can investigate the dynamic changes of surface structure at the oxide-metal interface and elsewhere on the surface of the active catalyst.

If the predominant reaction mechanism involves CO dissociation (as appears to be the case over nickel and most other transition-metal catalysts), methane formation may be expressed by writing the following elementary surface reaction steps:

$$CO \rightleftharpoons C + O$$
 $CO + O \rightleftharpoons CO_2$
 $C + H \rightleftharpoons CH + 3H \rightleftharpoons CH_2 + 2H \rightleftharpoons CH_3 + H \rightleftharpoons CH_4 \uparrow$

All of the species are reacting in their adsorbed states. If enol species form as reaction intermediates as suggested for CO hydrogenation over molybdenum, the elementary surface reaction sequence may be expressed as follows:

CO + 2H
$$\rightleftharpoons$$
 CHOH
CHOH + H \rightleftharpoons CH + H₂O \uparrow
CH + 3H \rightleftharpoons CH₂ + 2H \rightleftharpoons CH₃ + H \rightleftharpoons CH₄ \uparrow

7.8.2.5 Methanol Production. Kinetics, Surface Science, and Mechanisms Methanol production from CO, CO_2 , and H_2 is an industrial process that yields about 3×10^6 kg per day. The relevant thermodynamic parameters for the two reactions are [127]

CO + 2H₂
$$\rightleftharpoons$$
 CH₃OH $\Delta H_{600}^0 = -100.5 \text{ kJ/mole}$
 $\Delta G_{600}^0 = +45.4 \text{ kJ/mole}$
CO₂ + 3H₂ \rightleftharpoons CH₃OH + H₂O $\Delta H_{600}^0 = -61.6 \text{ kJ/mole}$
 $\Delta G_{600}^0 = +61.8 \text{ kJ/mole}$

Over copper-based catalysts the water-gas shift reaction may also occur in the presence of the three reacting molecules [127].

The activation energy for the reaction is about 64 kJ/mole, and it is usually carried out in the 530- to 580-K temperature range and a few atmospheres of total pressure [127].

The first catalyst utilized was a mixed ZnO/Cr_2O_3 oxide catalyst that operated at high temperatures (700 K) and at high pressures (100 atm). The catalyst presently used is Cu/ZnO with Al or Cr promoters that operates at much lower temperatures and atmospheric pressures [127].

There are continuing questions about the oxidation state of copper during the reaction. The observation that indicates that metallic copper plays an important role during the reaction is that reaction rate appears to be proportional to the metallic copper surface area over Al-promoted Cu/ZnO catalysts. However, over the binary Cu/ZnO catalyst no correlation between the rate of methanol formation and copper surface area is found. The presence of partially oxidized copper on the catalyst surface was detected by recent EXAFS studies and by temperature-programmed reduction [127]. Surface-science studies using Cu(310) crystal surfaces covered with ZnO islands indicate the presence of strongly chemisorbed oxygen on the metal and that oxygen from zinc oxide can readily spill over to the copper.

There is evidence that the hydrogenation of both CO and CO_2 can produce methanol, depending on catalyst formulation and the reaction conditions. Over a cesium-promoted Cu/ZnO catalyst, methanol forms from CO and H_2 without the presence of CO_2 . In this circumstance CO is the primary reactant. Isotope labeling studies using ^{14}C -labeled $^{14}CO_2$ in a reactant mixture of $H_2/^{12}CO/^{14}CO_2$ over $Cu/ZnO/Al_2O_3$ catalysts detected only ^{14}C -labeled methanol, implicating CO_2 as the primary reactant. It appears that over most Cu/ZnO catalysts both CO and CO_2 may hydrogenate to produce methanol and that CO hydrogenation is retarded by CO_2 , but the reverse is not true [127].

The presence of H₂O accelerates methanol production at low concentrations, and

the use of D_2O yields $CH_2DOH(D)$. H_2O is a reaction inhibitor at high concentrations. These results implicate water as a possible reactant and point to the importance of the water-gas shift reaction during the synthesis of methanol [127].

Surface-science studies using copper single-crystal surfaces of (110) and (310) orientation onto which ZnO islands had been deposited indicate that CO and CO₂ chemisorption can be used to identify the metal and the oxide sites, respectively. Methanol chemisorption produces both formate and methoxy species. The concentration of formate is enhanced by the presence of ZnO-copper interfaces, implicating these species as a reaction intermediate.

Palladium dispersed on silica or on other supports (La₂O₃, ZrO₂, etc.) can also form methanol selectively [127]. Surface-science investigations produced methanol on the Pd(110) crystal face without the presence of any oxide near atmospheric pressures and at 550 K. The activation energy was 74 kJ/mole.

Because the catalysts, copper, palladium, and zinc oxide do not dissociate CO, the hydrogenation of molecular CO is one of the likely mechanisms for methanol formation:

$$CO + 2H \rightleftharpoons CH - OH + H \rightleftharpoons CH_2 - OH + H \rightleftharpoons CH_3OH$$
 (7.35)

Carbon dioxide may dissociate to CO and O or it may also hydrogenate to produce a formate intermediate, $CO_2 + H \rightleftharpoons HCOO$. Further hydrogenation leads to the formation of methanol and water by a series of elementary reaction steps that are yet to be investigated.

7.8.2.6 Production of Higher-Molecular-Weight Hydrocarbons. Kinetics, Surface Science, and Mechanisms The hydrogenation of carbon monoxide over iron, cobalt, and ruthenium surfaces produces a mixture of hydrocarbons with a wide range of molecular-weight distribution. Most of the hydrocarbons produced are normal paraffins; however, olefins and alcohols in smaller concentrations are also obtained.

The wide product distribution indicates that a polymerization mechanism may be operative. Some of the reaction intermediates serve as chain initiators; then the chain propagation proceeds rapidly until termination by hydrogen occurs before the molecule desorbs from the catalyst surface. The distribution of reaction products, which has been shown to follow a Schulz-Flory [128, 129] distribution of molecular weights frequently encountered in polymerization processes, is given by

$$M(P) = (\ln \alpha)^2 P \alpha^P \tag{7.36}$$

where M(P) is the weight fraction of hydrocarbons containing P carbon atoms. The chain-growth probability factor is defined as

$$\alpha = R_P / (R_P + R_T) \tag{7.37}$$

where R_P and R_T are the rate of propagation and termination, respectively. Equation 7.36 can be expressed in logarithmic form as

$$\ln \frac{M(P)}{P} = \ln (\ln^2 \alpha) + P \ln \alpha \tag{7.38}$$

A plot of $\ln (M(P)/P)$ versus P yields a value of α from either the slope or the ordinate intercept. Agreement between the slope and intercept is used as a criterion of the soundness of Schulz-Flory fit. A typical product distribution of CO hydrogenation that reflects the polymerization kinetics is shown in Figure 7.34.

Dwyer and Somorjai [130] have studied the Fischer-Tropsch reaction using a polycrystalline iron foil of 1-cm² surface area; and the reaction was carried out with a hydrogen/carbon monoxide ratio of 3:1, at 6 atm and 600 K. At the low conversions (below 1%) obtained under these conditions, the products are primarily methane and ethylene, with trace amounts of other α -olefins up to C₅. This product distribution is compared with that obtained from pilot-plant studies over iron catalysts under industrial conditions and at high conversions (85%). Under industrial conditions, high-molecular-weight paraffins are obtained in large concentrations. In order to simulate the experimental conditions that exist at high conversions, Dwyer and Somorjai [130] have added ethylene to the synthesis gas, since C₂H₄ was one of the products detected. The fate of ethylene was then monitored as a function of reaction time. The majority of the ethylene was hydrogenated to ethane. However, about 10% of the added ethylene was converted to other hydrocarbons. The conversion of ethylene to other hydrocarbons had a significant impact on the product distribution of the CO-H₂ reaction. The relative amount of C₃ to C₅ hydrocarbons increased due to the presence of ethylene in the synthesis gas. The influence of ethylene concentration on the product distribution was investigated by varying the partial pressure of ethylene between 2 and 150 torr, while the H₂/CO ratio was held constant at 3:1 and at a total pressure of 6 atm. As the initial ethylene partial pressure is increased, the relative amount of methane in the product distribution decreased, although the amount of methane formed remains largely unchanged. The C₅₊ fraction, however, increases with increasing ethylene in an almost linear fashion. The C_3 and C_4 fractions increase to limiting values.

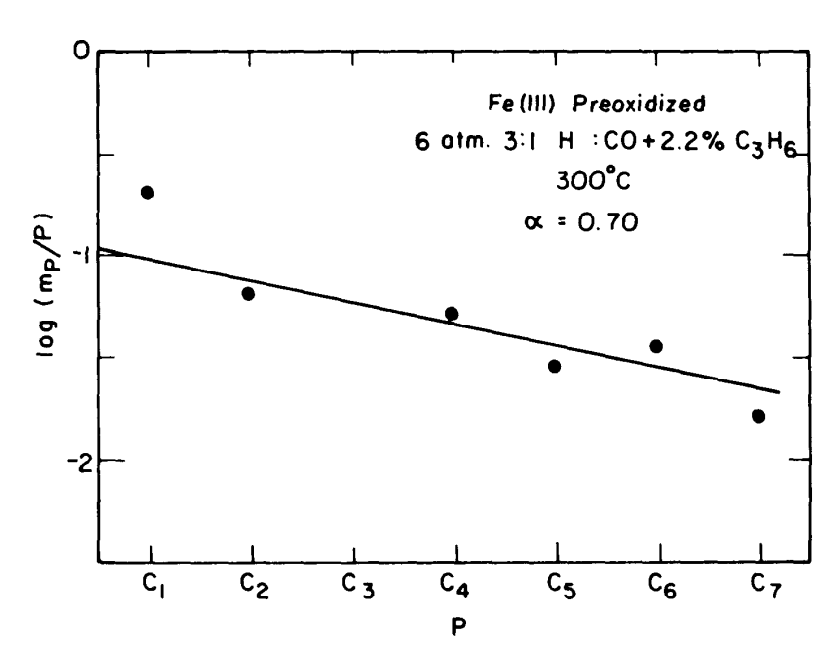


Figure 7.34. Plot of the hydrocarbon distribution in the CO-H₂ reaction over iron that reflects the polymerization kinetics [130].

Experiments in which propylene was added to synthesis gas produced results similar to those when ethylene was added. Propylene seems to produce larger molecules than did the same amount of added ethylene. By adding small concentrations of propylene, it is possible to obtain the product distribution found under high-conversion conditions.

Considerable work has been published concerning the incorporation of radioactive-isotope-labeled olefins in hydrocarbons during Fischer-Tropsch reactions. The pioneering work of Kummer and Emmett [89] and of Hall et al. [88] suggested that ethylene acted as a chain initiator over iron catalysts. The same results were obtained over cobalt catalyst by Eidus et al. [131].

It has long been suspected that α -olefins are the primary products of Fischer-Tropsch synthesis, although they are thermodynamically unstable under the reaction conditions. It appears that readsorption and subsequent secondary reactions of α -olefins occur readily under Fischer-Tropsch conditions. Readsorption and secondary reaction of these olefins may be a major reaction pathway leading to the growth of hydrocarbon molecules during Fischer-Tropsch synthesis. In standard flow reactors with large-surface-area catalysts, it is expected that at the leading edge of the bed, the product distribution will be similar to that obtained at low conversions. As these initial reaction products proceed along the bed, they will be readsorbed and undergo secondary reactions, leading to higher-molecular-weight products. As a result of the changing product distribution along the catalyst bed, the surface composition of the catalyst is also likely to change. The presence of readsorption as an important reaction step should permit one to devise ways of controlling the product distribution. Various additives to the reactant mixture, changing the size and geometry of the catalyst bed, and mixing of catalysts are among the experimental variables that may be used to tailor product distribution in the Fischer-Tropsch reaction.

We may then write the formation of high-molecular-weight hydrocarbons over iron or ruthenium surfaces as a two-step process, starting with olefin production:

$$2CO + 4H_2 \underset{550-650 \text{ K}}{\rightleftharpoons} C_2H_4(C_3H_6) + 2H_2O$$
 (7.39)

This is followed by the readsorption of olefins that induces polymerization:

CO +
$$H_2$$
 $\xrightarrow{\text{Fe, C}_2\text{H}_4(\text{C}_3\text{H}_6)}$ $C_{5-9}H_{12-20} + 2H_2\text{O}$ (7.40)

Recent studies of the CO-H₂ reaction on ruthenium surfaces have also shown the importance of readsorption on the metal catalyst surface. The presence of a multiple-step reaction that proceeds via the readsorption of the initial products provides opportunities for altering the product distribution by using several different catalysts simultaneously in the reaction mixture. By physical mixing of two catalysts, for example, experimental conditions can be realized where the olefins readsorb and further react on the other catalyst instead of on the iron catalyst surface. This way the product distribution can be changed to obtain molecules that are more desirable than the saturated straight-chain hydrocarbons. Chang and Silvestri [132] and Lechthaler and co-workers [133] have reported on a process that converts CO and

H₂ to aromatic molecules or to high-octane-number gasoline. First, methanol and olefins are produced by the catalytic reactions of CO and H₂, as discussed above. Then, using a zeolite shape-selective catalyst that is introduced along with the ruthenium or other metal catalyst in the same reaction chamber, methanol and the olefins are converted to aromatic molecules, cycloparaffins, and paraffins. The mechanism involves the dehydration of methanol to dimethyl ether. The light olefins that also form are alkylated by methanol and by the dimethyl ether [134] to produce higher-molecular-weight olefins and then the final cyclic and aromatic products.

The formation of aromatic molecules from CO and H_2 over ThO_2 surfaces has been reported at higher temperatures [87], whereas C_4 isomers were produced at lower temperatures and high pressures over the same catalyst (isosynthesis). However, the mechanism of this reaction has not yet been subjected to detailed scientific scrutiny.

During CO hydrogenation over transition-metal surfaces, the presence of potassium usually increases the rate and also selectivities for C_{2+} hydrocarbon production as expected if the CO dissociation rate is increased. As noted earlier, potassium adsorbed on transition metals exists in largely ionic states; this results from the transfer of valence charge density into the metal d-band, which reduces the metal work function. This charge transfer has a profound influence on the adsorption behavior of CO a revealed by thermal desorption and vibrational spectroscopy studies using platinum, nickel, and ruthenium single-crystal surfaces. In all cases, the CO desorption temperature is increased by 100-200 K in the presence of potassium [135, 136] reflecting a 5- to 12-kcal/mole increase in the heat of molecular CO chemisorption. In addition, the CO bond is weakened substantially as compared to adsorption on clean metal surfaces. Figure 7.35 illustrates the HREELS spectra for CO coadsorbed with potassium at several coverages on the hexagonal (111) platinum surface. With increasing coverage, there is a continued shift of the CO stretching frequencies from 1875 and 2120 cm⁻¹ to 1565 cm⁻¹. These shifts correlate with a change in bonding from mostly top sites to bridge sites and a decrease in CO bond order from 2.0 to 1.5. This dramatic bond weakening reflects enhanced population of the CO $2\pi^*$ antibonding orbital as a result of the increased density of metal electronic states in the presence of potassium. One should anticipate that the weakened CO bond and strengthened metal-carbon bond would facilitate CO dissociation. This was demonstrated by Campbell and Goodman [137] using nickel (100) where the CO dissociation rate was increased fourfold at potassium coverage of 10% of a monolayer. The activation energy for CO dissociation was also lowered from about 23 to 10 kcal/mole.

It is now clearly established that potassium chemisorbed on transition metals functions as an unusually powerful donor. This increases the density of surface electron states available for back-bonding with certain adsorbates, if they possess orbitals with energy and symmetry that correlate near the Fermi energy of the metal. Examples of such orbitals would be the $2\pi^*$ of CO and N_2 . The important general consequences of this interaction include increased heat of molecular adsorption and increased dissociation probability.

On the clean rhodium (111) surface, CO stays molecularly adsorbed at low pressures while it dissociates in the presence of potassium [138, 139]. This can be studied by the adsorption of a mixture of ¹²C¹⁸O and ¹³C¹⁶O and detecting ¹³C¹⁸O and ¹²C¹⁶O, the products of scrambling, which clearly identify the dissociation of mo-

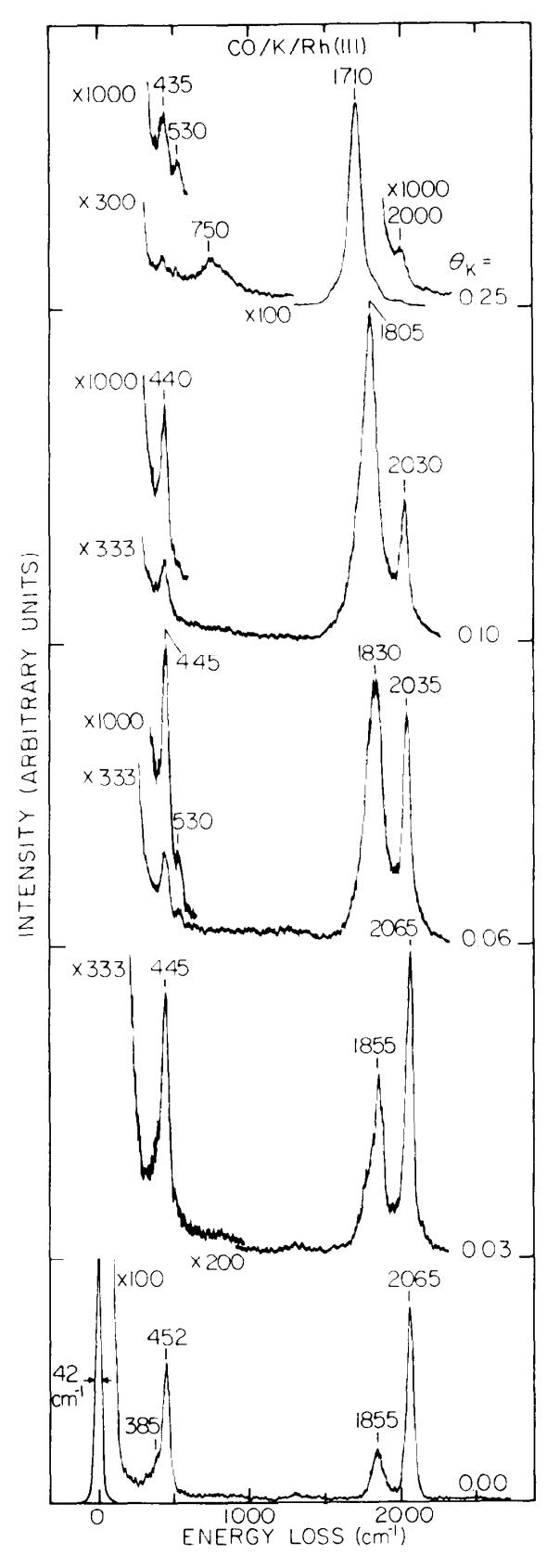


Figure 7.35. Vibrational spectra of CO at saturation coverage when chemisorbed on Rh(111) at 300 K as a function of preadsorbed potassium coverage [139].

lecular CO on the metal surface. In Figure 6.26, we show that three CO molecules may dissociate per potassium atom at a potassium coverage where maximum charge transfer to the transition metal occurs. The reduction of the hydrogenation ability of the catalyst induced by potassium is another reason for the markedly altered product distribution. Manganese oxides, when used as promoters, also increase the olefin selectivities. Thorium oxide and lanthanum oxide promote the formation of branched hydrocarbons and also enhance the selectivity for light olefins. Alkali-promoted molybdenum proves to be an excellent, sulfur-resistant catalyst.

When titania is used as a support for cobalt iron or ruthenium, very active catalysts are prepared, indicating the importance of certain oxide-metal interfaces as active sites for CO hydrogenation.

Zeolites as co-catalysts shift the product distribution because their acid sites can carry out secondary reactions such as alkylation, cracking, oligomerization, and isomerization. These reactions can be important in shifting selectivities toward high-octane gasoline or olefins.

7.8.2.7 Formation of Oxygenated Hydrocarbons from CO and H_2 and Organic Molecules The carbonylation of methanol produces acetic acid:

$$CH_3OH + CO \rightleftharpoons CH_3COOH$$
 (7.41)

This reaction is carried out over rhodium carbonyls as catalyst using HI as a promoter. Acetic anhydride is produced from the carbonylation of methylacetate over lithium-iodide-promoted rhodium catalyst:

$$CH_3COOCH_3 + CO \rightleftharpoons (CH_3CO)_2O$$
 (7.42)

The hydroformylation reaction produces aldehydes from olefins, CO and H_2 . For example,

$$CH_2 = CH_2 + CO + H_2 \rightleftharpoons H_3C - CH_2 - CHO$$
 (7.43)

Rhodium, cobalt, and ruthenium are the most frequently used catalysts to carry out this family of reactions.

7.8.3 Hydrocarbon Conversion on Platinum

7.8.3.1 Introduction Platinum is one of the most versatile, all-purpose, heterogeneous metal catalysts. It is employed under reducing conditions (in the presence of excess hydrogen) for the conversion of aliphatic straight-chain hydrocarbons to aromatic molecules (dehydrocyclization) and to branched molecules (isomerization), and for hydrogenation on a large scale in the chemical and petroleum-refining industries [140–142]. It is also used as an oxidation catalyst for ammonia oxidation, an important step in the process of producing fertilizers [143, 144]. Platinum is the catalyst for the oxidation of carbon monoxide and unburned hydrocarbons in the control of car emissions [145, 146]. Platinum is perhaps the most widely used and most active electrode for catalyzed reactions in electrochemical cells [147–150]. Its chemical stability in both oxidizing and reducing conditions makes this metal an

ideal catalyst in many applications. Mined mostly in South Africa and in Russia, platinum, along with rhodium (which occurs as an impurity in platinum ores), is very rare and therefore expensive. Its regeneration and recovery must be an important part of any technology that uses this metal.

For this reason it is of considerable importance to scrutinize the catalytic activity of platinum on the atomic scale, to learn what makes this metal so versatile as a catalyst and so selective for important catalytic transformations after suitable preparation. Once the elements of catalytic activity are revealed, it should be possible to use this metal more economically or perhaps to find ways to synthesize new catalyst systems to substitute for this excellent but rare catalyst.

Let us concentrate on the atomic-scale study of the platinum surface under the reducing conditions used during hydrocarbon conversion reactions. In this circumstance H-H, C-H, and C-C bond-breaking processes are essential. In Figure 7.36 the various hydrocarbon conversion reactions of interest are listed. Dehydrogenation involves C-H bond breaking only, while hydrogenolysis necessitates the breaking of C-C bonds. Dehydrocyclization must involve the complex process of dehydrogenation and ring closure.

Figure 7.36 shows several reactions that are all catalyzed by platinum. The simpler hydrogenation and dehydrogenation reactions have turnover frequencies in the

Figure 7.36. Several competing hydrocarbon reactions that occur on platinum catalyst surfaces.

range 0.1 to 10 sec^{-1} under the usual conditions of 400 to 600 K, atmospheric pressures of reactant and excess hydrogen) that are employed in the chemical industry [151, 152]. However, platinum is really noted for being an excellent catalyst for the more complex reactions of dehydrocyclization (e.g., n-heptane to toluene) and isomerization (for n-pentane to 2-methylbutane) that have turnover frequencies of about 10^{-4} to 10^{-2} sec⁻¹ under experimental conditions similar to those used to carry out the more facile reactions [153, 154]. One of the key questions in the molecular-scale study of the hydrocarbon catalysis of platinum is how this metal selectively catalyzes the complex, low-turnover frequency reactions while blocking the simpler, high-rate dehydrogenation and hydrogenation reactions and the slower, but unwanted, hydrogenolysis reaction. This happens after suitable preparation of the platinum catalyst prior to exposure to the reaction mixture.

Various crystal faces of platinum single crystals 1 mm thick with surface areas of about 1 cm² serve as excellent model catalysts. These samples can be prepared with quite uniform and ordered surface structures that can be analyzed by the various surface-science techniques. Low-energy electron diffraction was particularly useful for the determination of the structure of single-crystal surfaces. The flat surfaces where each platinum atom is surrounded by six and four nearest neighbors, respectively, are the two closest-packed platinum crystal faces of the highest atomic density (Figure 7.37). Stepped crystal faces can also be prepared easily; these faces display close-packed terraces several atoms in width, which are separated by atomic steps one atom in height. The lowered coordination of the step atoms is responsible for the unique chemical activity that is often displayed at these surfaces sites. There can be kinks in the steps, and atoms at these ledges have even lower coordination. The structure and concentration of steps and kinks, along with the structure and

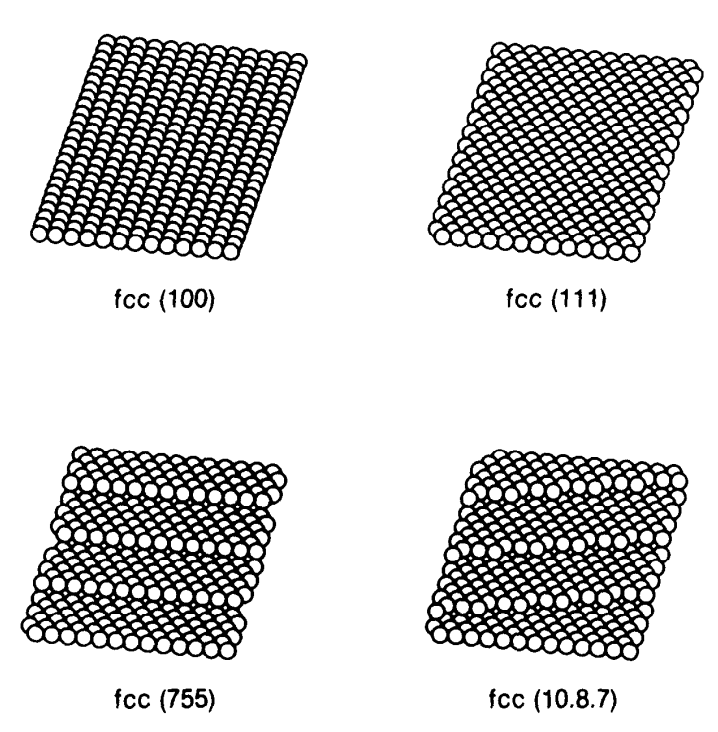


Figure 7.37. Idealized atomic surface structures for the flat Pt(100) and Pt(111), the stepped Pt(755), and the kinked Pt(10, 8, 7) surfaces.

width of the terraces, can be varied by cutting the platinum single crystals along different crystals planes and then by appropriately polishing and etching them to remove the surface damage introduced by the mechanics of surface preparation.

7.8.3.2 Structure Sensitivity of Hydrocarbon Conversion Reactions on Platinum Surfaces How does the reaction rate depend on the atomic structure of the platinum catalyst surface? To answer this question, reaction rate studies using flat, stepped, and kinked single-crystal surfaces with variable surface structure were very useful indeed. For the important aromatization reactions of n-hexane to benzene and n-heptane to toluene, it was discovered that the hexagonal platinum surface where each surface atom is surrounded by six nearest neighbors is three to seven times more active than the platinum surface with the square unit cell [155, 156]. Aromatization reaction rates increase further on stepped and kinked platinum surfaces. Maximum aromatization activity is achieved on stepped surfaces with terraces about five atoms wide with hexagonal orientation, as indicated by reaction rate studies over more than 10 different crystal surfaces with varied terrace orientation and step and kink concentrations (Figure 7.38).

The reactivity pattern displayed by platinum crystal surfaces for alkane isomerization reactions is completely different from that for aromatization. Studies revealed that maximum rates and selectivity (rate of desired reaction/total rate) for butane isomerization reactions are obtained on the flat crystal face with the square unit cell. Isomerization rates for this surface are four to seven times higher than those for the hexagonal surface. Isomerization rates are increased to only a small extent by surface irregularities (steps and kinks) on the platinum surfaces (Figure 7.39).

For the undesirable hydrogenolysis reactions that require C-C bond scission,

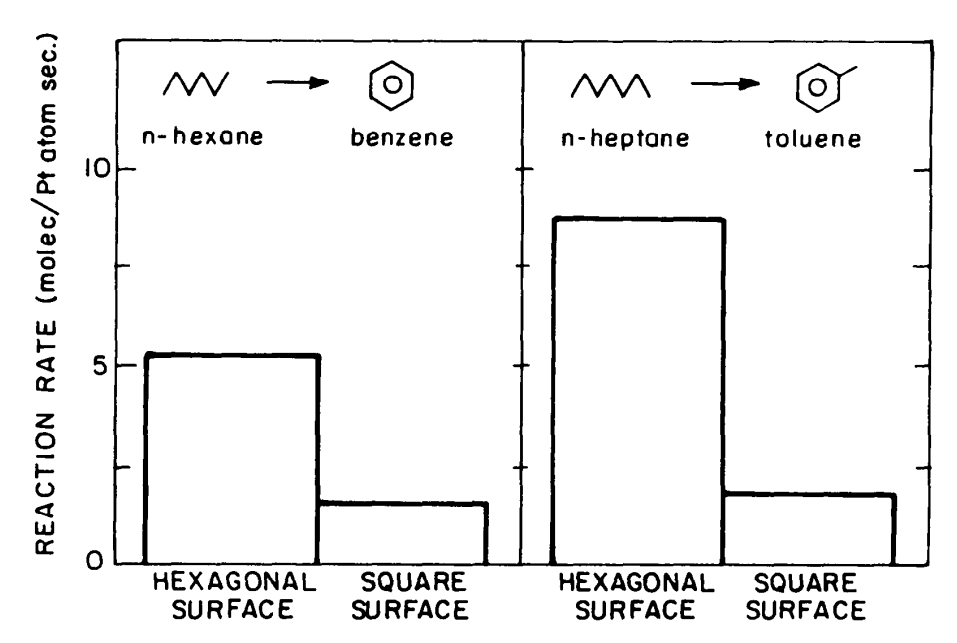


Figure 7.38. The structure sensitivity of dehydrocyclization of alkanes to aromatic hydrocarbons. The bar graphs compare reaction rates for *n*-hexane and *n*-heptane catalyzed at 573 K and atmospheric pressure over the two flat platinum single-crystal faces with different atomic structure. The Pt surface with a hexagonal atomic arrangement is several times more active than the surface with a square unit cell over a wide range of reaction conditions [155].

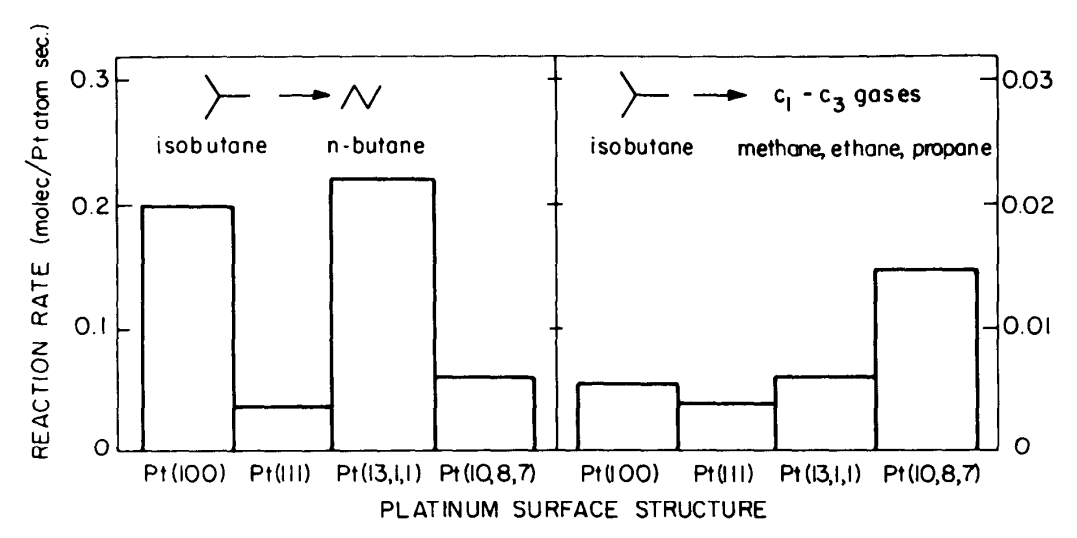


Figure 7.39. The structure sensitivity of light alkane isomerization and hydrogenolysis. Shown here are the reaction rates of isobutane catalyzed at 570 K and atmospheric pressure over four platinum surfaces shown in Figure 7.37. Isomerization is favored over Pt surfaces that have a square atomic arrangement. Hydrogenolysis rates are maximized when kink sites are present in high concentrations on the platinum surface [155].

the two flat surfaces with highest atomic density exhibit very similar reaction rates. However, the distribution of hydrogenolysis products varies sharply over these two surfaces. The hexagonal surface displays high selectivity for scission of the terminal C-C bonds, whereas the surface with a square unit cell always prefers cleavage of C-C bonds located in the center of the reactant molecule. The hydrogenolysis rates increase markedly (three- to fivefold) when kinks are present in high concentrations on the platinum surfaces.

Because different reactions are sensitive to different structural features of the catalyst surface, we must prepare the catalyst with the appropriate structure to obtain maximum activity and selectivity. The terrace structure, the step or kink concentrations, or a combination of these structural features is needed to achieve optimum reaction rates for a given reaction. Studies indicate that H-H and C-H bondbreaking processes are more facile on stepped surfaces than on the flat crystal faces, while C-C bond scission is aided by kink sites that appear to be the most active for breaking any of the chemical bonds that are available during the hydrocarbon conversion reactions. Because molecular rearrangement must also occur, in addition to bond breaking, it is not surprising that the terrace structure exerts such an important influence on the reaction path that the adsorbed molecules are likely to take. The difference in chemical behavior of terrace, step, and ledge atoms arises not only from their different structural environment but also from their different electronic charge densities that result from variation of the local atomic structure. Electron spectroscopy studies reveal altered density of electronic states at the surface irregularities: there are higher probabilities of electron emission into vacuum at these sites (lower work function), indicating the redistribution of electrons [157].

One of the important attributes of transition-metal surfaces is that they atomize diatomic molecules with large binding energy $(H_2 \text{ or } O_2)$ by forming strong M-H or M-O bonds and hold the atoms in high surface concentrations so that they are readily available during the surface reaction (see Section 7.2). The hydrogen atom

surface concentration is especially important in permitting catalyzed hydrocarbon conversion reactions to proceed unimpeded. The presence of excess hydrogen facilitates removal of product molecules and also inhibits catalyst deactivation. For this reason the reforming reaction of organic molecules is always catalyzed in the presence of excess hydrogen.

7.8.3.3 Carbonaceous Overlayers What is the composition of the working platinum catalyst surface? When the surface is examined after carrying out any one of the hydrocarbon conversion reactions, it is always covered by a near-monolayer amount of carbonaceous deposit.

In order to determine the surface residence time of the carbonaceous deposit, the platinum surface was dosed by the ¹⁴C-labeled organic molecules under the reaction conditions. Carbon-14 is a β -particle emitter. The β -particle detector was used to monitor its surface concentration as a function of time during the catalytic reaction. The hydrogen content of the adsorbed organic layer is determined by detecting the amount of desorbing hydrogen with a mass spectrometer. These investigations reveal that the residence time of the adsorbed carbonaceous layer depends on its hydrogen content, which in turn depends on the reaction temperature (Figure 7.40).

Although the amount of deposit does not change much with temperature, the composition does; it becomes much poorer in hydrogen as the reaction temperature is increased. The adsorption reversibility decreases markedly with increasing temperature as the carbonaceous deposit becomes more hydrogen-deficient. As long as

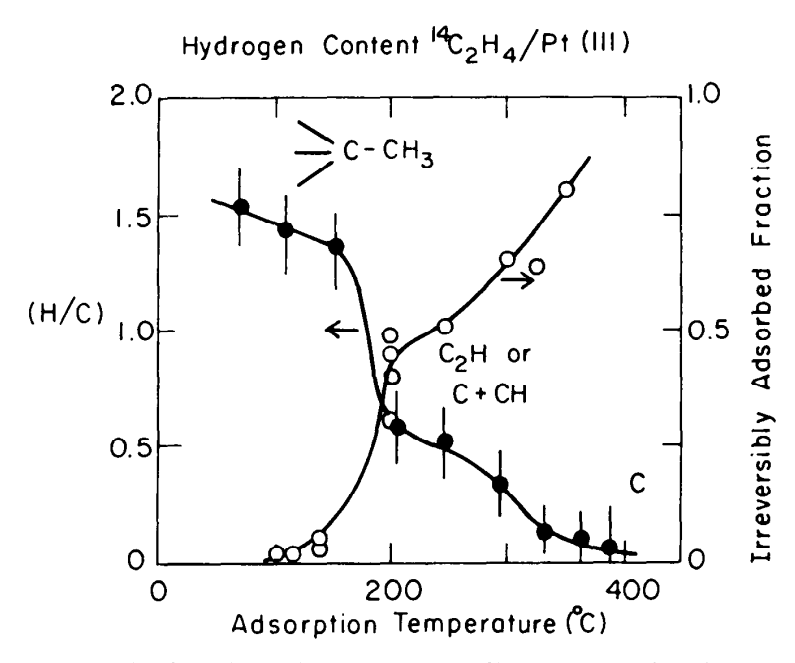


Figure 7.40. Carbon-14-labeled ethylene (or other alkenes) was chemisorbed as a function of temperature on the flat Pt(111) crystal face. The (H/C) ratio of the adsorbed species was determined from hydrogen thermal desorption. The amount of preadsorbed alkene that could not be removed by subsequent treatment in 1 atm of hydrogen represents the irreversibly adsorbed fraction. The adsorption reversibility decreases markedly with increasing adsorption temperature as the surface species become more hydrogen-deficient. The irreversibly adsorbed species have long residence times, on the order of days [195].

the composition is about $C_nH_{1.5n}$ and below 450 K, the organic deposit can be removed readily in hydrogen with increasing reaction temperatures (>450 K), it converts to an irreversible adsorbed deposit with a composition of $C_{2n}H_n$ that can no longer be readily removed (hydrogenated) in the presence of excess hydrogen [158].

Nevertheless, the catalytic reaction proceeds readily in the presence of this active carbonaceous deposit [158, 159]. Above 750 K this active carbon layer is converted to a graphitic layer that deactivates the metal surface, and all chemical activity for any hydrocarbon conversion reaction ceases. Hydrogen exchange studies indicate rapid exchange between the hydrogen atoms in the adsorbing reactant molecules and the hydrogen in the active but irreversibly adsorbed deposit. Only the carbon atoms in this layer do not exchange. Thus, one important property of the carbonaceous deposit is its ability to store and exchange hydrogen [158–160].

The structure of the adsorbed hydrocarbon monolayers was submitted to detailed studies by LEED and HREELS [161]. In the temperature range of 300-400 K the adsorbed alkenes form alkylidyne molecules that are shown in Chapter 6. The C-C bond closest to the metal is perpendicular to the surface plane, and its 1.5-Å length corresponds to a single bond. The carbon atom that bonds the molecule to the metal is located in a threefold site equidistant 2.0 Å from the nearest metallic neighbors [162]. This bond is appreciably shorter than the covalent metal—carbon bond (2.2) A) and is indicative of multiple metal—carbon bonds of the carbene or carbyne type. Although this layer is ordered, on being heated to about 100°C it disorders and hydrogen evolution is detectable by a mass spectrometer that is attached to the system. As the molecules dehydrogenate, the disordered layer is composed of CH₂-, C₂H-, and CH-type fragments that can be identified by HREELS [161]. Only after being heated to about 400°C do the fragments lose all their hydrogen and the graphite overlayer forms. These sequential bond-breaking processes, which occur as a function of temperature, are perhaps the most important and unique characteristics of the surface chemical bond (Chapter 6). Although the surface remains active in the presence of organic fragments of C₂H stoichiometry, it loses all activity when the graphite monolayer forms.

How is it possible that the hydrocarbon conversion reaction exhibits great sensitivity to the surface structure of platinum, while under the reaction conditions the metal surface is covered with a near-monolayer of carbonaceous deposit? In fact, often more than a monolayer amount of carbon-containing deposit is present, as indicated by surface-science measurements. Recent scanning tunneling microscopy studies that were carried out at high hydrocarbon and hydrogen pressures (atm) and hydrocarbon reaction temperatures indicate that CH₂, C₂H, and CH fragments are mobile on the surface; they move around by surface diffusion in the presence of coadsorbed molecular reactants. While they do not desorb, their mobility makes the active metal sites on the surface available to the molecular reactants. When the carbonaceous species polymerize at higher temperatures to form a graphite deposit, they lose their mobility and deactivate the metal surface by permanently blocking the active sites.

In order to determine how much of the platinum surface is exposed and remains uncovered, the adsorption and subsequent thermal desorption of carbon monoxide was utilized. This molecule, although readily adsorbed on the metal surface at 300 K at low pressures, does not adsorb on the carbonaceous deposit. The results indicate that up to 10-15% of the surface remains uncovered metal sites decreases slowly

with increasing reaction temperature. The structure of these uncovered metal islands is not very different from the structure of the initially clean metal surface during some of the organic reactions.

As a result of catalyzed hydrocarbon conversion reaction studies on platinum crystal surfaces, a model for the working platinum reforming catalyst could be proposed [163] and is shown in Figure 7.41. Between 80% and 95% of the catalyst surface is covered with an irreversibly adsorbed carbonaceous deposit that stays on the surface for times much longer than the reaction turnover time. The structure of this carbonaceous deposit varies continuously from two-dimensional to three-dimensional with increasing reaction temperature. There are platinum patches that are not covered by this deposit. These metal sites can accept the reactant molecules which then compress the carbonaceous deposit by surface diffusion to free up the active sites where the reactions occur. Upon desorption of the products, the carbonaceous species may diffuse back to cover the metal sites. The adsorption of new reactant molecules repeats the process; compression of the carbonaceous deposit by surface diffusion, reaction at the metal sites and product desorption. There is evidence that the carbonaceous deposit participates in some of the reactions by hydrogen transfer by providing sites for rearrangement and desorption while remaining inactive in other reactions; its chemical role requires further exploration.

7.8.3.4 Catalysis in the Presence of a Strongly Adsorbed Overlayer Reactions of this type do not occur directly on the metal surface and therefore are usually structure-insensitive [164]. In fact, the role of the metal could be reduced to providing atoms, hydrogen for example, via the dissociation of diatomic molecules. The metal is usually covered by strongly adsorbed overlayers and thus the incoming reactants (other than hydrogen) cannot form strong metal-adsorbate bonds. An example of

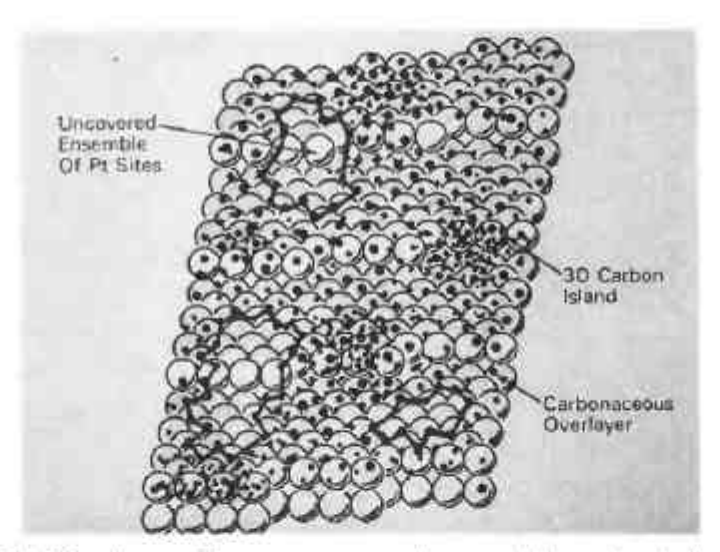


Figure 7.41. Model for the working structure and composition of a platinum dehydrocyclization catalyst. Most of the surface is continuously covered by a strongly bound carbonaceous deposit whose structure varies from two-dimensional to three-dimensional with increasing reaction temperature. Uncovered patches or ensembles of platinum surface sites always exist in the presence of this carbonaceous deposit. Bond breaking and chemical rearrangement in reacting hydrocarbon molecules take place readily at these uncovered sites [158].

this type of reaction is the hydrogenation of ethylene [165]. This facile reaction occurs at 300 K and at atmospheric pressures on many transition metal surfaces. It has been the subject of investigations of many researchers [166-172]. Table 7.48 shows that hydrogenation occurs equally well on platinum crystals, films, foils, and supported particles, indicating that the reaction is structure-insensitive [173]. When the clean metal surfaces are exposed to ethylene, a strongly adsorbed overlayer of ethylidyne (C₂H₃) forms. This molecule, shown in Figure 2.26 along with its vibration spectrum (Figure 2.25), is obtained by high-resolution electron-energy-loss spectroscopy (HREELS) [174]. The kinetics of ethylene hydrogenation and those of ethylidyne have been studied extensively over the (111) faces of rhodium and platinum, and the rates of these processes are displayed in Figure 7.42. Ethylene hydrogenation occurs at a rate six orders of magnitude higher than the rehydrogenation of the strongly adsorbed ethylidyne [165]. Even the deuteration of the methyl group of ethylidyne occurs very slowly. Studies using ¹⁴C labeling of ethylidyne and vibrational spectroscopy confirm these findings.

The (111) faces of platinum of rhodium are instantly covered with a monolayer of ethylidyne during ethylene hydrogenation because reaction rates are nearly identical over initially clean surfaces and surfaces precovered with ethylene. Vibrational spectroscopy studies confirm that the adsorbed monolayer structure on these surfaces following hydrogenation is ethylidyne. Thus ethylene hydrogenation occurs rapidly on the C_2H_3 -covered surfaces. The packing of the ethylidyne on the overlayer does not permit C_2H_4 adsorption directly on the metal surface, as proven by exchange studies with C_2H_4 and C_2D_4 . On the other hand, thermal desorption studies have

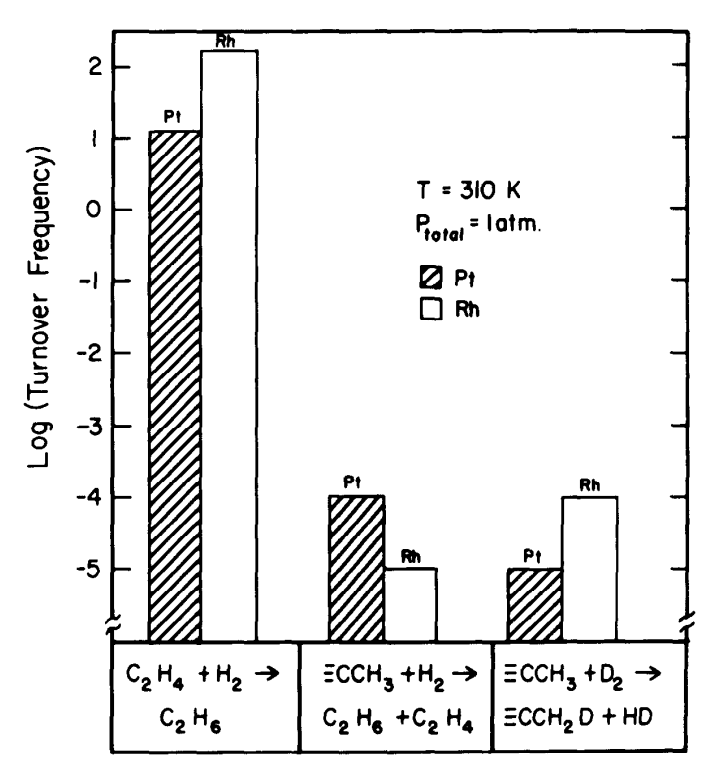


Figure 7.42. Turnover rates for ethylene hydrogenation, the rehydrogenation of ethylidyne, and the deuteration of the methyl- group of ethylidyne on platinum and rhodium crystal surfaces [190]. Note that ethylene hydrogenation rates are orders of magnitude faster than the rate of removal of chemisorbed ethylidyne.

shown that H_2 (D_2) can be dissociated and readsorbed on the ethylidyne-covered surfaces up to about one-fourth monolayer coverage.

One reaction model that explains these results has been proposed [165]. The hydrogen atom is transferred to the ethylene molecule that is weakly adsorbed on top of the ethylidyne and in the second layer perhaps by forming an ethylidene intermediate. This model of hydrogen transfer from hydrocarbons to ethylene was first proposed by Thomson and Webb [175]. This mechanism is of the Eley-Rideal type and is characterized by low activation energy and structure insensitivity.

Another reaction model involves the compression of the ethylidyne overlayer at high pressure of ethylene. Because of repulsive adsorbate-adsorbate (ethylene-ethylidyne) interaction, and the expected small activation energy of ethylidyne surface diffusion, ethylene could adsorb on the metal in the small hole created near the compressed ethylidyne. Compression of this type has been detected by STM upon the adsorption of hydrocarbons on platinum and the coadsorption of CO and sulfur on both platinum and rhenium surfaces [218].

However, there are other mechanisms of C_2H_4 for hydrogenation that studies have uncovered [165]. At higher temperatures, the rate of rehydrogenation of C_2H_3 is significant and the bare metal becomes available, in part, for C_2H_4 hydrogenation. During the electrochemical hydrogenation of C_2H_4 , the platinum surface is covered with a layer of hydrogen atoms (hydride) that react rapidly with the approaching C_2H_4 and do not permit the formation of ethylidyne. The complexity of surface reactions cannot be underestimated.

Nevertheless, ethylene hydrogenation may provide an example of reactions of weakly adsorbed molecules or high coverages in the second layer, an important class of catalytic reactions that could occur at low temperatures or high pressures. It should be noted that most catalyzed biochemically important reactions occur at 300 K and at high turnover rates, virtually excluding the possibility of forming strong chemical bonds with the enzyme catalyst surface by the adsorbed reactants or reaction intermediates.

These types of structure-insensitive reactions may be compared with homogeneous catalytic reactions that are facile, occurring at lower temperatures, and include hydrogenation or hydroformylation. Because the metal plays secondary roles in this process, high coordination sites are not needed to carry out the reaction. It is hoped that future studies will reveal the possible correlation between homogeneous catalytic reactions and heterogenous reactions of this type.

The organic overlayer may also serve as a template to orient or align the reactants. LEED surface crystallography and HREELS studies of the structure of these monolayers indicate that their structural integrity is preserved at temperatures as high as 400 K; thus their presence only allows us to carry out various specific reactions below this temperature. Above 400 K, fragmentation to small organic CH and C₂H groups occurs (Figure 2.30). While at low temperatures [176], benzene and ethylene maintain their molecular identify on the platinum and rhodium crystal surfaces, above 400 K the fragments are the same small organic moieties. Thus catalysis that requires an organic template to properly line up the reactant molecules can be carried out only below 400 K.

7.8.3.5 Structure Modifiers

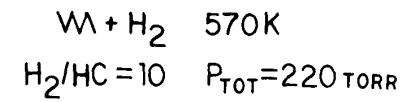
7.8.3.5.1 Site Blocking by Sulfur Let us consider the interaction of coadsorbed sulfur with thiophene which occurs during the hydrodesulfurization of thiophene on

the molybdenum (100) crystal surface [177]. This gentle reaction removes the sulfur from the molecule as H_2S in the presence of hydrogen, leaving behind the C_4 species that readily hydrogenates to butadiene, butenes, and butane without fragmentation. Molybdenum metal strongly adsorbs and decomposes thiophene and butenes as shown by surface studies, and thus the clean surface cannot be an active catalyst. MoS_2 is a layer compound, and its basal plane holds thiophene so weakly that its thermal desorption occurs at 165 K [178]. Thus this surface is not chemically active. The active molybdenum surface contains about one-half monolayer of strongly adsorbed sulfur. These atoms block the metal sites where thiophene decomposition would occur. Studies using ^{35}S labeling indicate that these sulfur atoms remain permanently on the metal surface during the catalytic reactions. The sulfur atom that is removed from the thiophene molecule occupies sites of weaker bonding where hydrogenation to H_2S and subsequent desorption occurs, while the C_4 species becomes partly hydrogenated and desorbs.

Thus the blockage of certain adsorption sites on the surface of early transition metal attenuates the strong bonding and permits the catalytic reaction to occur.

The hydrogenolysis of organic molecules over platinum is frequently an undesirable reaction that leads to the production of lower-molecular-weight products. Kink sites on transition metal surfaces are especially active for the C-C bond-breaking reaction [179]. While their surface concentration is no more than about 5% of the total number of metal sites, they may account for 90% of hydrogenolysis activity. These hydrogenolysis sites can often be poisoned by the chemisorption of controlled amounts of sulfur (produced by H_2S decomposition) that bonds more strongly to kink sites as compared to terrace sites. In this way, the hydrogenolysis reaction can be poisoned selectively as the kink sites are blocked and rendered inactive.

7.8.3.5.2 Ensemble Effect in Alloy Catalysis and the Creation of New Sites by Alloys As compared to pure platinum, bimetallic alloys such as platinum-rhenium and platinum-gold frequently exhibit superior activity, selectivity, and deactivation resistance while catalyzing reforming reactions. The influence of gold on hydrocarbon conversion catalysis by platinum was recently studied by evaporating gold onto platinum single-crystal surfaces [180]. At low temperatures, gold forms epitaxial overlayers on platinum, but upon heating it dissolves to form an alloy in the near surface region. This Pt-Au alloy displays markedly different activity and selectivity for the conversion of n-hexane as shown in Figure 7.43. Isomerization activities increase substantially as compared to those for clean platinum, whereas the aromatization and hydrogenolysis rates decrease exponentially with increasing gold surface concentration. This remarkable change in catalytic behavior can be explained by a change in the geometric distribution of platinum sites that are present in the (111) alloy surface. Substitution of gold atoms dilutes the surface platinum atoms such that the high-coordination threefold platinum sites are eliminated much faster than the twofold bridge and single-atom top sites. This change in the distribution of the available reaction sites is frequently called the *ensemble effect* [180]. As a result of this effect, catalyzed reactions that involve adsorption and rearrangement at threefold sites are eliminated, whereas reactions that require one or two atoms sites are attenuated to a much lesser extent. Although minor changes in electronic structure may also occur at the alloy surface sites, most of the reaction results can be explained by this high-coordination-site elimination model. Similar results revealing pro-



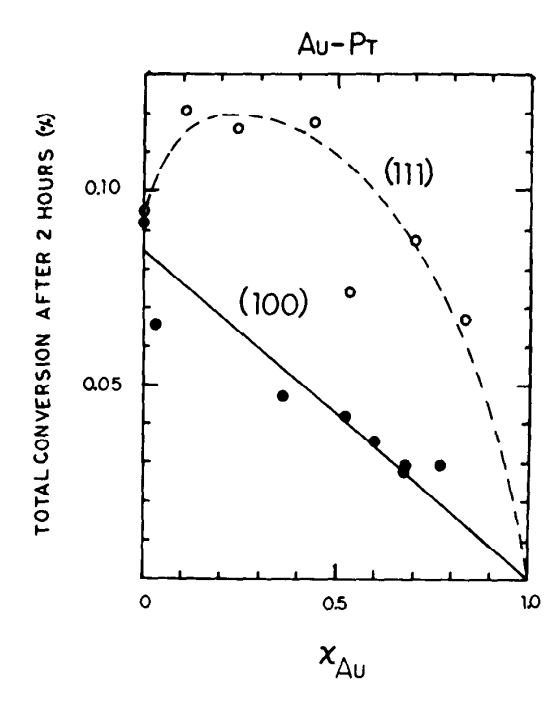


Figure 7.43. Rates of formation of various products from n-hexane conversion as a function of fractional gold coverage for gold-platinum alloys that were prepared by vaporizing gold onto platinum (111) and platinum (100) crystal surfaces, respectively [180, 190].

nounced changes in catalytic behavior with alloy composition were reviewed by Ponec [181] and Sinfelt [182]. For a variety of hydrocarbon reactions, catalyzed over metal films and high-area-supported catalysts, in most cases the geometrical ensemble effect is decisive in controlling the reaction selectivity.

The effect of alloying is also surface-structure-sensitive, as shown by studies where gold was the alloying constituent in the Pt(100) crystal face instead of the Pt(111) surface [183]. The (100) surface has a square unit cell that contains fourfold bridge and top sites, and unlike the (111) surface it does not have threefold sites. When this surface is alloyed with gold, all reaction rates decline in proportion to the concentration of inactive gold on the Pt(100) surface when *n*-hexane was used as a reactant. This is shown in Figure 7.43. Thus the enhancement of the isomerization activity requires a presence of threefold sites. When gold is used as an alloying agent, there are three types of threefold sites available. One contains only platinum atoms, whereas the other two mixed Pt-Au sites contain one and two atoms, respectively. Thus alloying produces new mixed metal sites with catalytic behavior that can modify the selectivity. Figure 7.43 clearly indicates that the high isomerization rate of n-hexane is sustained until the surface was covered up to two-thirds monolayer gold [183]. Thus all three threefold sites are active for isomerization. The mixed Pt-Au sites are then responsible for the enhanced isomerization activity of the Pt-Au alloy that exhibits markedly higher rates than the pure platinum (111) crystal surface.

Boudart and co-workers [184] have shown a 50-fold increase in the rate of $\rm H_2/O_2$ reaction to produce water over Pd-Au alloys. Such large effects cannot be explained by site-blocking ensemble effects. The new sites that are created by alloying have unique structure and bonding. In fact, a new catalyst is created with structural and

bonding properties that are not derived from the structural and bonding properties of the pure alloy constituents.

7.8.3.6 The Building of Improved Platinum and Other Metal Catalysts The atomic-scale ingredients of selective hydrocarbon catalysis by platinum have been identified and a model of the working catalyst has been constructed. Attention now turns toward building improved catalyst systems. Additives are being used to alter the surface structure beneficially, to reduce the amount of carbon deposit, or to slow down its conversion to the inactive graphitic form. Bimetallic or multimetallic platinum catalyst systems have been developed by the addition of one or more other transition metals (Re, Pd, Ir, or Au) that can be operated at higher reaction temperatures to obtain higher reaction rates [185]. They show slower rates of deactivation (have longer lifetimes) and can also be more selective for a given chemical reaction (dehydrocyclization or isomerization) than the one-component catalyst [185].

One of the major challenges in preparing scientifically tailored, high-technology metal catalysts is to deposit the metal particles with the specific surface structure needed to obtain optimum reaction selectively. The structure of the support and its chemical interaction with the metal are utilized to achieve this goal. Deposition of ordered platinum monolayers on sulfides or oxides with well-defined substrate structure is one important approach in this direction. Zeolites, aluminosilicates that are available with variable but well-defined pore structure and Al/Si ratio, could perhaps provide the structural definition that was obtained on the low-surface-area single-crystal catalysts without sacrificing the availability of high surface area [186]. There are attempts to prepare metal catalyst particles with uniform size and equal distances of separation by using microelectronic circuitry fabrication technology. Using electron beam lithography (or perhaps X-ray lithography in the future), metal particles in the size range of $10^2 \text{ Å} - 10^3 \text{ Å}$ can be deposited in ordered arrays on silica or alumina substrates. The reactivity and the stability of these metal "nanocluster" arrays are under investigation in my laboratory. Strong chemical interaction between the metal particles and the support induces charge transfer toward or away from the metal that again could beneficially alter its catalytic properties [187]. Other additives are being investigated that increase catalytic activity by decreasing the surface residence times required for the reaction and product desorption, thereby reducing the amount of platinum required in conventional reforming catalysts. Identification of new, less expensive catalyst materials with platinum-like chemical activity and selectivity is another important direction of research for catalysis science. Many transition-metal materials are in short supply worldwide and are not readily available in the United States.

As combined surface-science and catalytic-reaction studies develop working models for catalysts of many types, the building of new high-technology catalysts, using this molecular-level understanding, will become more frequent. This transition from art to catalysis science can come none too soon. The rising cost of petroleum necessitates the use of new fuel sources (natural gas, coal, shale, tar sand) and the use of new feedstocks for chemicals (methane, $CO + H_2$, coal liquids). The fuel and chemical technologies based on these new feedstocks require the development of an entirely new generation of catalysts. Ultimately, our fuels and chemicals must be produced form the most stable and abundant molecules we live with on our planet, including CO_2 , H_2O , N_2 and O_2 . To build the catalytic chemistry starting from these species is a considerable challenge that will be met by catalysis science in the future.

7.9 SUMMARY AND CONCEPTS

- Surface catalysis aims to carry out the same reaction repeatedly at high rates (activity) and selectivity.
- The catalytic process can be characterized by its kinetic parameters (rate constant, preexponential factor, activation energy, reactant pressure dependencies, reaction probability).
- The preparation, activation, deactivation, and regeneration of high-surface-area catalyst materials are dominant concerns of surface catalysis.
- Catalysis by transition-metal surfaces exhibit trends across the periodic table whereby metals that form chemical bonds of intermediate strength have the highest activities.
- Important catalytic reaction concepts include: structure sensitivity and insensitivity of reactions, mechanistic classifications (Langmuir-Hinshelwood, Eley-Rideal), the compensation effect, the presence of strongly chemisorbed overlayer, and the roles of structure and bonding modifier additives (promoters).
- Acid-base catalysis produces mostly carbenium ions by electron or by proton transfer. Among the solid acids, microporous, crystalline alumina silicates (zeolites) are utilized most frequently.
- Surface-science studies of catalysis employ mostly small-surface-area (1 cm²) crystal surfaces or model catalysts that are well-characterized on the atomic scale. Promoters are deposited on such a surface with known concentration and composition.
- The state and accomplishments of catalysis science are demonstrated through discussions of the ammonia synthesis, carbon monoxide hydrogenation, and hydrocarbon conversion over platinum.

7.10 PROBLEMS

- 7.1 Calculate the reaction probability of a catalytic reaction that has a turnover rate of 10^{-3} molecules/surface site/sec at 1 atm.
- *7.2 The hydrogenation of carbon monoxide and carbon dioxide to methane can be described by a series of elementary reaction steps [194, 196] that are given below:

(1)
$$CO_{(g)} + S \rightleftharpoons CO_{(a)}$$

(2)
$$H_2 + 2S \rightleftharpoons 2H_{(a)}$$

(3)
$$2H_{(a)} + CO_{(a)} \rightleftharpoons H_2CO_{(a)} + 2S$$

(4)
$$H_2CO_{(a)} + S \rightleftharpoons CH_{2(a)} + O_{(a)}$$

(5)
$$O_{(a)} + H_{(a)} \rightleftharpoons HO_{(a)} + S$$

(6)
$$HO_{(a)} + H_{(a)} \rightleftharpoons H_2O_{(g)} + 2S$$

(7)
$$CH_{2(a)} + H_{(a)} \rightleftharpoons CH_{3(a)} + S$$

(8)
$$CH_{(a)} + H_{(a)} \rightleftharpoons CH_{4(a)} + 2S$$

Write the rate expression that gives the CO and H_2 pressure dependencies of the reaction rate assuming that (a) step 3 or (b) step 4 is rate-determining.

- **7.3 The determination of the equilibrium constant of ammonia formation N₂ + 3H₂ = 2NH₃ has been performed by Haber and Nerst. Using different catalysts they obtained different results. Review the literature [197] on these studies and describe the outcome of this important debate in the history of catalysis.
- **7.4 Search the literature to find the important surface catalyzed processes that are used to convert crude oil to gasoline and describe them in sequence of application in the refining technology [198, 199].
- **7.5 The partial oxidation of ethylene to ethylene oxide is an important chemical reaction in the chemical technology [198, 200, 201]. Describe the process, the catalyst that is employed, and the nature of the catalyst promoters.
- **7.6 Acrylonitrile (CH₂CHCN) is produced from propylene, ammonia, and oxygen over a mixed oxide catalyst [198, 199, 202]. Describe the process.
- **7.7 The hydrogenation of nitriles (R-CN) to amines (R-NH₂) is carried out using Raney nickel as a catalyst. Describe what Raney nickel is and describe the process [198].
- **7.8 Microporous, crystalline oxides (alumina, silicates, phosphates, etc.) are used as catalyst is in the petroleum and in the chemical technologies in large volume to carry out cracking, isomerization, alkylation, and many other important hydrocarbon conversion reactions [198, 199, 203]. Discuss the structure of these so-called "zeolites" that have one-dimensional and two-dimensional micropores. How can the acidity of the catalysts be altered? How do their acid strengths compare with concentration H₂SO₄ and HF?
- **7.9 The catalytic reduction of nitrogen oxides, NO_x, that are produced by combustion of fuels at high temperatures (≈ 1800°C during electric power generation) is one of the important environmental catalytic problems. Review the process that uses ammonia or small hydrocarbons as reducing agents, and list the catalysts that are employed [204, 205].
- **7.10 The "three-way" catalytic converter used in automobiles catalyzes the oxidation of unburned hydrocarbons and CO while reducing simultaneously NO to N₂ [198, 206]. Describe the process.
- **7.11 The water-gas-shift reaction [207] is utilized to produce hydrogen by the reaction of CO and H₂O. Describe the process.
- **7.12 The oxidation of CO to CO₂ and the reduction of NO by NH₃ are complex catalyzed surface reactions that have two or more branches depending on

the composition of the reactant mixture and the temperature. There are periodic oscillations in the reaction rates including instabilities [208]. Review the literature describing the ratio rate oscillations for these two processes and discuss the experimental conditions that give rise to this phenomenon.

- **7.13 The removal of sulfur from organosulfur compounds is an important catalytic reaction during petroleum refining [198, 199]. A test reaction for this process is the hydrodesulfurization of thiophene to butenes. Describe the process [209]. The removal of nitrogen from organonitrogen compounds is equally important. Describe the process [210].
- **7.14 The polymerization of ethylene over chromium compounds is responsible for the production of much of the polyethylene that is produced [211]. Describe the process.
- **7.15 The catalyzed gasification (using steam) of carbon solids (coals, chars, organic solid waste, graphite) to H₂, CO₂, and CO is utilized to convert these materials to gaseous fuels (coal gasification) [23, 212]. Describe the process.
- **7.16 The conversion of methane by oxydehydrogenation to ethane, ethylene, oxygen-containing organic molecules, or CO and H₂ are important reactions that are at the frontier of catalyst research. Methane, which is the most abundant fraction of natural gas, is an increasingly significant source of fuels as the supply of crude oil diminishes. Review the processes [213–217].

REFERENCES

- [1] J. Berzelius. Jahres-Bericht über die Fortschritte der Physichen Wissenschaften, Volume 15, H. Laupp, Tübingen, 1836.
- [2] P. Emmett. Fifty Years of Progress in Surface Science. CRC Crit. Rev. Solid State Sci. 4:127 (1974).
- [3] A. Gaydon. Dissociation Energies and Spectra of Diatomic Molecules. Chapman and Hall, London, 1953.
- [4] G.W. Koeppl. Best *Ab Initio* Surface Transition State Theory Rate Constants for the D+H₂ and H+D₂ Reactions. *J. Chem. Phys.* **59:**3425 (1973).
- [5] M. Salmerón, R.J. Gale, and G.A. Somorjai. A Modulated Molecular Beam Study of the Mechanism of the H₂-D₂ Exchange Reaction on Pt(111) and Pt(332) Crystal Surfaces. J. Chem. Phys. **70**:2807 (1979).
- [6] H. Bonzel, G. Brodén, and G. Pirug. Structure Sensitivity of NO Adsorption on a Smooth and Stepped Pt(100) Surface. *J. Catal.* **53:**96 (1978).
- [7] M.P. Kiskinova. Electronegative Additives and Poisoning in Catalysis. Surf. Sci. Rep. 8:359 (1988).
- [8] G.A. Somorjai. On the Mechanism of Sulfur Poisoning of Platinum Catalysts. *J. Catal.* 27:453 (1972).
- [9] S. Bhatia, J. Beltramini, and D.D. Do. Deactivation of Zeolite Catalysts. *Catal. Rev. Sci. Eng.* 31:431 (1989/1990).

- [10] E.E. Petersen and A.T. Bell, editors. Catalyst Deactivation. Chemical Industries, Volume 30. Marcel Dekker, New York, 1987.
- [11] L. Falicov and G.A. Somorjai. Correlation between Catalytic Activity and Bonding and Coordination Number of Atoms and Molecules on Transition Metal Surfaces: Theory and Experimental Evidence. *Proc. Natl. Acad. Sci. USA* 82:2207 (1985).
- [12] M. Boudart. Catalysis by Supported Metals. Adv. Catal. Relat. Subj. 20:153 (1969).
- [13] H.P. Bonzel and R. Ku. Mechanisms of the Catalytic Carbon Monoxide Oxidation on Pt(110). Surf. Sci. 33:91 (1972).
- [14] I. Langmuir. The Mechanism of the Catalytic Action of Platinum in the Reactions $2CO + O_2 \rightleftharpoons 2CO_2$ and $2H_2 + O_2 \rightleftharpoons 2H_2O$. Trans. Faraday Soc. 17:621 (1922).
- [15] D.D. Eley. Catalysis, an Art Becoming a Science. Chem. Ind. (1), 1976:12 (1976).
- [16] T. Engel and G. Ertl. A Molecular Beam Investigation of the Catalytic Oxidation of CO on Pd(111). J. Chem. Phys. 69:1267 (1978).
- [17] A.K. Galway. Compensation Effect in Heterogeneous Catalysis. *Adv. Catal.* **26:**247 (1977).
- [18] M.A. Vannice. The Catalytic Synthesis of Hydrocarbons from H₂/CO Mixtures over the Group VIII Metals. II. The Kinetics of the Methanation Reaction over Supported Metals. J. Catal. 37:462 (1975).
- [19] O.V. Krylov. Catalysis by Non-Metals. Academic Press, New York, 1970.
- [20] P.B. Venuto and E.T. Habib. Catalyst-Feedstock-Engineering Interactions in Fluid Catalytic Cracking. *Catal. Rev. Sci. Eng.* 18:1 (1978).
- [21] D.P. Burke. Catalysts I. A \$600-Million Market in Cars and Refineries. *Chem. Week* 124:42 (1979).
- [22] K.C. Taylor. Automobile Catalytic Converters. In: J.R. Anderson and M. Boudart, editors, *Catalysis: Science and Technology*, Volume 5. Springer-Verlag, New York, 1984.
- [23] J.A. Cusumano, R.A. Dalla Betta, and R.B. Levy. *Catalysis in Coal Conversion*. Academic Press, New York, 1978.
- [24] G.W. Parshall. Industrial Applications of Homogeneous Catalysis. A Review. *J. Mol. Catal.* **4:**243 (1978).
- [25] G.A. Somorjai. Active Sites in Heterogeneous Catalysis. Adv. Catal. 26:1 (1977).
- [26] D.R. Kahn, E.E. Petersen, and G.A. Somorjai. The Hydrogenolysis of Cyclopropane on a Platinum Stepped Single Crystal at Atmospheric Pressure. *J. Catal.* 34:294 (1974).
- [27] B.A. Sexton and G.A. Somorjai. The Hydrogenation of CO and CO₂ on Polycrystalline Rhodium: Correlation of Surface Composition, Kinetics, and Product Distributions. J. Catal. 46:167 (1977).
- [28] M. Temkin and V. Pyzhev. Acta Physicochim. URSS 12:327 (1940).
- [29] M. Temkin and V. Pyzhev. Kinetics of the Synthesis of Ammonia on Promoted Iron Catalysts. J. Phys. Chem. (USSR) 13:851 (1939).
- [30] A. Nielsen. Review of Ammonia Catalysis. Catal. Rev. 4:1 (1970).
- [31] A. Nielsen. An Investigation on Promoted Iron Catalysts for the Synthesis of Ammonia. J. Gjellerups Forlag, Copenhagen, 1968.
- [32] A. Ozaki, H. Taylor, and M. Boudart. Kinetics and Mechanism of the Ammonia Synthesis. *Proc. R. Soc. London* **A258:47** (1960).
- [33] G. Ertl. Elementary Steps in Ammonia Synthesis: The Surface Science Approach. In: J.R. Jennings, editor, Catalytic Ammonia Synthesis: Fundamentals and Practice, Fundamental and Applied Catalysis. Plenum Press, New York, 1991.
- [34] J.W. Geuss and K.C. Waugh. Chemisorption at More Elevated Pressures on Indus-

- trial Ammonia Synthesis Catalysts. In: J.R. Jennings, editor, Catalytic Ammonia Synthesis: Fundamentals and Practice, Fundamental and Applied Catalysis. Plenum Press, New York, 1991.
- [35] S.R. Tennison. Alternative Noniron Catalysts. In: J.R. Jennings, editor, Catalytic Ammonia Synthesis: Fundamentals and Practice. Fundamental and Applied Catalysis. Plenum Press, New York, 1991.
- [36] C.A. Vancini. Synthesis of Ammonia. Macmillan Press, London, 1971. Translated by L. Pirt.
- [37] N.D. Spencer, R.C. Schoonmaker, and G.A. Somorjai. Iron Single Crystals as Ammonia Synthesis Catalysts. Effect of Surface Structure on Catalyst Activity. *J. Catal.* **74:**129 (1982).
- [38] D.R. Strongin, J. Carrazza, S.R. Bare, and G.A. Somorjai. The Importance of C₇ Sites and Surface Roughness in the Ammonia Synthesis Reaction over Iron. *J. Catal.* **103**:213 (1987).
- [39] R. Smoluchowsky. Anisotropy of the Electronic Work Function of Metals. *Phys. Rev.* **60:**661 (1941).
- [40] J. Hölzl and F.K. Schulte. Work Function of Metals. In: G. Höhler, editor, Solid Surface Physics. Springer Tracts in Modern Physics, Volume 85. Springer-Verlag, Berlin, 1979.
- [41] J. McAllister and R.S. Hansen. Catalytic Decomposition of Ammonia on Tungsten (100), (110), and (111) Crystal Faces. J. Chem. Phys. **59:**414 (1973).
- [42] J.A. Dumesic, H. Topsøe, and M. Boudart. Surface, Catalytic, and Magnetic Properties of Small Iron Particles. III. Nitrogen Induced Surface Reconstruction. J. Catal. 37:513 (1975).
- [43] F. Bozso, G. Ertl, and M. Weiss. Interaction of Nitrogen with Iron Surfaces. II. Fe(110). J. Catal. 50:519 (1977).
- [44] F. Bozso, G. Ertl, and M. Weiss. Interaction of Nitrogen with Iron Surfaces. I. Fe(100) and Fe(111). J. Catal. 49:18 (1977).
- [45] P.H. Emmett and S. Brunauer. The Adsorption of Nitrogen by Iron Synthetic Ammonia Catalysts. J. Am. Chem. Soc. 56:35 (1934).
- [46] J.J. Scholten, P. Zwietering, J.A. Konvalinka, and J.H. de Boer. Chemisorption of Nitrogen on Iron Catalysts in Connection with Ammonia Synthesis. Part 1. The Kinetics of the Adsorption and Desorption of Nitrogen. *Trans. Faraday Soc.* 55:2166 (1959).
- [47] S.R. Bare, D.R. Strongin, and G.A. Somorjai. Ammonia Synthesis over Iron Single-Crystal Catalysts: The Effects of Alumina and Potassium. *J. Phys. Chem.* **90:**4726 (1986).
- [48] D.R. Strongin, S.R. Bare, and G.A. Somorjai. The Effects of Aluminum Oxide in Restructuring Iron Single Crystal Surfaces for Ammonia Synthesis. *J. Catal.* **103:**289 (1987).
- [49] I. Sushumna and E. Ruckenstein. Role of Physical and Chemical Interactions in the Behavior of Supported Metal Catalysts: Iron on Alumina—A Case Study. *J. Catal.* **94:**239 (1985).
- [50] E. Paparazzo. XPS Analysis of Iron Aluminum Oxide Systems. *Appl. Surf. Sci.* **25:1** (1986).
- [51] E. Paparazzo, J.L. Dormann, and D. Fiorani. X-Ray Photoemission Study of Fe-Al₂O₃ Granular Thin Films. *Phys. Rev. B* 28:1154 (1983).
- [52] W.S. Borghard and M. Boudart. The Textural Promotion of Metallic Iron by Alumina. J. Catal. 80:194 (1983).
- [53] H. Ludwiczek, A. Preisinger, A. Fischer, R. Hosemann, A. Schönfeld, and W. Vo-

- gel. Structure, Formation, and Stability of Paracrystalline Ammonia Catalysts. J. Catal. 51:326 (1978).
- [54] G. Fagherazzi, F. Galante, F. Garbassi, and N. Pernicone. Structural Study of the Al₂O₃-Promoted Ammonia Synthesis Catalyst. II. Reduced State. *J. Catal.* **26:**344 (1972).
- [55] W.G. Frankenburg. The Catalytic Synthesis of Ammonia from Nitrogen and Hydrogen. In: P.H. Emmett, editor, *Hydrogenation and Dehydrogenation. Catalysis*, Volume 3. Reinhold, New York, 1955.
- [56] G. Ertl, S.B. Lee, and M. Weiss. Adsorption of Nitrogen on Potassium Promoted Fe(111) and (100) Surfaces. Surf. Sci. 114:527 (1982).
- [57] G. Ertl. Surface Science and Catalysis—Studies on the Mechanism of Ammonia Synthesis: The P.H. Emmett Award Address. *Catal. Rev. Sci. Eng.* **21**:201 (1980).
- [58] Z. Paál, G. Ertl, and S.B. Lee. Interactions of Potassium, Oxygen, and Nitrogen with Polycrystalline Iron Surfaces. *Appl. Surf. Sci.* 8:231 (1981).
- [59] D.R. Strongin and G.A. Somorjai. The Effects of Potassium on Ammonia Synthesis over Iron Single Crystal Surfaces. J. Catal. 109:51 (1988).
- [60] T.E. Madey and C. Benndorf. Influence of Surface Additives (Na and O) on the Adsorption and Structure of NH₃ on Ni(110). *Surf. Sci.* **152/153:587** (1985).
- [61] C. Benndorf and T.E. Madey. Interaction of NH₃ with Adsorbed Oxygen and Sodium on Ru(001): Evidence for Both Local and Long Range Interactions. *Chem. Phys. Lett.* **101**:59 (1983).
- [62] D.R. Strongin and G.A. Somorjai. On the Rate Enhancement of Ammonia Synthesis over Iron Single Crystals by Coadsorption of Aluminum Oxide with Potassium. *Catal. Lett.* 1:61 (1988).
- [63] K. Altenburg, H. Bosch, J.G. van Ommen, and P.J. Gellings. The Role of Potassium as a Promoter in Iron Catalysts for Ammonia Synthesis. *J. Catal.* **66:**326 (1980).
- [64] S. Khammouma. Ph.D. thesis, Stanford University, Palo Alto, CA, 1972.
- [65] G.A. Somorjai. *Chemistry in Two Dimensions: Surfaces*. Cornell University Press, Ithaca, NY, 1981.
- [66] A. Ozaki and K. Aika. Catalytic Activation of Dinitrogen. In: J.R. Anderson and M. Boudart, editors, *Catalysis: Science and Technology*, Volume 1. Springer-Verlag, Berlin, 1981.
- [67] M. Bowker, I. Parker, and K.C. Waugh. Extrapolation of the Kinetics of Model Ammonia Synthesis to Industrially Relevant Temperatures and Pressures. *Appl. Catal.* **14**:101 (1985).
- [68] M. Bowker, I. Parker, and K.C. Waugh. The Application of Surface Kinetic Data to the Industrial Synthesis of Ammonia. *Surf. Sci.* 197:L223 (1988).
- [69] P. Stolze and J.K. Nørskov. Comment on "The Application of Surface Kinetic Data to the Industrial Synthesis of Ammonia" by M. Bowker, I. Parker, and K.C. Waugh. Surf. Sci. 197:L230 (1988).
- [70] P. Stolze and J.K. Nørskov. An Interpretation of the High-Pressure Kinetics of Ammonia Synthesis Based on a Microscopic Model. J. Catal. 110:1 (1988).
- [71] J.K. Nørskov and P. Stolze. Theoretical Aspects of Surface Reactions. *Surf. Sci.* **189**/ **190:**91 (1987).
- [72] P. Stolze. Surface Science as the Basis for the Understanding of the Catalytic Synthesis of Ammonia. *Phys. Scr.* **36:824** (1987).
- [73] P. Stolze and J.K. Nørskov. A Description of the High-Pressure Ammonia Synthesis Reaction Based on Surface Science. J. Vacuum Sci. Technol. A 5:581 (1987).
- [74] P. Stolze and J.K. Nørskov. Bridging the "Pressure Gap" between Ultrahigh-Vacuum Surface Physics and High-Pressure Catalysis. *Phys. Rev. Lett.* **55:**2502 (1985).

- [75] J.R. Rostrup-Nielsen. Catalytic Steam Reforming. In: J.R. Anderson and M. Boudart, editors, *Catalysis Science and Technology*, Volume 5. Springer-Verlag, New York, 1984.
- [76] D.A. Hickman and L.D. Schmidt. Production of Syngas by Direct Catalytic Oxidation of Methane. *Science* **259**:343 (1993).
- [77] M.A. Vannice. The Catalytic Synthesis of Hydrocarbons from H₂/CO Mixtures over the Group VIII Metals. I. The Specific Activities and Product Distributions of Supported Metals. J. Catal. 37:449 (1975).
- [78] D.J. Dwyer and G.A. Somorjai. Hydrogenation of CO and CO₂ over Iron Foils: Correlations of Rate, Product Distribution, and Surface Composition. *J. Catal.* **52**:291 (1978).
- [79] M. Araki and V. Ponec. Methanation of Carbon Monoxide on Nickel and Nickel Copper Alloys. J. Catal. 44:439 (1976).
- [80] P.R. Ventreek, B.J. Wood, and H. Wise. The Role of Surface Carbon in Catalytic Methanation. J. Catal. 43:363 (1976).
- [81] J.A. Rabo, A.P. Risch, and M.L. Poutsma. Reactions of Carbon Monoxide and Hydrogen on Co, Ni, Ru, and Pd Metals. *J. Catal.* 53:295 (1978).
- [82] P. Biloen, J.L. Helle, and W.M.H. Sachtler. Incorporation of Surface Carbon into Hydrocarbons during Fischer-Tropsch Synthesis: Mechanistic Implications. *J. Catal.* **58:95** (1979).
- [83] L.L. Kesmodel, L.H. Dubois, and G.A. Somorjai. LEED Analysis of Acetylene and Ethylene Chemisorption on the Pt(111) Surface: Evidence for Ethylidyne Formation. *J. Chem. Phys.* **70:**2180 (1979).
- [84] J.E. Demuth and H. Ibach. Identification of CH Species on Ni(111) by High Resolution Electron Energy Loss Spectroscopy. *Surf. Sci.* 78:L238 (1978).
- [85] M.L. Poutsma, L.F. Elek, P. Ibarbia, H. Risch, and J.A. Rabo. Selective Formation of Methanol from Synthesis Gas over Palladium Catalysts. *J. Catal.* 52:157 (1978).
- [86] M.A. Vannice. The Catalytic Synthesis from Carbon Monoxide and Hydrogen. *Catal. Rev. Sci. Eng.* **14:**153 (1976).
- [87] H. Pichler. Twenty-five Years of Synthesis of Gasoline by Catalytic Conversion of Carbon Monoxide and Hydrogen. *Adv. Catal. Relat. Subj.* **4:**271 (1952).
- [88] W.K. Hall, R.J. Kokes, and P.H. Emmett. Mechanism Studies of the Fischer-Tropsch Synthesis: The Incorporation of Radioactive Ethylene, Propionaldehyde and Propanol. J. Am. Chem. Soc. 82:1027 (1960).
- [89] J.T. Kummer and P.H. Emmett. Fischer-Tropsch Synthesis Mechanism Studies. The Addition of Radioactive Alcohols to the Synthesis Gas. J. Am. Chem. Soc. 75:5177 (1953).
- [90] J.A. Rabo, L.F. Elek, and J.N. Francis. The Reaction of Surface Carbon with Water on Ni and Co Catalysts; a New Process for the Production of Concentrated Methane from Dilute Carbon Monoxide Waste Streams. In: T. Seiyama and K. Tanabe, editors, New Horizons in Catalysis. Studies in Surface Science and Catalysis, Volume 7A. Elsevier, New York, 1981, p. 490.
- [91] D.G. Castner, R. Blackadar, and G.A. Somorjai. CO Hydrogenation on Clean and Oxidized Rhodium Foil and Single Crystal Catalysts. Correlations of Catalyst Activity, Selectivity, and Surface Composition. J. Catal. 66:257 (1980).
- [92] G.M. Schwab. Metal Electrons and Catalysis. Trans. Faraday Soc. 42:689 (1946).
- [93] S.J. Tauster. Strong Metal Support Interactions. Acc. Chem. Res. 20:389 (1987).
- [94] S.J. Tauster, S.C. Fung, R.T.K. Baker, and J.A. Horsley. Strong Interactions in Supported Metal Catalysts. *Science* 211:1121 (1981).

- [95] S.J. Tauster, S.C. Fung, and R.L. Garten. Strong Metal Support Interactions. Group 8 Noble Metals Supported on TiO₂. J. Am. Chem. Soc. 100:170 (1978).
- [96] V. Andera. Investigation of the Rh/TiO₂ System by XPS and XAES. Appl. Surf. Science 51:1 (1991).
- [97] J.P. Belzunegui, J.M. Rojo, and J. Sanz. ¹H NMR Procedure to Estimate the Extent of Metal Surface Covered by TiO_x Overlayers in Reduced Rh/TiO₂ Catalysts. *J. Phys. Chem.* **95**:3463 (1991).
- [98] A. Dauscher, L. Hilaire, F. le Normand, G. Maire, G. Mueller, and A. Vasquez. Characterization by XPS and XAS of Supported Pt/TiO₂-CeO₂ Catalysts. *Surf. Interface Anal.* 16:341 (1990).
- [99] A.N. Murty, M. Seamster, A.N. Thorpe, and R.T. Obermyer. NMR Evidence of Metal-Support Interaction in Syngas Conversion Catalyst Co-TiO₂. J. Appl. Phys. 67:5847 (1990).
- [100] G. Munuera, A.R. González-Elipe, and J.P. Espinós. XPS Study of Phase Mobility in Ni/TiO₂ Systems. *Surf. Sci.* 211/212:1113 (1989).
- [101] M.G. Cattania, F. Parmagiani, and V. Ragaini. A Study of Ruthenium Catalysts on Oxide Supports. Surf. Sci. 211/212:1097 (1989).
- [102] F. Boccuzzi, A. Chiorino, and G. Ghiotti. IR Study of the CO Adsorption on Pt/ZnO Samples. Evidence for a PtZn Phase Formation in the SMSI State. Surf. Sci. 209:77 (1989).
- [103] D. Gazzoli, G. Minelli, and M. Valigi. The FeO_x-TiO₂ System: An X-Ray Diffraction, Thermogravimetric and Magnetic Susceptibility Study. *Mater. Chem. Phys.* 21:93 (1989).
- [104] K. Matsuo and K. Nakano. Performances of Platinum Metal Catalysts Supported on Titania Coated Silica Prepared from Metal Organics. *Appl. Surf. Sci.* 33/34:269 (1988).
- [105] A.D. Logan, E.J. Braunschweig, A.K. Datye, and D.J. Smith. Direct Observation of the Surfaces of Small Metal Crystallites; Rhodium Supported on TiO₂. Langmuir 4:827 (1988).
- [106] K. Tamura, U. Bardi, and Y. Nihei. An Investigation by Angular Resolved X-Ray Photoelectron Spectroscopy of Strong Metal-Support Interaction (SMSI) in the Pt/TiO₂ System. Surf. Sci. 197:L281 (1988).
- [107] G. Munuera, A.R. González-Elipe, J.P. Espinós, J.C. Conesa, J. Soria, and J. Sanz. Hydrogen-Induced TiO_x Migration onto Metallic Rh in Real Rh/TiO₂ Catalysts. J. Phys. Chem. 91:6625 (1987).
- [108] A. Katrib, C. Petit, P. Legare, L. Hilaire, and G. Maire. An Investigation of Metal-Support Interaction in Bimetallic Pt-Mo Catalysts Deposited on Silica and Alumina. Surf. Sci. 189/190:886 (1987).
- [109] A.B. Anderson and D.Q. Dowd. Co-Adsorption on Pt(111) Doped with TiO, FeO, ZnO, and Fe, and Pt Ad-Atoms. Molecular Orbital Study of Co-Dopant Interactions. *J. Phys. Chem.* **91:**869 (1987).
- [110] C. Ocal and S. Ferrer. A New CO Adsorption State on Thermally Treated Pt/TiO₂ Model Catalysts. *Surf. Sci.* 178:850 (1986).
- [111] C. Ocal and S. Ferrer. The Strong Metal-Support Interaction (SMSI) in Pt-TiO₂ Model Catalysts. A New CO Adsorption State on Pt-Ti Atoms. *J. Chem. Phys.* 89:4974 (1985).
- [112] J. Cunningham and G.H. Al-Sayyed. Metal-Support Interaction in Benzene Hydrogenation over Pt-TiO₂. Influence of O₂ and UV. Surf. Sci. 169:289 (1986).
- [113] J. Sanz and J.M. Rojo. NMR Study of Hydrogen Adsorption on Rh/TiO₂. J. Phys. Chem. 89:4974 (1985).

- [114] H. Orita, S. Naito, and K. Tamuru. Nature of SMSI Effect on CO + H₂ Reaction over Supported Rh Catalysts. *J. Phys. Chem.* 89:3066 (1985).
- [115] S. Takatani and Y.W. Chung. Effect of High Temperature Reduction on the Surface Composition of and CO Chemisorption on Ni/TiO₂. *Appl. Surf. Sci.* **19:**341 (1984).
- [116] H.R. Sadeghi and V.E. Henrich. Rh on TiO₂. Model Catalyst Studies of the Strong Metal-Support Interaction. *Appl. Surf. Sci.* 19:330 (1984).
- [117] K. Tanaka, K. Miyahara, and I. Toyoshima. Adsorption of CO₂ on TiO₂ and Pt/TiO₂ Studied by X-Ray Photoelectron Spectroscopy and Auger Electron Spectroscopy. *J. Phys. Chem.* 88:3504 (1984).
- [118] J.C. Conesa, J. Soria, P. Malet, G. Munuera, and J. Sanz. Magnetic Resonance Studies of Hydrogen-Reduced Rh/TiO₂ Catalysts. J. Phys. Chem. 88:2986 (1984).
- [119] D.N. Belton, Y.M. Sun, and J.M. White. Thin-Film Models of Strong Metal-Support Interaction Catalysts. Platinum on Oxidized Titanium. J. Phys. Chem. 88:1690 (1984).
- [120] T. Pannaparayil, M. Oskooie-Tabrizi, C. Lo, L.N. Mulay, G.A. Melson, and V.U.S. Rao. Magnetic and Mössbauer Study of Metal-Zeolite Interaction in Catalysts. *J. Appl. Phys.* 55:2601 (1984).
- [121] J.E.E. Baglin, G.J. Clark, and J.F. Ziegler. Catalyst Metal-Support Interactions. Rutherford Backscattering Spectrometry Applied to Discontinuous Films. *Nucl. Instrum. Methods Phys. Res.* 218:445 (1983).
- [122] T. Huizinga, H.F.J. van't Blik, J.C. Vis, and R. Prins. XPS Investigations of Pt and Rh Supported on γ-Al₂O₃ and TiO₂. Surf. Sci. 135:580 (1983).
- [123] B.H. Chen and J.M. White. Properties of Platinum Supported on Oxides of Titanium. J. Phys. Chem. 86:3534 (1982).
- [124] H. Poppa and F. Soria. The Interaction of CO and O₂ with Thin Islands of Pd. Surf. Sci. 115:L105 (1982).
- [125] M. Valigi, D. Gazzoli, and D. Cordischi. A Structural, Thermogravimetric and ESR Study of the RhO_x-TiO₂ System. J. Mater. Sci. 17:1277 (1982).
- [126] J.A. Horsley. A Molecular Orbital Study of Strong Metal-Support Interaction between Platinum and Titanium Dioxide. J. Am. Chem. Soc. 101:2870 (1979).
- [127] R.G. Herman. Classical and Non-Classical Route for Alcohol Synthesis. In: L. Guczi, editor, *New Trends in CO Activation. Studies in Surface Science and Catalysis*, Volume 64. Elsevier, Amsterdam, 1991.
- [128] P.J. Flory. *Principles of Polymer Chemistry*. Cornell University Press, Ithaca, NY, 1953.
- [129] G.V. Schulz. Über die Kinetik der Kettenpolymerisationen. V. Der Einfluß verschiedener Reaktionsarten auf die Polymolekularität. Z. Phys. Chem. Abt. B 43:25 (1939).
- [130] D.J. Dwyer and G.A. Somorjai. The Role of Readsorption in Determining the Product Distribution During CO Hydrogenation over Fe Single Crystals. *J. Catal.* **56:**249 (1979).
- [131] Y.T. Eidus, N.D. Zelinski, and N.I. Ershov. Dokl. Akad. Nauk USSR 60:599 (1948).
- [132] C.D. Chang and A.J. Silvestri. The Conversion of Methanol and Other O-Compounds to Hydrocarbons over Zeolite Catalysts. *J. Catal.* 47:249 (1977).
- [133] S.L. Meisel, J.P. McCullough, C.H. Lechthaler, and P.B. Weisz. Gasoline from Methanol in One Step. *Chemtech* **6:**86 (1976).
- [134] W.W. Kaeding and S.A. Butter. Production of Chemicals from Methanol. I. Low Molecular Weight Olefins. J. Catal. 61:155 (1980).
- [135] J.K. Nørskov. Adsorbate-Adsorbate Interactions and Surface Reactivity. In: H.P. Bonzel, A.M. Bradshaw, and G. Ertl, editors, *Physics and Chemistry of Alkali Metal Adsorption. Materials Science Monographs*, Volume 57. Elsevier, Amsterdam, 1989.

- [136] J.E. Crowell, E.L. Garfunkel, and G.A. Somorjai. The Coadsorption of Potassium and CO on the Pt(111) Crystal Surface: A TDS, HREELS, and UPS Study. Surf. Sci. 121:303 (1982).
- [137] C.T. Campbell and D.W. Goodman. A Surface Science Investigation of the Role of Potassium Promoters in Nickel Catalysts for CO Hydrogenation. *Surf. Sci.* 123:413 (1982).
- [138] J.E. Crowell, W.T. Tysoe, and G.A. Somorjai. Potassium Coadsorption Induced Dissociation of CO on the Rh(111) Crystal Face: An Isotope Mixing Study. J. Phys. Chem. 89:1598 (1985).
- [139] J.E. Crowell and G.A. Somorjai. The Effect of Potassium on the Chemisorption of Carbon Monoxide on the Rh(111) Crystal Face. *Appl. Surf. Sci.* 19:73 (1984).
- [140] J.H. Sinfelt. Heterogeneous Catalysis by Metals. *Prog. Solid State Chem.* 10:55 (1975).
- [141] F.G. Ciapetta and D.N. Wallace. Catalytic Naphtha Reforming. *Catal. Rev.* 5:67 (1972).
- [142] G.A. Mills, H. Heineman, T.H. Milliken, and K.G. Oblad. Catalytic Mechanism. *Ind. Eng. Chem.* 45:135 (1953).
- [143] N.I. Il'chenko and G.I. Golodets. Catalytic Oxidation of Ammonia. I. Reaction Kinetics and Mechanism. J. Catal. 39:57 (1975).
- [144] J.K. Dixon and J.E. Longfield. Hydrocarbon Oxidation. In: P.H. Emmett, editor, Oxidation, Hydration, Dehydration and Cracking Catalysis. Catalysis, Volume 7. Reinhold, New York, 1960.
- [145] C.C. Chang and L.L. Hegedus. Surface Reactions of NO, CO, and O₂ near the Stoichiometric Point. I. Pt-Alumina. J. Catal. 57:361 (1976).
- [146] M. Shelef. Nitric Oxide: Surface Reactions and Removal from Auto Exhaust. *Catal. Rev. Sci. Eng.* 11:1 (1975).
- [147] E. Segal, R.J. Madon, and M. Boudart. Catalytic Hydrogenation of Cyclohexane. I. Vapor-Phase Reaction on Supported Platinum. *J. Catal.* **52:**45 (1978).
- [148] P. Stonehart and P.M. Ross. The Commonality of Surface Processes in Electrocatalysis and Gas-Phase Heterogeneous Catalysis. *Catal. Rev. Sci. Eng.* 12:1 (1975).
- [149] J.C. Schlatter and M. Boudart. Hydrogenation of Ethylene on Supported Platinum. J. Catal. 24:482 (1972).
- [150] A.J. Appleby. Electrocatalysis and Fuel Cells. Catal. Rev. 4:221 (1970).
- [151] J. Haro, R. Gómez, and J.M. Ferreira. The Role of Palladium in Dehydrogenation of Cyclohexane over Pt-Pd/Al₂O₃ Bimetallic Catalysts. J. Catal. **45**:326 (1976).
- [152] M. Kraft and H. Spindler. Studies on Some Relations between Structural and Catalytical Properties of Alumina-Supported Platinum. In: *Proceedings of the 4th International Congress on Catalysis. Preprints of the Papers*, 1960, paper #69.
- [153] C. Leclerq, L. Leclerq, and R. Maurel. Hydrogenolysis of Saturated Hydrocarbons. III. Selectivity in Hydrogenolysis of Various Aliphatic Hydrocarbons on Platinum/Alumina. J. Catal. **50:**87 (1977).
- [154] J.R. Anderson and N.R. Avery. The Isomerization of Aliphatic Hydrocarbons on Evaporated Films of Platinum and Palladium. J. Catal. 5:446 (1966).
- [155] G.A. Somorjai. Surface Science View of Catalysis: The Past, Present, and Future. In: 8th International Congress on Catalysis. Proceedings. Volume 1: Plenary Lectures, 1984.
- [156] S.M. Davis, F. Zaera, and G.A. Somorjai. Surface Structure and Temperature Dependence of *n*-Hexane Skeletal Rearrangement Reactions Catalyzed over Platinum Single Crystal Surfaces: Marked Structure Sensitivity of Aromatization. *J. Catal.* **85**:206 (1984).

- [157] K. Besocke, B. Krahl-Urban, and H. Wagner. Dipole Moments Associated with Edge Atoms; a Comparative Study on Stepped Pt, Au, and W Surfaces. *Surf. Sci.* **68:**39 (1977).
- [158] G.A. Somorjai and F. Zaera. Heterogeneous Catalysis on the Molecular Scale. *J. Phys. Chem.* **86:**3070 (1982).
- [159] M. Salmerón and G.A. Somorjai. Desorption, Decomposition, and Deuterium Exchange Reactions of Unsaturated Hydrocarbons (Ethylene, Acetylene, Propylene, and Butenes) on the Pt(111) Crystal Face. J. Phys. Chem. 86:341 (1982).
- [160] S.M. Davis and G.A. Somorjai. Molecular Ingredients of Heterogeneous Catalysis: New Horizons for High Technology. *Bull. Soc. Chim. France* 3:(3), 271 (1984).
- [161] G.A. Somorjai, J.E. Crowell, R.J. Koestner, L.H. Dubois, and M.A. Van Hove. The Study of the Structure of Adsorbed Molecules on Solid Surfaces by High Resolution Electron Energy Loss Spectroscopy and Low Energy Electron Diffraction. In: K. Fuwa, editor, *Recent Advances in Analytical Spectroscopy*. Pergamon Press, Oxford, 1982.
- [162] L.H. Dubois, D.G. Castner, and G.A. Somorjai. A Low Energy Electron Diffraction (LEED), High Resolution Electron Energy Loss (ELS), and Thermal Desorption Mass Spectrometry (TDS) Study. *J. Chem. Phys.* **72:**5234 (1980).
- [163] S.M. Davis, F. Zaera, and G.A. Somorjai. The Reactivity and Composition of Strongly Adsorbed Carbonaceous Deposits on Platinum. Model of the Working Hydrocarbon Conversion Catalyst. *J. Catal.* 77:439 (1982).
- [164] G.A. Somorjai. Surface Science and Catalysis. *Philos. Trans. R. Soc. London* A318:81 (1986).
- [165] A. Wieckowski, S. Rosasco, G. Salaita, A. Hubbard, B. Bent, F. Zaera, D. Godbey, and G.A. Somorjai. Comparison of Gas-Phase and Electrochemical Hydrogenation of Ethylene at Platinum Surfaces. J. Am. Chem. Soc. 107:5910 (1985).
- [166] A. Farkas, L. Farkas, and E.K. Rideal. Experiments on Heavy Hydrogen. IV. The Hydrogenation and Exchange Reaction of Ethylene with Heavy Hydrogen. *Proc. R. Soc. London* A146:630 (1934).
- [167] D.D. Eley and J.L. Tuck. On the Microthermoconductivity Method for the Estimation of *Para*-Hydrogen and Deuterium. *Trans. Faraday Soc.* 32:1425 (1936).
- [168] O. Beek. Hydrogenation Catalysts. Discuss. Faraday Soc. 8:118 (1950).
- [169] G.H. Twigg and E.K. Rideal. The Exchange Reaction between Ethylene and Deuterium on a Nickel Catalyst. *Proc. R. Soc. London* A171:55 (1939).
- [170] J. Horiuti and M. Polanyi. Exchange Reactions of Hydrogen on Metallic Catalysts. Trans. Faraday Soc. 30:1164 (1934).
- [171] R.W. Roberts. A Study of the Adsorption and Decomposition of Hydrocarbons on Clean Iridium Surfaces. J. Phys. Chem. 67:2035 (1963).
- [172] J. Horiuti and K. Miyahara. *Hydrogenation of Ethylene on Metallic Catalysts*. National Standard Reference Data Series 13, National Bureau of Standards, 1968.
- [173] F. Zaera and G.A. Somorjai. Hydrogenation of Ethylene over Platinum (111) Single-Crystal Surfaces. J. Am. Chem. Soc. 106:2288 (1984).
- [174] R.J. Koestner, M.A. Van Hove, and G.A. Somorjai. A LEED Crystallography Study of the (2×2) - C_2H_3 Structure Obtained after Ethylene Adsorption on Rh(111). *Surf. Sci.* 121:321 (1982).
- [175] S.J. Thomson and G. Webb. Catalytic Hydrogenation of Olefins on Metals, a New Interpretation. J. Chem. Soc. Chem. Commun. 13:526 (1976).
- [176] B.E. Koel, J.E. Crowell, B. Bent, C.M. Mate, and G.A. Somorjai. Thermal Decomposition of Benzene on the Rh(111) Crystal Surface. *J. Phys. Chem.* **90:**2949 (1986).
- [177] A.J. Gellman, D. Neiman, and G.A. Somorjai. Catalytic Hydrodesulfurization over

- the Mo(100) Single Crystal Surface. I. Kinetics and Overall Mechanism. J. Catal. 107:92 (1987).
- [178] M.H. Farias, A.J. Gellman, G.A. Somorjai, R.R. Chianelli, and K.S. Liang. The CO and Coadsorption and Reactions of Sulfur, Hydrogen, and Oxygen on Clean and Sulfided Mo(100) and on MoS₂ Crystal Faces. *Surf. Sci.* **140**:181 (1984).
- [179] W.D. Gillespie, R.K. Herz, E.E. Petersen, and G.A. Somorjai. The Structure Sensitivity of *n*-Heptane Dehydrocyclization and Hydrogenolysis Catalyzed by Platinum Single Crystals at Atmospheric Pressure. *J. Catal.* 70:147 (1981).
- [180] J.W.A. Sachtler and G.A. Somorjai. Influence of Ensemble Size on CO Chemisorption and Catalytic *n*-Hexane Conversion by Au-Pt(111) Bimetallic Single-Crystal Surfaces. *J. Catal.* **81:**77 (1983).
- [181] V. Ponec. Catalysis by Alloys in Hydrocarbon Reactions. Adv. Catal. 32:149 (1983).
- [182] J.H. Sinfelt. Bimetallic Catalysts: Discoveries, Concepts, and Applications. John Wiley & Sons, New York, 1983.
- [183] R.C. Yeates and G.A. Somorjai. Surface Structure Sensitivity of Alloy Catalysis: Catalytic Conversion of *n*-Hexane over Au-Pt(111) and Au-Pt(100) Alloy Crystal Surfaces. *J. Catal.* **103**:208 (1987).
- [184] Y.L. Lam, J. Criado, and M. Boudart. Enhancement by Inactive Gold of the Rate of the H₂-O₂ Reaction on Active Palladium: a Ligand Effect. *Nouv. J. Chim.* 1:461 (1977).
- [185] G.A. Somorjai. Building and Characterization of Catalysts on Single Crystal Surfaces. *Catal. Lett.* **15:25** (1992).
- [186] J.A. Rabo, editor. Zeolite Chemistry and Catalysis. ACS Monograph, Volume 171. American Chemical Society, Washington, D.C., 1976.
- [187] Z. Karpiński, Z. Zhang, and W.M.H. Sachtler. Probing Palladium-Cobalt/NaY Catalysts by Neopentane Conversion. *Catal. Lett.* 13:123 (1992).
- [188] J.H. Sinfelt. Catalytic Hydrogenolysis on Metals. Catal. Lett. 9:159 (1991).
- [189] B.C. Gates. Catalytic Chemistry. John Wiley & Sons, New York, 1992.
- [190] G.A. Somorjai and J. Carrazza. Structure Sensitivity of Catalytic Reactions. *Ind. Eng. Chem. Fundam.* **25:**63 (1986).
- [191] D.W. Goodman. Model Catalytic Studies over Metal Single Crystals. Acc. Chem. Res. 17:194 (1984).
- [192] J.K. Nørskov, P. Stoltze, and U. Nielsen. The Reactivity of Metal Surfaces. *Catal. Lett.* 9:173 (1991).
- [193] C.H. Bartholomew, R.B. Pannell, and J.L. Butler. Support and Crystallite Size Effects in CO Hydrogenation on Nickel. *J. Catal.* **65:**335 (1980).
- [194] K.J. Williams, A.B. Boffa, M. Salmerón, A.T. Bell, and G.A. Somorjai. The Kinetics of CO₂ Hydrogenation on a Rh Foil Promoted by Titania Overlayers. *Catal. Lett.* **9:**415 (1991).
- [195] S.M. Davis, F. Zaera, B.E. Gordon, and G.A. Somorjai. Radiotracer and Thermal Desorption Studies of Dehydrogenation and Atmospheric Hydrogenation of Organic Fragments Obtained from [14C]Ethylene Chemisorbed over Pt(111) Surfaces. J. Catal. 92:240 (1985).
- [196] K.J. Williams. Titania Promotion of Rhodium Model Catalysts: A Surface Science and Reaction Study. Ph.D. thesis, University of California, Berkeley, 1991.
- [197] S.A. Topham. The History of the Catalytic Synthesis of Ammonia. In: J.R. Anderson and M. Boudart, editors, *Catalysis: Science and Technology*, Volume 7. Springer-Verlag, Berlin, 1985.

- [198] C.N. Satterfield. *Heterogeneous Catalysis in Practice*. McGraw-Hill Chemical Engineering Series. McGraw-Hill, New York, 1980.
- [199] B.C. Gates, J.R. Katzer, and G.C.A. Schuit. *Chemistry of Catalytic Processes*. McGraw-Hill Chemical Engineering Series. McGraw-Hill, New York, 1979.
- [200] R.A. van Santen and H.P.C.E. Kuipers. The Mechanism of Ethylene Epoxidation. *Adv. Catal.* **35:**265 (1987).
- [201] J.M. Berty. Ethylene Oxide Synthesis. In: B.E. Leach, editor, *Applied Industrial Catalysis*, Volume 1. Academic Press, New York, 1983.
- [202] R.K. Grasselly and J.D. Burrington. Selective Oxidation and Ammoxidation of Propylene by Heterogeneous Catalysis. *Adv. Catal.* **30:**133 (1981).
- [203] J. Dwyer and P.J. O'Malley. Relation between Acidic and Catalytic Properties of Zeolites. In: S. Kaliaguine, editor, Keynotes in Energy-Related Catalysis. Studies in Surface Science and Catalysis, Volume 35. Elsevier, Amsterdam, 1988.
- [204] M. Iwamoto. Catalytic Decomposition of Nitrogen Monoxide. In: M. Misano, Y. Morooka, and S. Kimura, editors, Future Opportunities in Catalytic and Separation Technology. Studies in Surface Science and Catalysis, Volume 54. Elsevier, Amsterdam, 1990.
- [205] H. Bosch and F. Janssen. Catalytic Reduction of Nitrogen Oxides: A Review on the Fundamentals and Technology. *Catal. Today* 2:369 (1988).
- [206] J.E. McEvoy, editor. Catalysts for the Control of Automobile Pollutants. Advances in Chemistry, Volume 143. American Chemical Society, Washington, D.C., 1975.
- [207] D.S. Newsome. The Water-Gas Shift Reaction. Catal. Rev. Sci. Eng. 21:275 (1980).
- [208] G. Ertl. Oscillatory Catalytic Reactions at Single-Crystal Surfaces. *Adv. Catal.* **37:**213 (1990).
- [209] P. Grange. Catalytic Dehydrosulfurization. Catal. Rev. Sci. Eng. 21:135 (1980).
- [210] T.C. Ho. Hydrodenitrogenation Catalysis. Catal. Rev. Sci. Eng. 30:117 (1988).
- [211] M.P. McDaniel. Supported Chromium Catalysts for Ethylene Polymerization. Adv. Catal. 33:48 (1985).
- [212] E.E. Donath. History of Catalysis in Coal Liquifaction. In: J.R. Anderson and M. Boudart, editors, *Catalysis: Science and Technology*, Volume 3. Springer-Verlag, Berlin, 1982.
- [213] J. Raskó, G.A. Somorjai, and H. Heinemann. Catalytic Low-Temperature Oxydehydrogenation of Methane to Higher Hydrocarbons with Very High Selectivity at 8-12% Conversion. *Appl. Catal. A* **84:**57 (1992).
- [214] J. Raskó, P. Pereira, G.A. Somorjai, and H. Heinemann. The Catalytic Low Temperature Oxydehydrogenation of Methane: Temperature Dependence, Carbon Balance and Effects of Catalyst Composition. *Catal. Lett.* **9:**395 (1991).
- [215] J.C. Mackie. Partial Oxidation of Methane: The Role of Gas Phase Reactions. *Catal. Rev. Sci. Eng.* **33:**169 (1991).
- [216] Y. Amenomiya, V.I. Birss, M. Goledzinowski, J. Galuszka, and A.R. Sanger. Conversion of Methane by Oxidative Coupling. *Catal. Rev. Sci. Eng.* 32:163 (1990).
- [217] J.H. Lunsford. The Catalytic Conversion of Methane to Higher Hydrocarbons. Catal. Today 6:235 (1990).
- [218] Surface Science as a Basis for Understanding Heterogeneous Catalysis. In: R.W. Joyner and R.A. van Santen, editors, *Elementary Reaction Steps in Heterogeneous Catalysis*. Kluwer Academic Publishers, Dordrecht, The Netherlands, in press, (1993).